METEOROLOGICAL DRIVERS OF LIGHTNING IN ALASKA ON

SEASONAL AND SUB-SEASONAL TIMESCALES

By

Jonathan Chriest, B.S.

A Thesis Submitted in Partial Fulfillment of the Requirements

for the Degree of

Master of Science

in

Atmospheric Sciences

University of Alaska Fairbanks

May 2021

APPROVED:

Uma S. Bhatt, Committee Chair
Peter A. Bieniek, Committee Member
John E. Walsh, Committee Member
Gilberto J. Fochesatto, Chair
Department of Atmospheric Sciences
Kinchel Doerner, Dean
    College of Natural Science and Mathematics
Richard Collins
    Director of the Graduate School

Abstract

Wildfire has long been a part of the Boreal forest ecosystem in Alaska and the increasing number of large fire seasons over the past 2 decades has had substantial economic and health impacts. Boreal wildfires are expected to continue to increase over the next century in part due to a projected increase in lightning. This motivates developing lightning outlooks to inform fire management decisions regarding the economic allocation of shared firefighting resources including but not limited to personnel and air tankers. The goal of this research is to identify key meteorological parameters associated with lightning processes on a stroke-by-stroke spatial scale and at hourly-to-sub-seasonal timescales. This is a first step towards developing robust lightning outlooks. In order to identify the key parameters, lightning data for the Alaska Lightning Detection Network was paired with hourly European Center Reanalysis Version 5 (ERA5) over the 2012–2019 study period. This data was analyzed on the scale of Alaska Fire Service Predictive Service Areas (PSAs) and three sub-seasons of the Alaska fire season. This strategy helped to identify regional and sub-seasonal variability and made the research operationally relevant.

Key results from this research include the following. The majority of lightning occurs in the duff driven sub-season across all PSAs. Lightning, particularly in the Interior PSAs, follows a diurnal pattern with lightning on average beginning earlier in the day in the eastern portion of Alaska and later in the day in the western portion of Alaska. This distinctive pattern is not as well defined in the Coastal PSAs. Results also suggested that dry lightning may be more prevalent in portions of the western Interior than in other regions of Alaska. Lightning events were more common under specific atmospheric flow directions at 500 and 700 hPa, where these directions varied by PSA. Northeasterly and northwesterly flow aloft were most favorable for lightning in the Tanana Valley West PSA, while southerly flow aloft was more favorable for lightning in the

North Slope and Upper Yukon PSAs. Finally, easterly flow was a more common pattern during

lightning strokes in the Seward Peninsula and Kuskokwim Valley PSAs.

Table of Contents

List of Figures

List of Tables

List of Appendices

Acknowledgements

to thank the UAF ski trails for enabling me to ski almost daily to and from the office and whenever I needed to take a midday breath.

1. Introduction

Wildfire has long been a part of the Boreal forest ecosystem in Alaska in the summer (Lynch et al. 2004). Between 1940 and 2020, 70.4 million acres of Alaska burned due to wildland fire, the majority of which was in Interior Alaska between the Brooks Range and the Alaska Range (Figure 1). Since records began in 1950, most fires have been started by human activity, however 90% of acres burned have been due to wildfires started by lightning (Kasischke and Turetsky 2006). The large acreage burned in the Alaska fire seasons of 2004, 2005, and 2015 have been attributed to lightning ignitions (Wendler et al. 2011; Farukh and Hayasaka 2012; Partain et al. 2016). Boreal wildfires are also projected to continue to increase over the next century in part due to a projected increase in lightning (Romps et al. 2014; Veraverbeke et al. 2017). Organized convective storms in Alaska are projected to triple by 2100 under a high emissions scenario as a result of anthropogenic climate change, where the main drivers are the loss of sea ice and increased relative humidity over land (Poujol et al. 2021). Under anthropogenic climate change, the expected earlier snowmelt lengthens the fire season and the potential for more extreme fire conditions (Semmens and Ramage 2012). The prominent role of lightning in historical fires, along with the projected increases of lightning, motivates developing lightning outlooks to inform management decisions regarding the economic allocation of firefighting resources including personnel and air attack infrastructure normally shared with the contiguous United States (CONUS). To develop robust lightning outlooks, analysis at the seasonal time scale as well as at shorter time scales is needed. An understanding of lightning processes in Alaska at short (< daily) timescales is currently lacking and it would not only help identify meteorological linkages but would also assist with forecasting thunderstorms, enhancing the safety of fire crews.

1
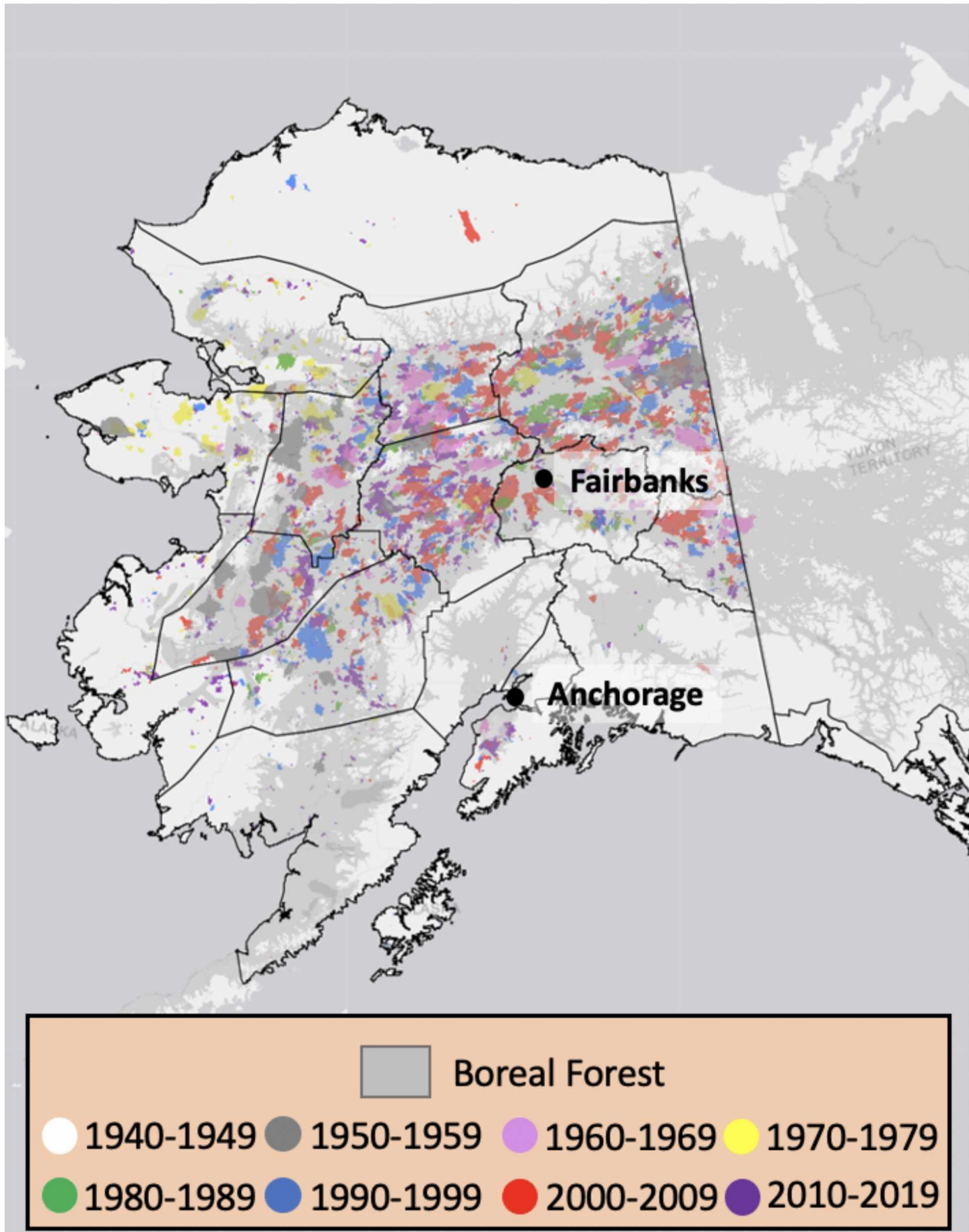
Figure 1: Wildland fires in Alaska from 1940-2019. Gray terrestrial shading highlights the boreal forest based on a shapefile by Brandt el al. (2009). Black outlines identify fire management divisions called Predictive Service Areas.

Research into the drivers of wildfire in Alaska has yielded some promising findings, though seasonal and sub-seasonal predictability to provide fire managers with skillful summer outlooks is still part of active research. Warm summer weather conditions are correlated with large fire years (Flannigan et al. 2009) and earlier spring snowmelt can increase the chance of large fires (Semmens and Ramage 2012). On the monthly timescale, Duffy et al. (2005) found that seven variables and an interaction term "explain 79% of the variability in the natural logarithm of the number of hectares burned annually by lightning-caused fires in Alaska from 1950 to 2003", with the top 3 variables being average June temperature, the East Pacific teleconnection pattern, and average April temperature.

Seasonal predictability of lightning in Alaska has been explored on monthly timescales, where Bieniek et al. (2019) found that the number of lightning flashes is correlated with convective precipitation, providing a potential proxy for lightning in meteorological observations and modeled parameters. Predicting lightning is a challenge even at short timescales (< day) as shown by steeper decline of skill for Alaska than for the CONUS using the Localized Aviation MOS Program (LAMP) forecasts of lightning (Charba et al. 2020). In another study of CONUS lightning, Romps et al. (2014) proposed the product of convective available potential energy (CAPE) and precipitation rate as a proxy for the number of cloud-to-ground (CG) lightning flashes. Consistent results from Tippett et al. (2019) also in the CONUS showed that cool season negative CG flash counts are well correlated with a product of CAPE and precipitation rate. The accuracy of this proxy is seasonally dependent, indicating that the proxy could benefit from utilizing additional parameters (e.g., warm cloud depth) that are not captured by precipitation rate and CAPE (Tippett et al. 2019). CONUS results are not necessarily applicable to Alaska. For example in the eastern CONUS, lifted condensation level (LCL) heights and cloud base heights are

generally lower than in Alaska, and they favor warm rain processes with greater precipitation efficiency (Tippett et al. 2019). In contrast, forecaster experience in Alaska (A. Young, personal communication 2019) suggests that cold rain processes dominate with droplets growing mainly in the ice phase and melting before reaching the surface. This is consistent with Mülmenstädt et al. (2015), who found that ice-phase clouds are more frequent in the Western CONUS, while liquid-phase clouds were more frequent east of the Rockies. Fuchs et al. (2015) also hypothesized that storms with high cloud base heights or shallow warm cloud depths have less warm-phase precipitation and more mixed-phase precipitation and lightning. These differences present a need to investigate lightning predictability in Alaska in relation to parameters differently than in the CONUS.

According to lightning climatologies developed as early as 1976 through satellite observations, most thunderstorm activity takes place in Interior Alaska in June and July (Biswas and Jayaweera 1976; Grice and Comiskey 1976; Reap 1991) and is driven by air-mass and synoptic forcing (Biswas and Jayaweera 1976). Instability is also known to be a potential proxy for lightning activity in Alaska (Sullivan 1963; Reap 1991; Farukh et al. 2011). Figures 2 and 3 show lightning activity in different fire sub-seasons. Lightning density is highest during the middle part of the Alaska fire season, the duff driven sub-season, in the Interior part of the state. Also notable is the fact that lightning density in western Alaska is higher during the early part of the Alaska fire season than during the latter portion of the season, while the opposite is true in eastern Alaska (Figure 2). Figure 3 highlights the seasonal evolution of daily lightning activity over both the 8 year period of study and the longer record from earlier years. Transitions in approximately mid-June and mid-July in both datasets coincide with Alaska fire sub-seasons outlined in Burrows (1987) and discussed further in the next section.

4
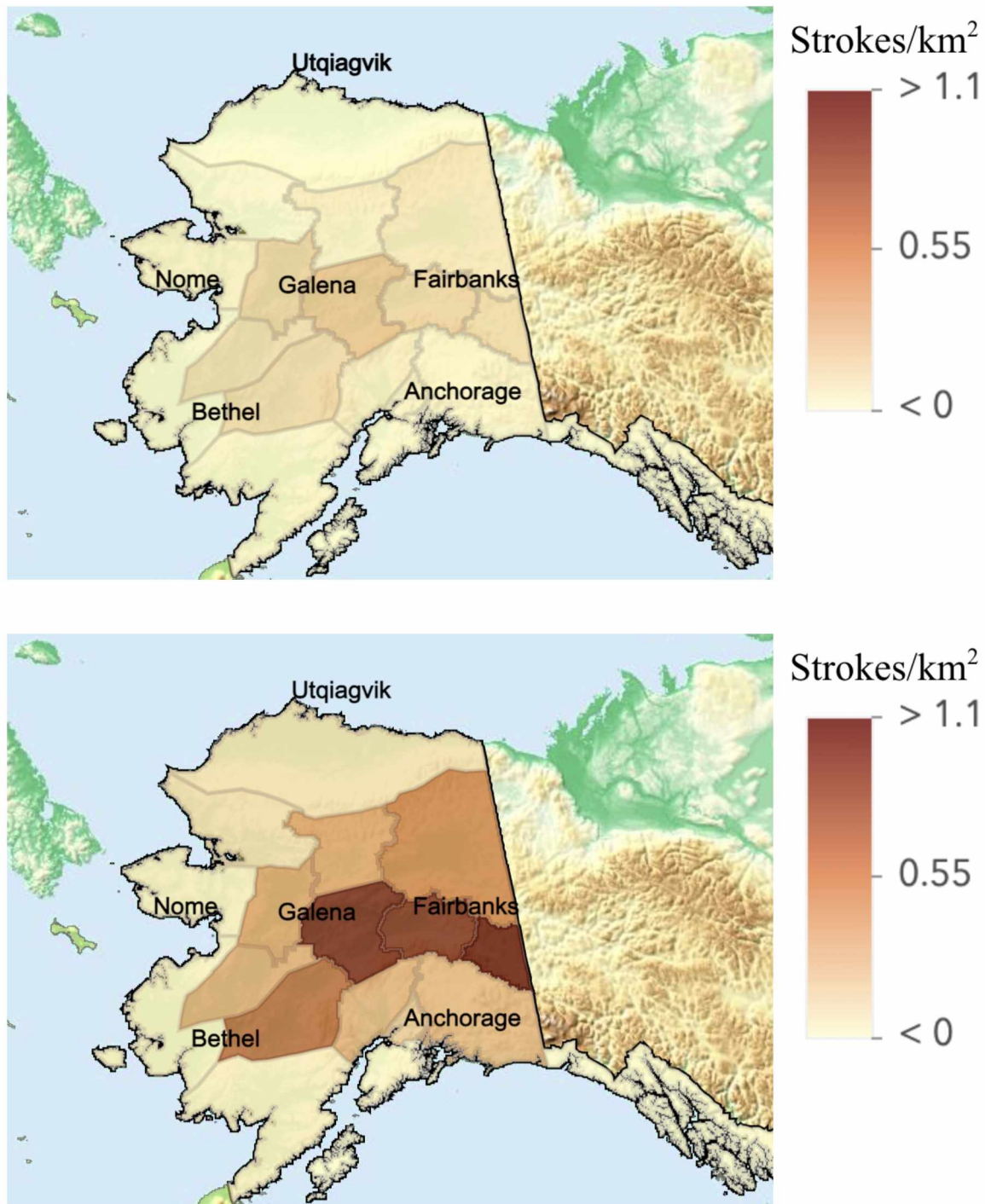
Figure 2: Lightning density (strokes/km2) using Alaska Lightning Detection Network data from 2012–2019 in different Alaska fire sub-seasons outlined in Burrows 1987. Top: Wind driven sub-season (May 1-June 10). Middle: Duff driven sub-season (June 11-July 20). Bottom: Drought driven sub-season (July 21-August 31). Black outlines identify fire management divisions called Predictive Service Areas.
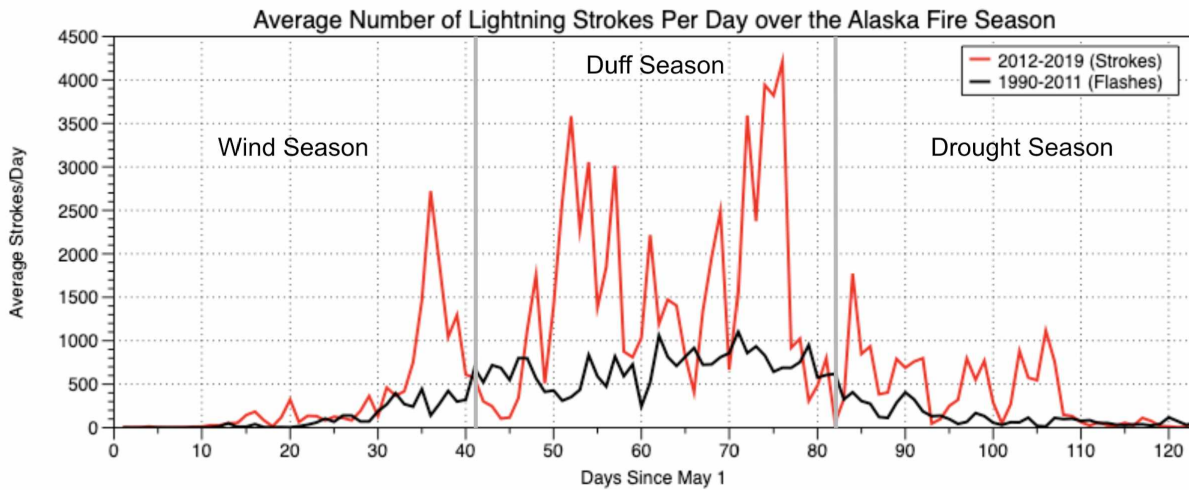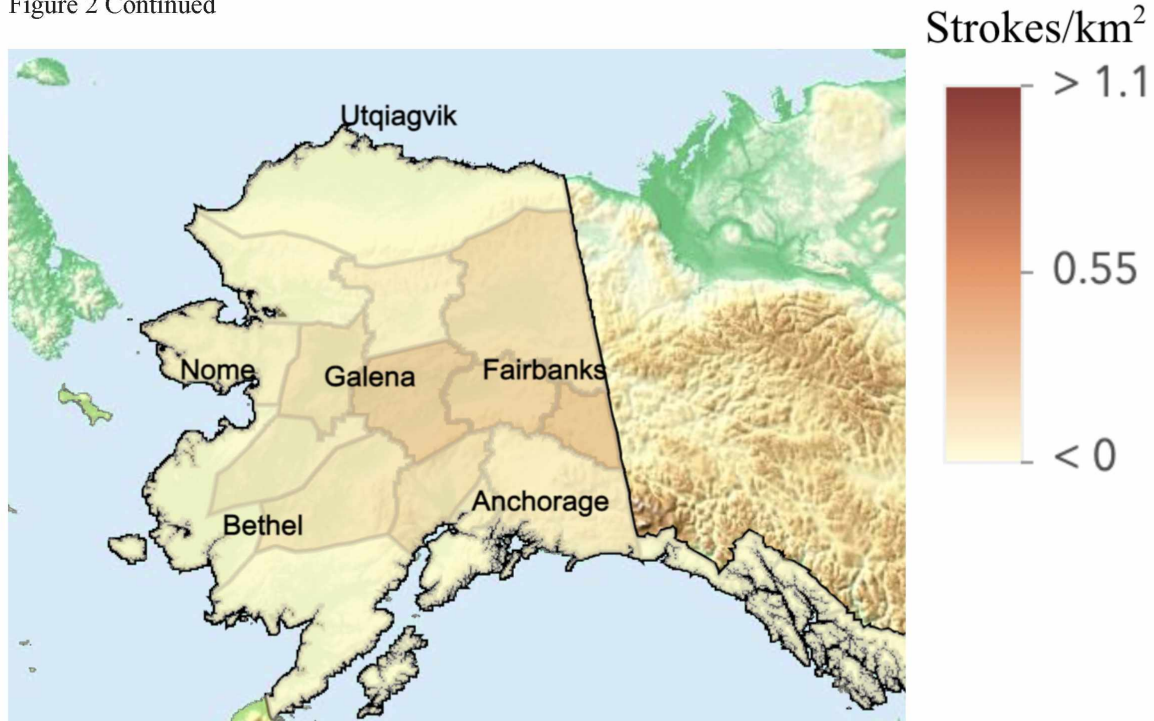
Figure 3: Alaska daily lightning counts. The seasonal cycle of lightning coincides well with Alaska fire sub-seasons outlined in Burrows (1987). 1990–2011 data encompasses lightning in Alaska from ~63–71°N and ~141–161°W, the area in which most lightning occurs. 2012–2019 data encompasses all land area in Alaska.

Statistical approaches (Reap 1991; Duffy et al. 2005; Farukh et al. 2011) and map analyses (Henry 1978) have been used in efforts to better predict lightning and lightning-caused fires. With the knowledge that extreme fire behavior often occurs on a less than monthly timescale (Flannigan and Harrington 1988; Alvarado et al. 1998), the goal of this research is to identify meteorological parameters associated with lightning on a stroke-by-stroke spatial scale at hourly-to-sub-seasonal timescales. This process-level understanding for Alaska will then be combined with seasonal analysis to make progress in developing lightning outlooks on the seasonal time scale. Through this short timescale and more precise spatial scale approach, thresholds in weather parameters for lightning occurrences can be determined on an operationally relevant Bureau of Land Management (BLM) Predictive Service Area (PSA) scale, the same scale used for Alaska Fire Service operational decision making. With the goal to characterize lightning related meteorological variables on the PSA scale, Alaska Interagency Coordination Center's (AICC) historical lightning dataset (Alaska Lightning Detection Network, ALDN) was analyzed with hourly European Center for Medium Range Weather Forecasting (ECMWF) ERA5 ~30 km resolution reanalysis. Meteorological thresholds for lightning in space and time will be applicable to daily lightning forecasting as well as interpretation of seasonal fire weather forecasts. This study is not intended to be an all-inclusive study of fire weather and fire growth in Alaska, since acres burned each year may be influenced by weather conditions after the fire has started (Farukh and Hayasaka 2012), such as what happened in Southcentral Alaska during the summer of 2019 (Bhatt et al. 2021). Weather conditions are only quantified during the hour of the lightning stroke in this study.

2. Data and Methods

2.1 Data

2.1.1 Lightning Data

The network of lightning sensors in Alaska (Figure 4) underwent initial testing in the late 1970s (Krider et al. 1980), but interest in lightning in Alaska by the fire weather community goes back farther. Changes over time to the detection efficiency and range of the Alaska Lightning Detection Network (ALDN) make it challenging to perform a robust trend analysis of lightning flashes or strokes. Positional accuracy of the network was determined to be 2-4 km with a detection efficiency of 40-80% up to 1999 (Dissing and Verbyla 2003). The detection accuracy and efficiency was improved to 0.5-2km and 80-90% from 2000 to 2011 (Farukh and Hayasaka 2012). An overhaul of the detection system was completed in 2012 and has not been studied for positional accuracy or detection efficiency. While not a main goal of this research, these inhomogeneities further motivate the need to investigate proxy data such as convective precipitation from reanalysis on an hourly timescale.

Figure 4: Location of ALDN lighting sensors from 2012-2019. In 2012, sensors in Whitehorse, Yukon and Ross River, Yukon were also part of the network (W. Beach, personal communication 2020)

The Alaska Lightning Detection Network (ALDN) has undergone significant changes since it became operational in 1986, but data since 2012 is fairly homogeneous in regards to the locations of the sensors and sensor configurations. The current network that has been operational since 2012 consists of 13 active Time of Arrival (TOA) sensors (Figure 4). These sensors detect in the Very Low Frequency (VLF, 3 to 30 kHz) to Low Frequency (LF, 30 to 300 kHz) range and have one antenna for satellite GPS locating and one for electromagnetic detection. The old network, called Impact Systems, which was used from 1986–2011 measured flashes with a multiplicity value, where the multiplicity value represents the number of strokes in the flash. The new TOA system records only the stroke data. In theory, stroke output from the TOA system could be post-processed to report flashes with multiplicity like the old system, but that process is not in place yet. There can be anywhere from 1 to 26 strokes per negatively charged flash, with 3

to 5 strokes per flash being the most common. Positively charged flashes typically consist of just 1 stroke, although multiple stroke positive flashes are possible but rare (Rakov 2016). This change in reporting between 2011 and 2012 resulted in an artificial "increase" in lightning records. The Alaska Fire Service reports that approximately 2.25 times as much lightning is being reported with TOA sensors compared to Impact Systems sensors. During 2012, the two networks (old and new) were operated side-by-side for comparison. For the entirety of 2012, 2.07 times as much lightning was reported by the TOA network than the Impact Systems network. However, the average flash multiplicity in that timeframe was only 1.28, thus changes in stroke vs. flash reporting between the two networks do not account for all of this difference. Different coverages, detection properties, and detection efficiencies explain this difference. The period of study in this research was constrained to 2012–2019 because the pre-2012 flash data is inconsistent with the post-2012 stroke data. Processing either the stroke data to make it flash data or turning flash data into stroke data would not be a straightforward process and would potentially add artifacts to the dataset.

  The number of strokes per flash is highly dependent on the time resolution allowed for the system to detect the next stroke. Smaller time resolutions would likely lead to the network detecting even more strokes. For the network to record a stroke, a certain number of sensors must detect the stroke. The default setting from Time of Arrival sensor networks requires 6 sensors to detect a stroke in order for it to be recorded. Currently, the Alaska system is configured to 5 sensors detecting a stroke in order to be recorded. This has been consistent throughout the 2012–2019 time period. Strokes may be counted even if 5 sensors do not detect it simultaneously. If 3 or 4 sensors detect a stroke, this activates the grid cell that the lightning stroke occurred in and the grid cell waits for one additional stroke to be detected. If another stroke occurs in the same

grid cell with 3 or 4 sensors detecting it, both strokes are deemed valid and recorded. Grid cell size was configured to be 2 degrees longitude by 4 degrees latitude in Alaska and has also been consistent throughout the 2012–2019 time period. The large cell size can cause issues, as other strokes may be detected in this grid cell that would validate two or more strokes, but could be from a completely different thunderstorm and not related to the first stroke detected. The more sensors that detect the stroke, the more accurate the location and time of detection. Based on the lightning network history, limiting the period of study in this research to 2012–2019 provides a consistent and high quality sensor record. In addition, focusing on the most recent period allows the findings to be operationally relevant for Alaska Fire Service decision making, since it is based on the current lightning detection network.

2.1.2 Fire Polygons

Acres burned in each PSA annually were calculated in ArcGIS based on Alaska Fire Service fire perimeters. These shapefiles outline human and lightning caused wildland fires and are shown by decade in Figure 1. The perimeters are collected through a variety of methods with varying accuracies from satellite imagery, to the use of GPS, to hand sketches on topographic maps. Prior to 1987, the Alaska Fire Service collected acres burned data based on fires greater than 1000 acres. From 1987 to 2015, this criteria was lowered to 100 acres and lowered again from 2016 to the present to 10 acres or larger. These changes to fire perimeter size thresholds in data collection and reporting by the Alaska Fire Service have resulted in 0.96% more acres burned being reported post 1987 than would have been reported pre–1987. The database includes information on the date and method of collection of the fire perimeters. Acres burned is a common indicator of fire season activity in Alaska (AICC 2020).

2.1.3 Predictive Service Areas

The impacts of wildfire and the required fire management response varies considerably across the Alaskan landscape so the state is subdivided into so-called Predictive Service Areas (PSAs) for this purpose. In 2001, Alaska established 21 PSAs based on climate, ecology, management responsibility, and fire history information (Figure 5). The Alaska Interagency Coordination Center's Predictive Services unit uses these spatial divisions to update 7-day fire potential outlooks throughout the fire season so all analysis in this study was conducted at the scale of these PSAs. Table 1 provides general information on these 21 PSAs including size, fire activity, latitude, and notable population centers. Table 1 also defines the group that each PSA was placed in for analysis based on its geographic location relative to the coast. The three groups are Interior, Semi-Interior, and Coastal. The North Slope was analyzed in a category of its own based on its unique climate.

Figure 5: Alaska Fire Service Predictive Service Areas shown with Alaska topography.

Table 1: Predictive Service Area characteristics. Population data from U.S. Census Bureau.

PSA Name	Largest Community (Population)	Latitude Range	Area (km^2)	Fire Density 1940-2020 (total acres burned per km^2)	PSA Group
North Slope	Utqiagvik (4,383)	67.8°–71.3°N	205,764.59	2.05	North Slope
Upper Yukon	Fort Yukon (561)	64.0°–68.9°N	153,903.25	125.14	Interior
Bristol Bay & Alaska Peninsula	Dillingham (2,215)	56.2°–61.0°N	130,437.55	3.15	Coastal
Copper River Basin	Valdez (3,847)	59.8°–63.6°N	107,862.46	2.13	Semi-Interior
Yukon-Kuskokwim (Y-K) Delta	Bethel (6,472)	59.2°–64.2°N	89,886.04	7.48	Coastal
Kuskokwim Valley	McGrath (304)	60.3°–63.7°N	87,941.44	67.72	Semi-Interior
Koyukuk & Upper Kobuk Valley	Kotzebue (3,287)	66.2°–68.9°N	82,426.12	34.27	Coastal
Tanana Zone (South)	Denali Park (872)	62.8°–65.9°N	74,006.09	149.64	Interior
Seward Peninsula	Nome (3,850)	64.1°–66.6°N	70,894.35	33.85	Coastal
Tanana Zone (North)	Allakaket (213)	65.5°–68.1°N	64,755.35	75.48	Interior
Lower Yukon	Marshall (261)	61.2°–64.0°N	60,085.79	103.45	Semi-Interior
Middle Yukon	Galena (495)	63.3°–66.7°N	54,691.69	120.03	Semi-Interior
Tanana Valley West	Fairbanks (31,551)	63.2°–65.4°N	52,706.49	120.82	Interior
Susitna Valley	Willow (1,987)	60.4°–63.5°N	50,451.44	0.66	Semi-Interior
Southern Panhandle	Ketchikan (8,228)	54.6°–57.2°N	35,701.39	0.003	Coastal
Tanana Valley East	Tok (1,289)	62.0°–64.5°N	32,842.4	61.10	Interior
Northern Panhandle	Haines (1,863)	58.2°–60.3°N	29,066.37	0.01	Coastal
Kenai Peninsula	Kenai (7,742)	59.1°–61.1°N	27,488.99	34.95	Coastal
Central Panhandle	Juneau (32,227)	56.2°–59.0°N	24,806.3	0.01	Coastal
Kodiak Island	Kodiak (6,022)	56.4°–58.6°N	12,491.53	4.99	Coastal
Matanuska Valley & Anchorage	Anchorage (293,531)	61.0°–62.5°N	12,460.45	6.56	Coastal

2.1.4 ERA5

The ECMWF has produced the newly available ERA5 reanalysis which performs well in the Arctic (Graham et al. 2019) with fewer heterogeneities than station data for precipitation in Alaska (White et al. 2020). ERA5 has ~30 km resolution with 137 vertical levels that span from the surface to 80 km and is available at an hourly resolution, making it appropriate to represent meteorological variables in this study. The hourly meteorological data were extracted and matched to lightning strokes at the nearest hour (e.g., 14:31 rounds to 15:00) and nearest grid point for all of the strokes in the study. The variables investigated were 2-meter temperature, 2-meter dew point temperature, convective available potential energy (CAPE), convective precipitation, relative humidity (calculated from temperature and dew point), 500 hPa geopotential heights, freezing level, warm cloud depth (calculated from freezing level and cloud base height), K-Index, 850 hPa temperature, and 700 and 500 hPa wind/flow direction. See Table 3 for additional details.

2.2 Methods

2.2.1 Alaska Fire Sub-Seasons

The Alaska fire season has four distinct sub-seasons during the summer which were originally delineated by Burrows et al. (1987). The dates of these sub-seasons are approximate and dependent on weather patterns that differ from year-to-year. The exact dates chosen in this study are those suggested by the Alaska Fire Service and reflect the seasonal cycle of lightning in Alaska. The *wind driven* sub-season, spanning from May 1 through June 10, begins with the timing of snow melt, is generally a period with low rainfall in Interior Alaska, and is when wind drives most fire growth. The *duff driven* sub-season begins around June 11 and runs through July

20, when longer days around the summer solstice produce heating of spruce canopies and drying of the surface and near surface fuels. The *duff driven* sub-season is considered the peak of the fire season and is when the most lightning occurs (Table 2). The sub-season from July 21 through August 31 will be referred to in this study as the *drought driven* sub-season, and combines the drought and diurnal driven sub-seasons of Burrows (1987). During the *drought driven* sub-season, fire activity is tied to the arrival or delay of the summer rains. If significant rains do not occur, the deeper layers of fuels continue to dry and fire can become difficult to suppress. Fires can easily become active again even after moderate precipitation, as boreal duff fuels can dry in a matter of days (~15). As the season comes to an end, fire spread becomes more limited due to shorter days and longer periods of nighttime radiational cooling. However, high levels of drought can allow fires to continue to spread despite unfavorable weather conditions (Burrows et al. 1987).

Table 2: Lightning strokes by PSA group by Alaska fire sub-season.

	Area (km^2)	Strokes in the Wind Driven Sub-Season	Strokes in the Duff Driven Sub-Season	Strokes in the Drought Driven Sub-Season
Interior	378,213.58	55,546	282,016	69,577
Semi-Interior	273,091.38	42,719	162,848	39,367
Coastal	405,173.47	12,957	34,797	13,836
North Slope	205,764.59	1,358	26,963	4,124

2.2.2 Data Pairing and Database Preparation

Lightning data from the AICC were paired with hourly ECMWF ERA5 reanalysis to develop an understanding of the relationships associated with weather conditions at the time of

each lightning stroke. The lightning strokes were analyzed within the AICC PSAs from 2012–2019 during the Alaska fire sub-seasons. TOA sensors report and specify a limited number of cloud-to-cloud strokes (or intercloud, IC strokes) in addition to CG strokes. For all analysis in this study, IC strokes were removed from the dataset, given that they do not have the potential to ignite a fire. Additionally, positively charged strokes with an amplitude of less than 10 kA were also eliminated, since the vast majority of these strokes are likely cloud strokes regardless of classification (Cummins et al. 1998; Biagi et al. 2007). This amounted to the elimination of 14,332 strokes from the dataset. While this process may have eliminated some CG strokes, a maximum of 7% of positive strokes less than 10 kA are believed to be CG strokes (Biagi et al. 2007). After these strokes were eliminated, 746,817 CG strokes were left for the analysis.

A database was developed through the data pairing process that could then be queried for the analysis. Each record within the database contains a single lightning stroke with information on the properties of the lightning stroke in addition to the ERA5 weather parameters paired to the stroke based on the grid point values at the time and place of the lightning stroke. A complete list of parameters in the database is available in Table 3.

Geodatabase (e.g., gdb file type) files of lightning activity from 2012–2019 were acquired from the AICC and added to an ArcGIS workspace as point data. All points (strokes) not over land area covered by Alaska PSAs were clipped out, as well as strokes meeting the various criteria for elimination outlined above. Files were converted from geodatabases to comma separated values (.csv) files and read into an NCAR Computing Language (NCL) script. This NCL script also read in ERA5 reanalysis data and determined the meteorological parameters at the time and place of each lightning stroke in the file. To manage such a large dataset, both lightning and ERA5 data were split up by year for computational efficiency to

avoid memory issues in dealing with all 746,817 strokes at once. Once these meteorological

parameters were assigned to the strokes, these data were divided into various other categories

including by PSA, by fire sub-season, and by month. Analysis was conducted on the data by fire

sub-season and by PSA.

Table 3: Weather and lightning variables investigated together from the Alaska Lightning Detection Network and ECMWF ERA5 Reanalysis.

Lightning	Surface	Thermodynamic	Middle & Upper Levels
Location (lat, lon, PSA)	2 m Temperature	CAPE	500 hPa Height
Hour of Day	2 m Dew Point	K-Index	850 hPa Temperature
Fire Season	Relative Humidity	Freezing Level	500 hPa Wind Direction
Polarity	Convective Precipitation	Cloud Base Height	700 hPa Wind Direction
		Warm Cloud Depth	

2.2.3 Statistics

This study used standard statistical measures of mean, median, and standard deviation in

quantifying the relationships between lightning and the meteorological variables. Statistics were

calculated using both computer programs and DataGraph, a plotting and analysis program.

19

3. Results

3.1 Timing of Lightning

3.1.1 Seasonal Timing of Lightning by PSA

The occurrence of lightning has a distinct spatial and temporal signal (Figure 6) where the majority of the lightning occurs in the duff driven sub-season across all PSAs but there are large differences across PSAs during the wind and drought driven seasons. The majority of lightning also occurs in Interior Alaska, while the lowest lightning counts are in Coastal PSAs consistent with the spatial view in Figure 2. Perhaps the most striking difference is that the Seward Peninsula experiences 36% of its lightning in the drought driven sub-season, while no other PSA experiences more than 26% (Figure 6). Lightning distributions range from the North Slope which experiences 4% of its lightning in the wind driven sub-season, 83% in the duff driven sub-season, and 13% in the drought driven sub-season to the Seward Peninsula with 27%, 37%, and 36% in wind, duff and drought driven sub-seasons, respectively. PSAs that experience more lightning in the wind driven season than the drought driven season are Bristol Bay and the Alaska Peninsula, the Kenai Peninsula, the Kuskokwim Valley, the Lower and Middle Yukon, and the Tanana Zone South. The remaining PSAs experience more lightning in the drought driven sub-season than in the wind driven sub-season. A distinct regional preference emerges in this comparison. PSAs that have more lightning in the wind driven sub-season than the drought driven sub-season are in the southwest portion of Alaska, while the PSAs that are more drought driven sub-season dominant for lightning are further north and east.
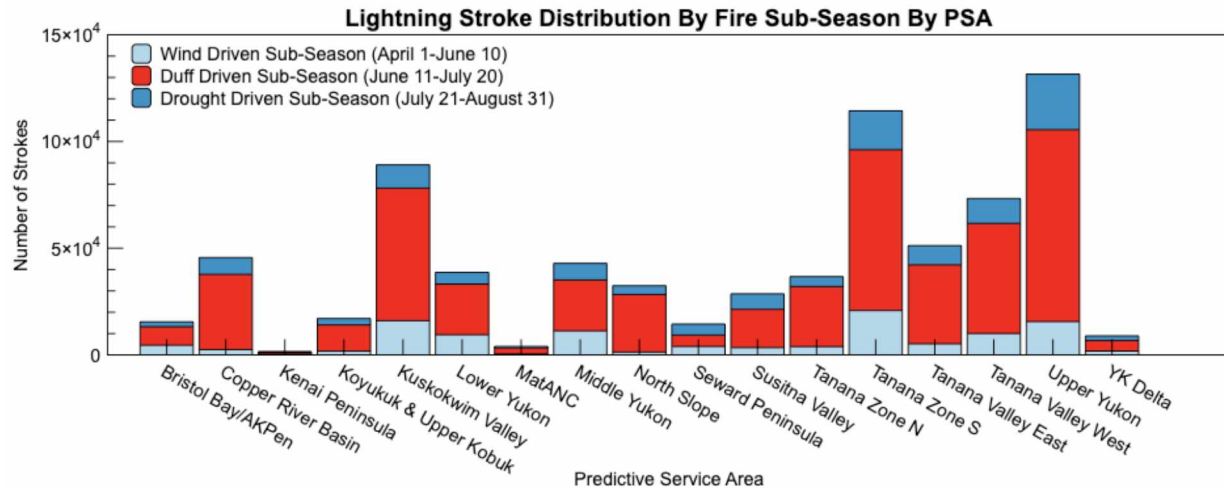
Figure 6: Lightning stroke distribution by fire season by PSA. Data covers the period from 2012–2019.

3.1.2 Diurnal Timing of Lightning by PSA

Afternoon lightning is dominant throughout both the Interior and Coastal PSAs with comparatively low amounts of lightning occurring in the overnight and early morning hours (Figure 7). It is important to note from these plots that lightning starts earlier farther east due to earlier sunrises initiating solar driven convection at an earlier hour of the day. The region of study, while large, is in a single time zone. This feature is well defined for Interior PSAs, which also have a more limited range of latitude from approximately 60.4–69°N. There is more variability in the Coastal PSAs, however the feature remains present across the wide range of latitudes from 56.5 to 71.2°N. Southeast Alaska (Northern, Central, and Southern Panhandle PSAs) and the Kodiak Island PSA were excluded due to little relevance for fire weather. The pre-2012 ALDN Impact Systems data were used to create Figures 7 and 8 in order to capture the largest sample size possible while maintaining consistent data.
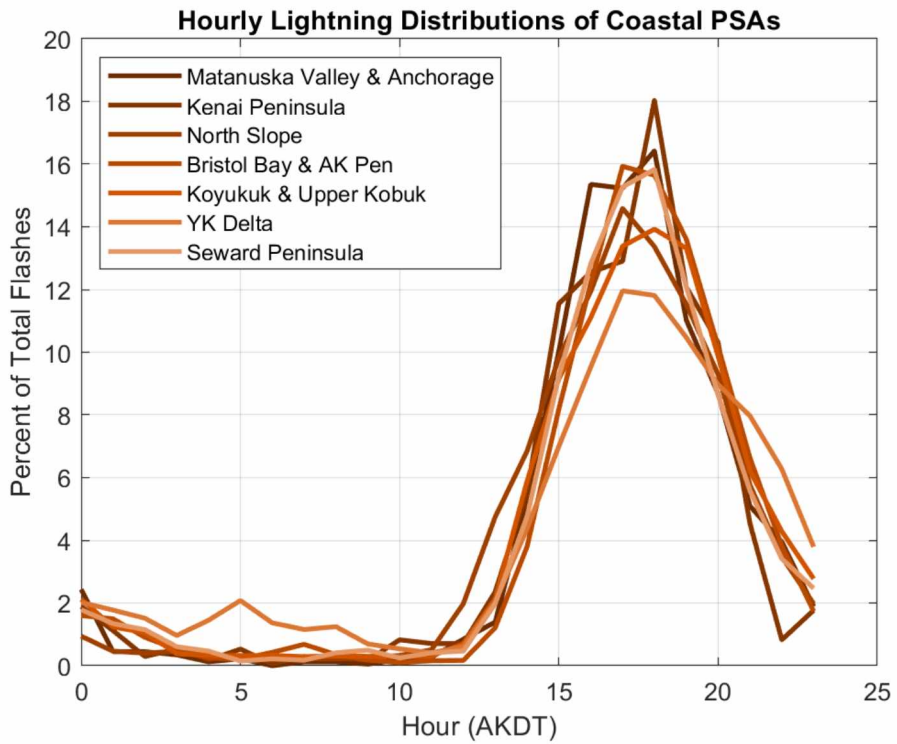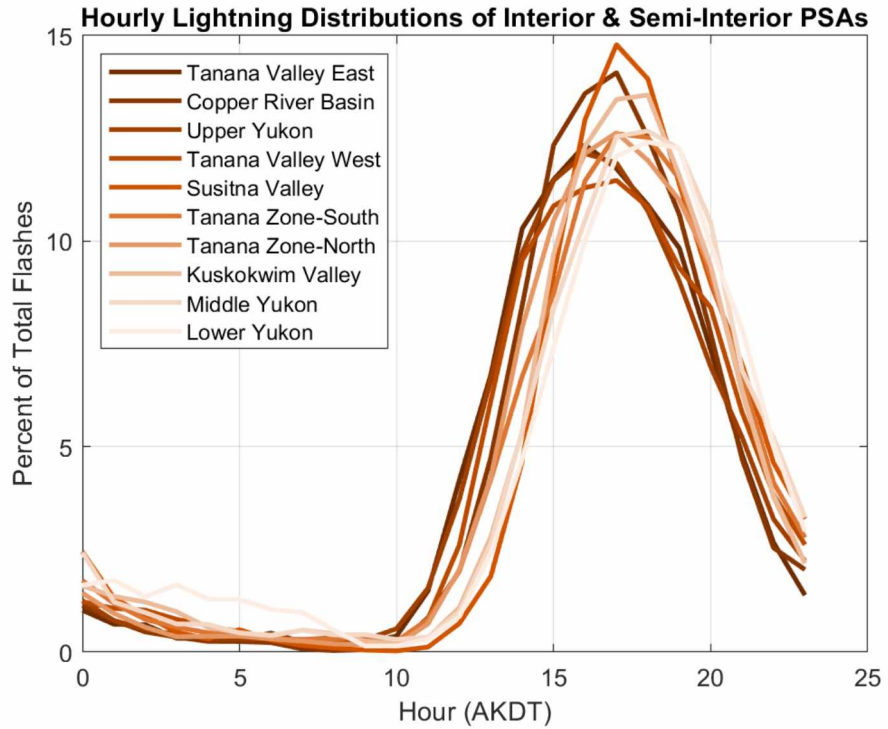
Figure 7: Hourly lightning distribution of Interior and Semi-Interior (top) and Coastal (bottom) PSAs. Colors are organized with the darkest lines representing PSAs further east and the lighter colored lines representing PSAs further west. Data used in figure 7 is the dataset from 1986-2011.

Nocturnal lightning is rare in Alaska, with summertime strokes between midnight and 5AM accounting for just 4.53% of total summer lightning strokes from 1986-2012. While the amount of lightning occurring at night is low, locations that experience a higher percentage of their total lightning at night are generally closer to the coast, with a few exception areas in the Interior (Figure 8). A possible explanation for elevated coastal nocturnal lightning is the dependence these areas have on an upper level feature such as a vorticity maximum to drive the lightning, while solar driven air-mass convection dominates the Interior. The local maximums in the Interior are intriguing and worthy of further research which is beyond the scope of this study.

Positively charged lightning strokes have a greater potential to ignite a wildfire because they have overall higher energy levels than negatively charged strokes. Since polarity data became available in 2012, 20.5% of nocturnal lightning in Alaska was positively charged, compared to 18.1% of overall lightning. Differences in multiplicity of nocturnal versus daytime and evening flashes from 1986-2012 were not observed, with the average overall multiplicity of lightning being 1.56 with a standard deviation of 1.17, while nocturnal flashes had an average multiplicity of 1.59 with a standard deviation of 1.18.

Percentage of Fire Season Lightning Occurring Between Midnight and 5AM
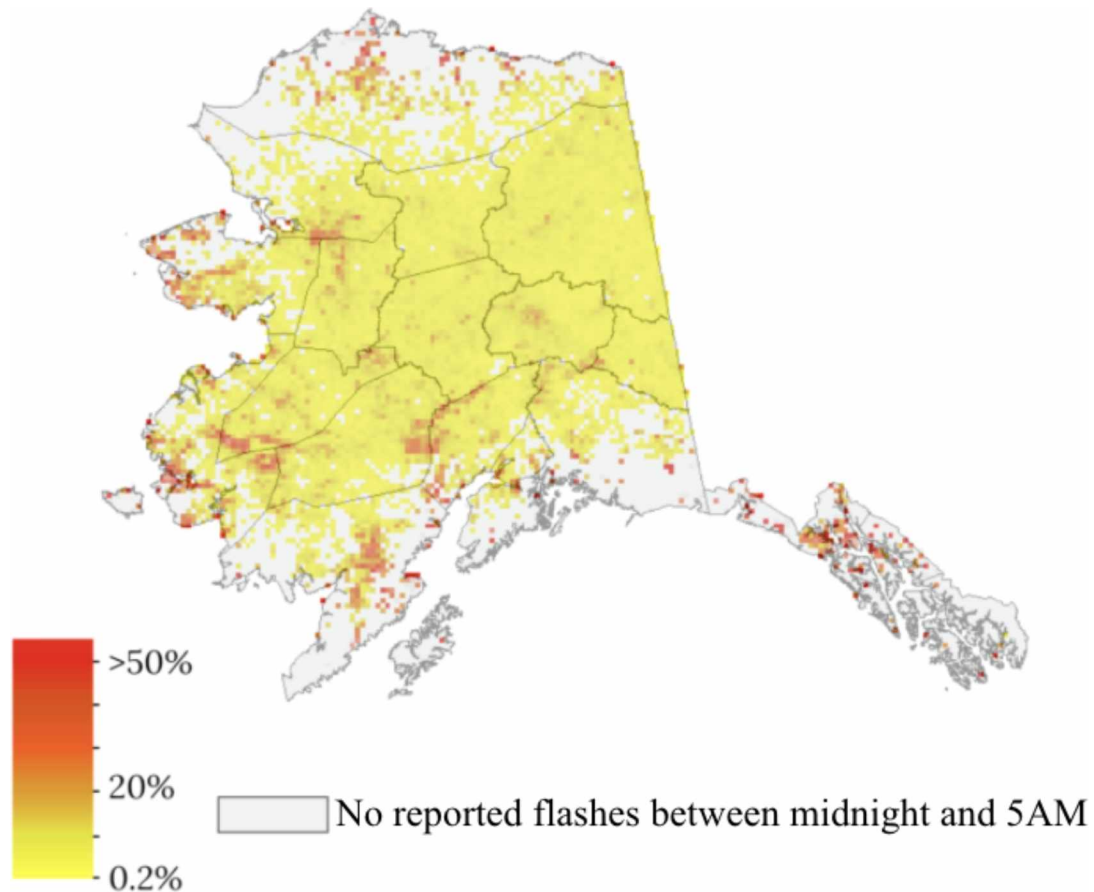
Figure 8: Percentage of total lightning occurring between midnight and 5AM for the 1986-2012 time period. Source: Alaska Interagency Coordination Center

3.2 Meteorological Variables Associated with Lightning

This section summarizes values of meteorological variables that coincide with lightning strokes over the sub-season for each PSA. These variables are chosen based on past knowledge of the parameters that are monitored operationally because they are critical to lightning activity (A. Young, personal communication 2019). These lightning proxies were analyzed at the scale of

each PSA during the 3 Alaska fire sub-seasons (wind driven, duff driven, and drought driven). The parameters in this analysis include air temperature, convective precipitation, and dew point temperature. This subset of parameters was chosen since air temperature has some skill in seasonal forecasts, convective precipitation was shown to be correlated with lightning (Bieniek et al. 2019), and dew point temperature is a simple measure of moisture at the surface. PSAs were organized into 4 geographical divisions. The Interior PSAs are characterized by their continental climates and inland location. The Semi-Interior PSAs are characterized by their closer location to the coast than Interior PSAs, and some may border the coast, though the majority of their area encompasses Interior locations. The Coastal PSAs are characterized by their strong maritime influence throughout much of the summer due to their location along the coast. The North Slope PSA was analyzed independently due to its large geographical area and unique Arctic climate. Table 4 provides a comparison of 2012-2019 average parameter values over the entire sub-season, henceforth referred to as 'climatological' as well as parameter averages during lightning strokes. Table 4 serves as a reference in the discussion of the box and whisker charts presented next.

Table 4: Mean values of 2-meter air temperature, 2-meter dew point temperature, and convective precipitation during lightning strokes as compared to mean values for all hours during the 2012-2019 period (shown in parentheses) over the same sub-season and area.

Wind Driven Sub-Season (May 1–June 10)				
	Interior PSAs	Semi-Interior PSAs	Coastal PSAs	North Slope
2m air temperature (°C)	16.2 (7.6)	16.5 (6.5)	16.3 (5.6)	13.4 (0.03)
2m Dew Point Temperature (°C)	7.4 (-0.2)	8.6 (0.6)	9.3 (1.2)	5.8 (-2.9)
Convective Precipitation (mm/hr)	0.386 (0.0032)	0.412 (0.0035)	0.554 (0.0026)	0.344 (0.001)
Duff Driven Sub-Season (June 11–July 20)				
	Interior PSAs	Semi-Interior PSAs	Coastal PSAs	North Slope
2m air temperature (°C)	19.2 (14.6)	17.9 (12.4)	18.0 (12.2)	15.8 (10.3)
2m Dew Point Temperature (°C)	11.2 (7.2)	11.9 (7.2)	11.4 (7.7)	10.1 (5.8)
Convective Precipitation (mm/hr)	0.366 (0.006)	0.454 (0.0054)	0.477 (0.0036)	0.423 (0.0036)
Drought Driven Sub-Season (July 21–August 31)				
	Interior PSAs	Semi-Interior PSAs	Coastal PSAs	North Slope
2m air temperature (°C)	17.9 (11.8)	17.7 (11.1)	18.0 (11.5)	14.2 (7.5)
2m Dew Point Temperature (°C)	11.5 (6.9)	12.0 (7.5)	12.7 (8.4)	11.4 (4.5)
Convective Precipitation (mm/hr)	0.361 (0.0044)	0.475 (0.0049)	0.431 (0.0041)	0.329 (0.0025)

3.2.1: The Wind Driven Sub-Season (May 1–June 10)

During the wind driven sub-season, climatological 2-meter air temperatures are highest in the Interior PSAs, followed by the Semi-Interior PSAs, the Coastal PSAs, and finally the North Slope PSA. However, differences in mean lightning-associated temperatures between the geographical divisions are minimal with the exception of the North Slope PSA. All mean temperatures during lightning strokes are much higher, 9°C or greater, than climatological values (Table 4). This is not unexpected, since lightning occurs during the warmer part of the day, as shown in Figure 7. The wind driven sub-season has much colder temperatures during lightning strokes in the Susitna Valley and Copper River Basin PSAs than other Semi-Interior PSAs (Figure 9, top). These PSAs contain the highest terrain in Alaska. The Tanana Valley East PSA was among the colder lightning PSAs as well, understandably so since it contains the Fortymile Uplands, which develop strong valley inversions well into the spring while the higher terrain heats up and allows for instability adequate for thunderstorm development to be diurnally induced above the inversion layer. Coastal PSAs exhibited the most variability in temperatures during lightning strokes, while Interior PSAs were the most uniform (Figure 9, top). Interestingly, the North Slope was most similar to the Copper River Basin in terms of temperatures, likely for entirely different reasons (Arctic climate vs. high terrain).

Climatological 2-meter dew point temperatures are highest in the Coastal PSAs, followed by the Semi-Interior PSAs, Interior PSAs, and finally the North Slope PSA (Table 4). Coincident with lightning strokes, this same order applies, though values are markedly above climatology. Dew point temperatures are higher during lightning strokes, indicating that more moisture is present near the surface compared to climatology. While lightning associated 2-meter temperatures was very similar across the geographical divisions, dew point temperatures varied

across the divisions. Dew point temperatures in the Copper River Basin PSA are the lowest of all

PSAs and most similar to the North Slope PSA, consistent with 2-meter temperatures (Figure 9,

middle). The Tanana Valley East PSA had the lowest dew point temperatures coincident with

lightning of the Interior PSAs. The highest dew point temperatures coincident with lightning

occur in Western Alaska, with the Seward Peninsula, Y-K Delta, and Lower and Middle Yukon

PSAs having the most surface moisture during lightning strokes.

During the wind driven sub-season, climatological convective precipitation is highest in

the Interior and Semi-Interior PSAs followed by the Coastal PSAs and lowest in the North Slope

PSA (Table 4). During lightning strokes, convective precipitation is above climatology for all

geographical divisions and largest in the Coastal PSAs followed by Semi-Interior and Interior

PSAs. The North Slope has the least convective precipitation coincident with lightning (Figure 9

bottom). The Seward Peninsula PSA was the wettest PSA in terms of convective precipitation

during lightning strokes in the wind driven sub-season, while the neighboring Koyukuk and

Upper Kobuk PSA was the driest (Figure 9, bottom). The range of the upper quartile of

convective precipitation during lightning strokes decreases from the Coastal to the Semi-Interior

and to the Interiors PSAs.

During the wind driven sub-season, PSAs with colder air temperatures during lightning

strokes generally had lower dew point temperatures as well. While the Middle Yukon PSA was

the warmest PSA and had relatively high dew point temperatures coincident with lightning,

convective precipitation during lightning strokes was very low. It is important to note that the

median convective precipitation (0.07 mm/hr) during lightning strokes is much lower than the

mean (0.37 mm/hr) in the Middle Yukon PSA. This indicates that in ERA5, lightning was often

coincident without any convective precipitation. A similar conclusion can be drawn for the

Koyukuk and Upper Kobuk PSA. Further investigation into the accuracy of ERA5 convective

precipitation during lightning strokes that are assigned as dry may be needed to validate this

result.

Air Temperature During Lightning Strokes in the Wind Driven Sub-Season

Interior PSA   Semi-Interior PSA   Coastal PSA

Predictive Service Area (y-axis):
- Upper Yukon
- Tanana Valley West
- Tanana Valley East
- Tanana Zone South
- Tanana Zone North
- North Slope
- Kuskokwim Valley
- Susitna Valley
- Middle Yukon
- Lower Yukon
- Copper River Basin
- Y-K Delta
- MatANC
- Seward Peninsula
- Koyukuk & Upper Kobuk
- Kenai Peninsula
- Bristol Bay & AK Peninsula

Air Temperature (°C)

Convective Precipitation During Lightning Strokes in the Wind Season

Interior PSA   Semi-Interior PSA   Coastal PSA

Predictive Service Area (y-axis):
- Upper Yukon
- Tanana Valley West
- Tanana Valley East
- Tanana Zone South
- Tanana Zone North
- North Slope
- Kuskokwim Valley
- Susitna Valley
- Middle Yukon
- Lower Yukon
- Copper River Basin
- Y-K Delta
- MatANC
- Seward Peninsula
- Koyukuk & Upper Kobuk
- Kenai Peninsula
- Bristol Bay & AK Peninsula

Hourly Accumulated Convective Precipitation (mm)

Figure 9: The 2-meter air temperature (top), convective precipitation (middle), 2-meter dew point temperature (bottom) during lightning events in the wind driven sub-season across different PSAs.

31

Dew Point Temperatures During Lightning Strokes in the Wind Season
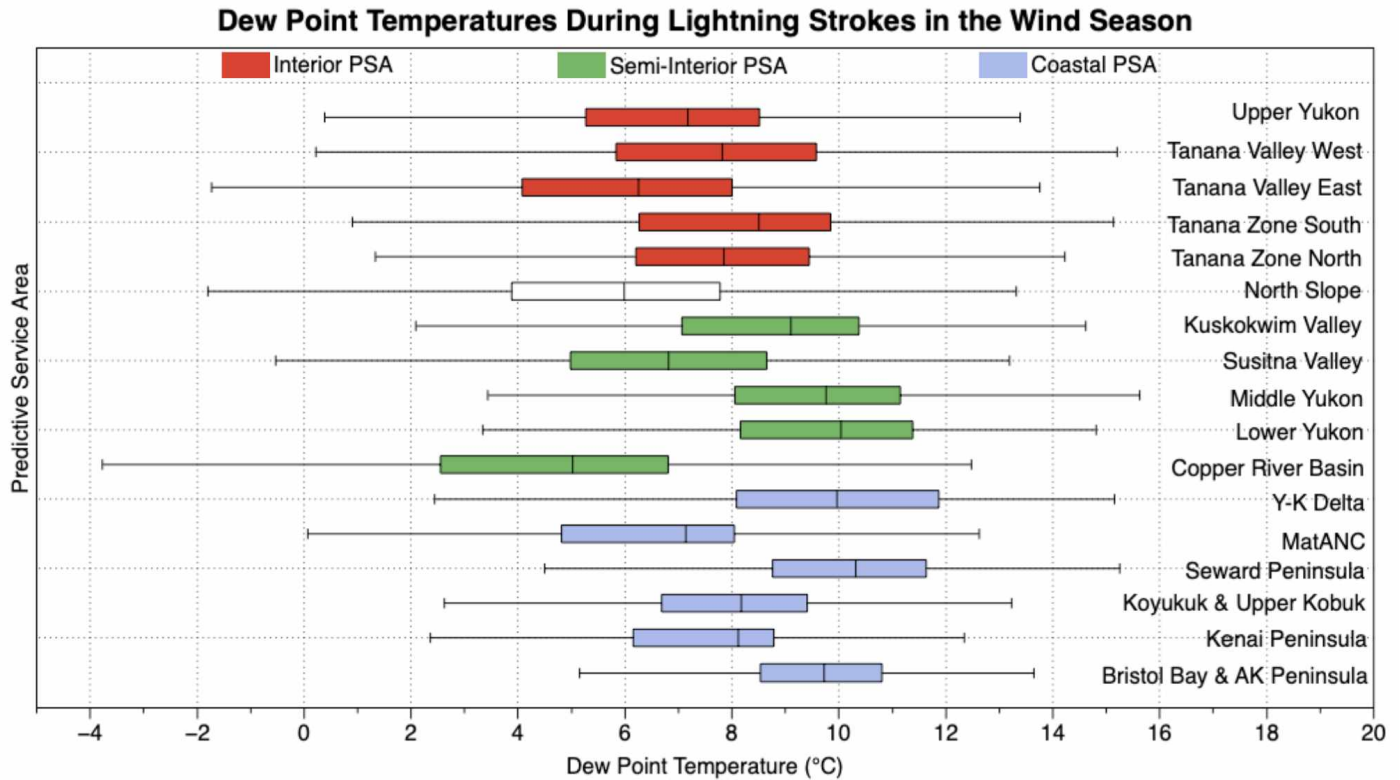
3.2.2: The Duff Driven Sub-Season (June 11–July 20)

The duff driven sub-season (June 11 through July 20) is the season with the most lightning activity and the most fire ignitions (H. Strader, personal communication 2020), making this the critical period to understand when producing a seasonal fire weather forecast. Climatologically, temperatures during the duff driven sub-season show a similar pattern to those during the wind driven season, where Interior PSAs are the warmest, followed by Semi-Interior PSAs, Coastal PSAs, and then the North Slope (Table 4). Temperatures during lightning strokes were also highest in the Interior PSAs, but were slightly lower in the Semi-Interior and Coastal PSAs. The North Slope PSA again exhibited the coldest temperatures during lightning strokes. Temperatures during lightning are on average around 5 °C warmer than climatology during the duff driven sub-season, though they are around 10 °C warmer than climatology during the wind

driven sub-season. Temperatures during lightning strokes were the coolest in the North Slope, Matanuska Valley and Anchorage and Kenai Peninsula PSAs. Temperatures during lightning strokes are warmest in the southern and western Interior PSAs (Figure 10, top).

Dew point temperatures during the duff driven sub-season across geographical divisions are very similar both climatologically and during lightning strokes with the exception of the North Slope PSA which had lower dew point temperatures for both (Table 4). However, during lightning strokes, dew point temperatures are approximately 4 °C higher than climatology. Between Interior, Semi-Interior, and Coastal PSAs, dew point temperatures during lightning strokes were the most uniform of all sub-seasons (Figure 10, middle). The Matanuska Valley and Anchorage PSA is the only PSA that experiences much lower dew point temperatures during lightning strokes than the rest (Figure 10, middle).

Climatologically, the Interior PSAs receive the most convective precipitation followed by the Semi-Interior PSAs, with the Coastal and North Slope PSAs receiving equally the least during the duff driven sub-season (Table 4). During lightning strokes Coastal PSAs have the highest amount of convective precipitation, followed by Semi-Interior, North Slope, and finally Interior PSAs (Table 4). The Semi-Interior, Interior, and North Slope PSAs have a lower range of convective precipitation during lightning strokes than the Coastal PSAs (Figure 10, bottom). The Semi-Interior PSA of Kuskokwim Valley is an exception to this feature with the second largest range among all PSAs. Similar to during the wind driven sub-season, the Middle Yukon PSA has a mean lightning associated convective precipitation of 0.41 mm/hour, but a corresponding median of 0.03 mm/hour, again suggesting a potentially elevated occurrence rate of dry lightning.

While the Tanana Zone South showed some of the highest temperatures and dew points during lightning strokes, it was not among the wettest PSAs in terms of convective precipitation during lightning strokes. Coastal and Western Interior PSAs experience more convective precipitation during lightning events than eastern Interior PSAs do during the duff driven sub-season.
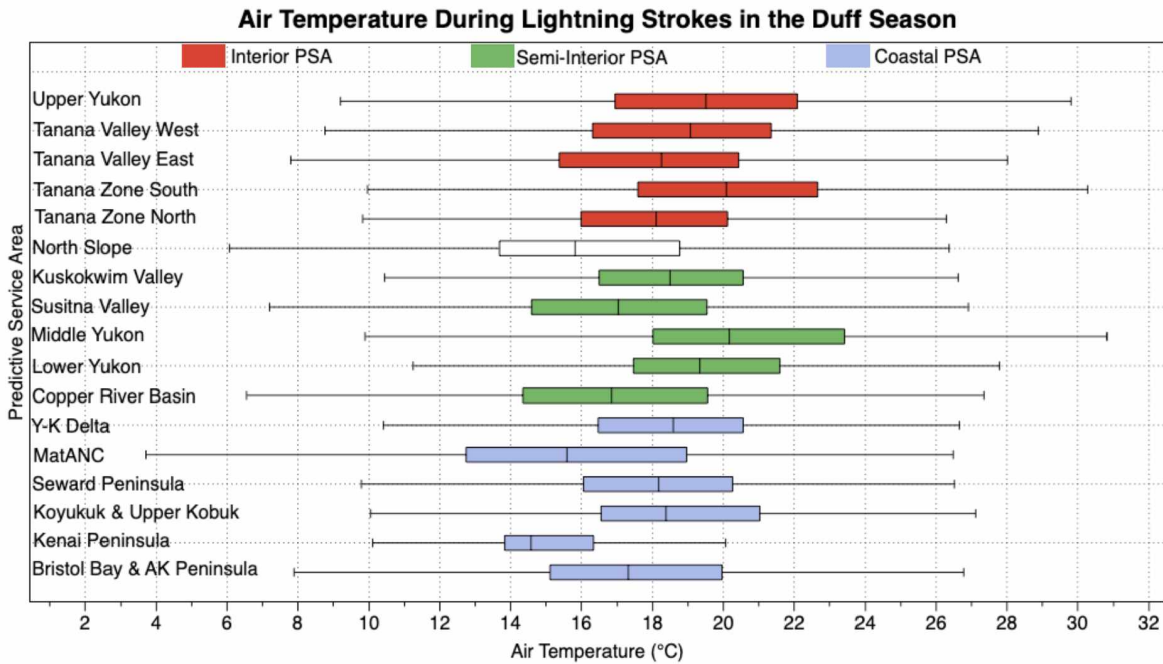
Figure 10: The 2-meter air temperature (top), convective precipitation (middle), 2-meter dew point temperature (bottom) during lightning strokes in the duff driven sub-season across different PSAs.

Figure 10 Continued

Convective Precipitation During Lightning Strokes in the Duff Season

Dew Point Temperature During Lightning Strokes in the Duff Season
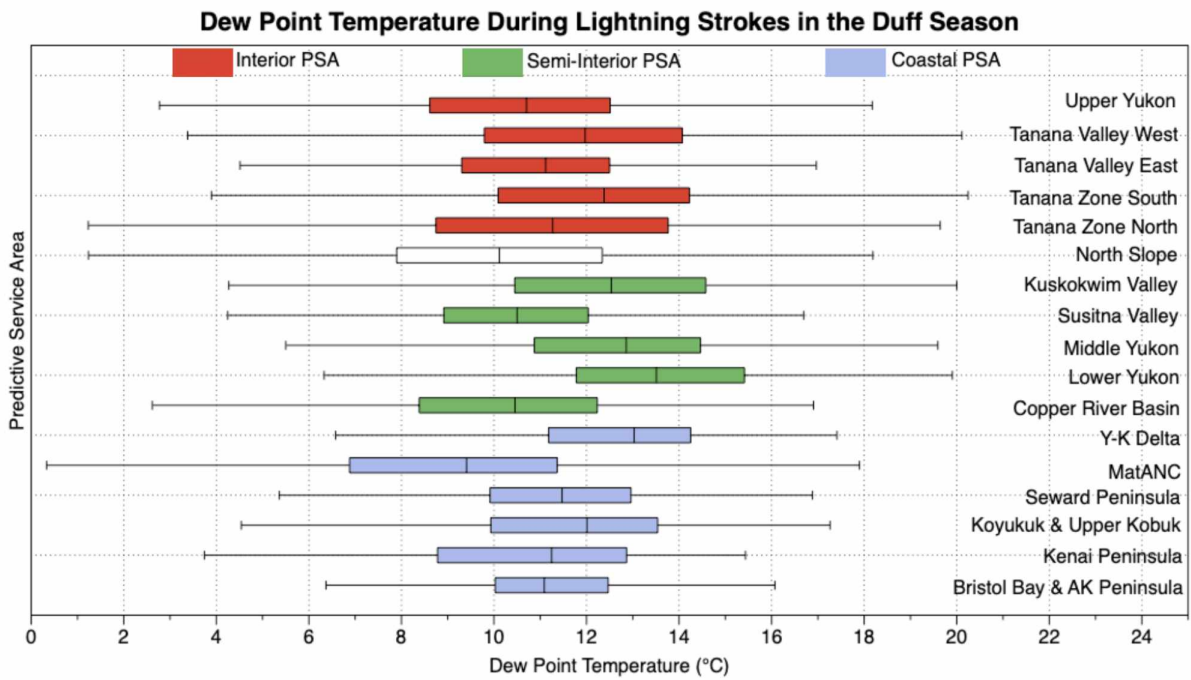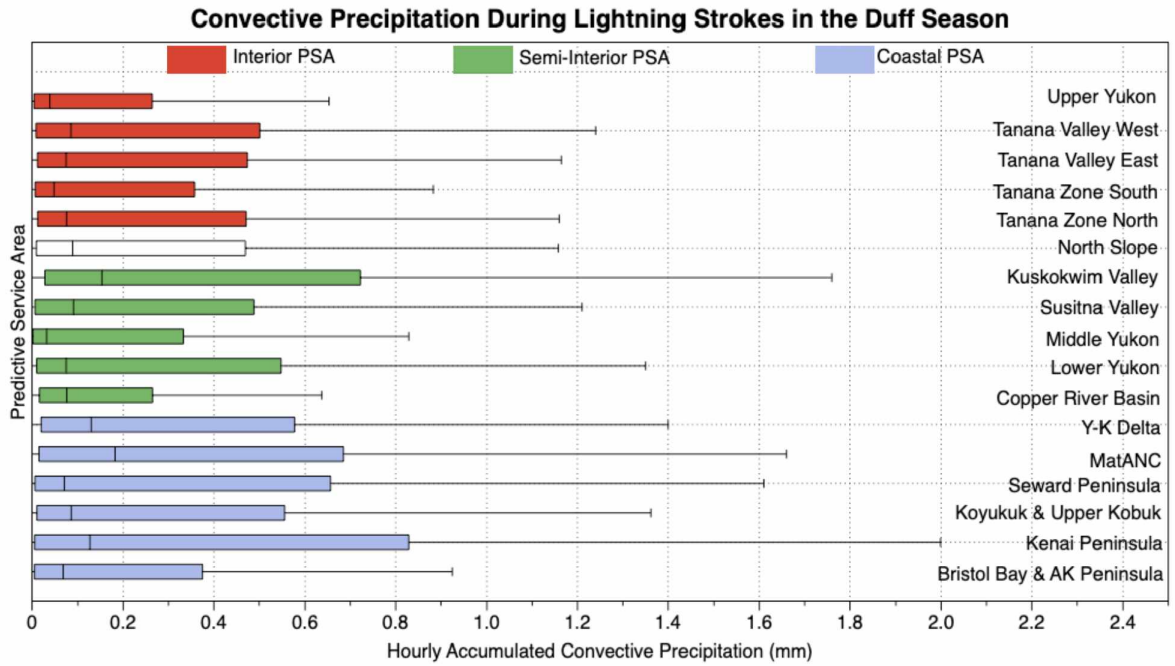
3.2.3: The Drought Driven Sub-Season (July 21–August 31)

Lightning activity during the drought driven sub-season can be important if conditions have been dry. Climatologically, 2-meter air temperatures during the drought driven sub-season are similar throughout the Coastal, Interior, and Semi-Interior PSAs, and colder in the North Slope PSA (Table 4). The same holds true for lightning associated 2-meter air temperatures. Lightning associated temperatures are fairly uniform with the exception of the Kenai Peninsula, the Matanuska Valley & Anchorage, and the Copper River Basin PSAs showing lower temperatures (Figure 11, top panel).

Climatological Coastal PSAs show the highest dew point temperatures followed by the Semi-Interior, the Interior, and finally the North Slope (Table 4). Lightning associated dew point temperatures are more similar across all geographical divisions though display the same ranks as the climatology (Table 4). While the North Slope PSA and the Interior PSAs have a climatological difference of 2.4°C, their lightning associated dew point temperatures are nearly identical (Table 4). Across different PSAs, there is more variability in dew point temperatures in the drought driven sub-season than in the duff driven sub-season (Figure 11, middle panel). Climatologically, the Coastal and Semi-Interior PSAs have higher dew point temperatures during the drought driven sub-season than during any other season, while the North Slope and Interior PSAs reach the seasonal maximum in the duff driven season. The Y-K Delta has the highest lightning associated dew point temperature of all PSAs during the drought driven sub-season.

Interior, Semi-Interior, and Coastal PSAs are climatologically similar in terms of convective precipitation, while the North Slope PSA is lower (Table 4). The Semi-Interior PSAs have the highest lightning associated convective precipitation in the drought driven sub-season (Table 4). In contrast, the Coastal PSAs showed the most lightning associated precipitation

during the wind and duff driven sub-seasons (Table 4). The Middle Yukon PSA once again shows the potential for elevated levels of dry lightning with mean lightning-associated convective precipitation of 0.44 mm/hour and a median of only 0.06 mm/hour. While the Matanuska Valley and Anchorage PSA showed the highest convective precipitation, the sample size for that PSA during the drought driven sub-season was only 705 strokes (Figure 11, bottom panel).

The Tanana Valley East PSA showed lower lightning associated temperatures and dew point temperatures than the other Interior PSAs during the drought driven season, but higher convective precipitation (Figure 11). This is likely due to the prevalence of easterly flow events over the area wrapping moisture and relatively cool air from the Gulf of Alaska through the Yukon, leading to instability and lightning as the cold front replaces warm air in place. Such a synoptic event occurred on August 1, 2020 in the eastern Interior.
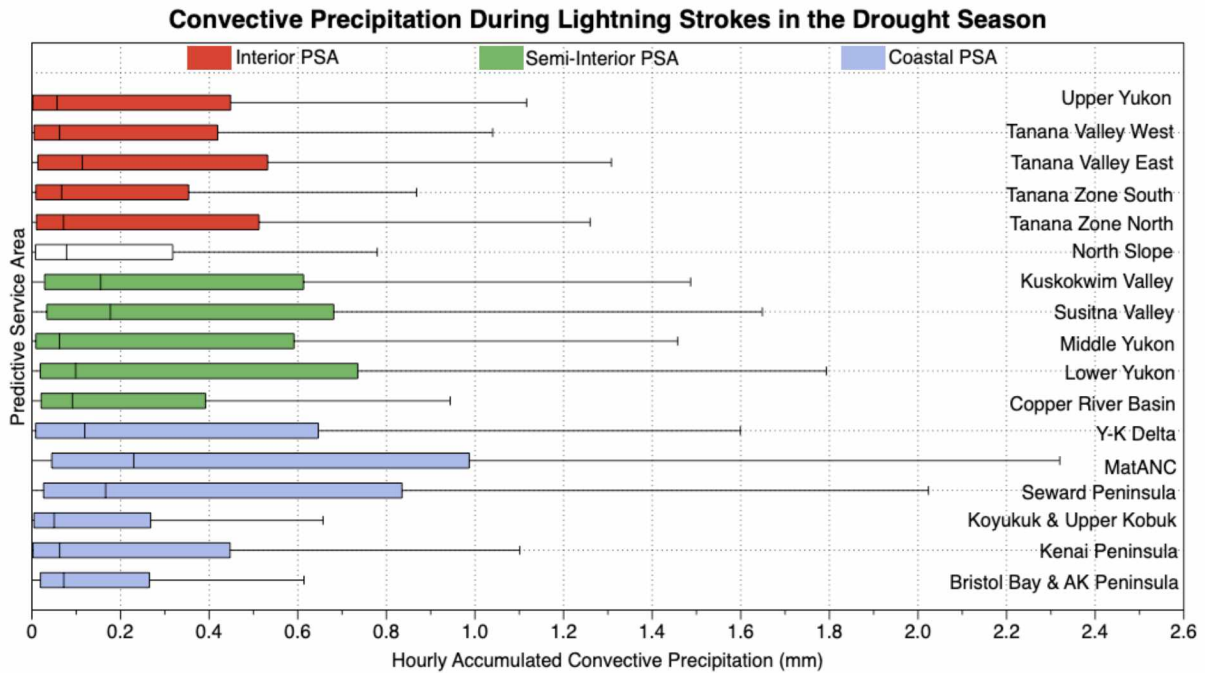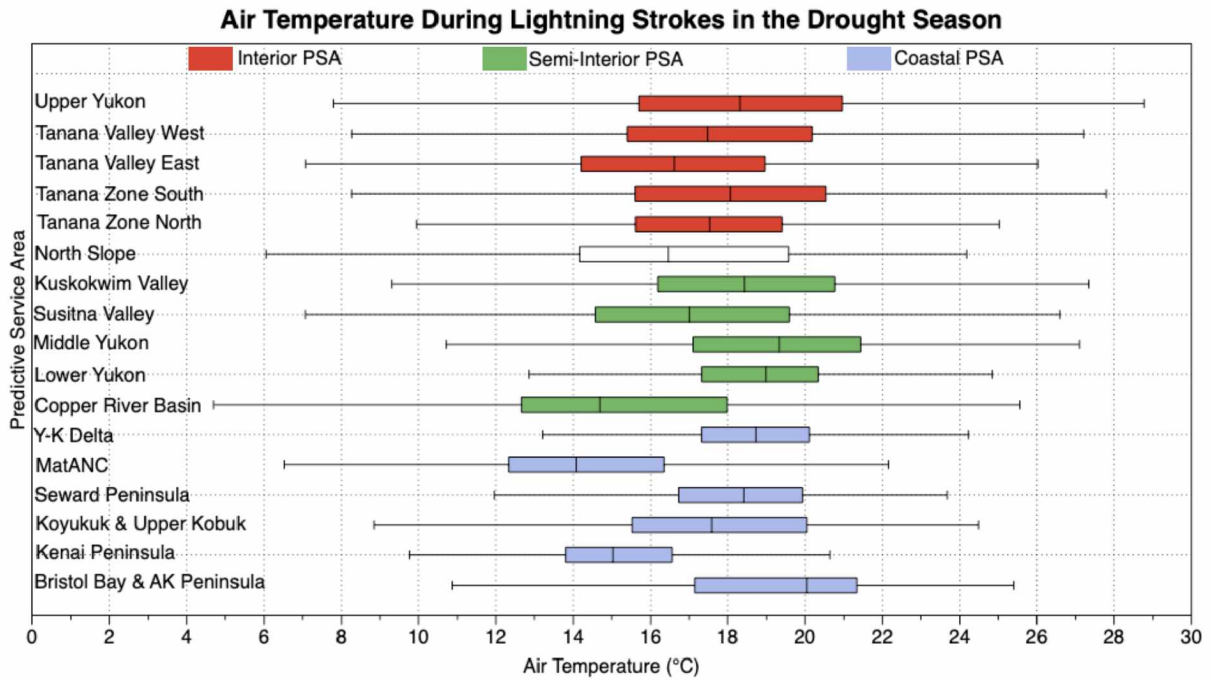
Figure 11: The 2-meter air temperature (top), convective precipitation (middle), 2-meter dew point temperature (bottom) during lightning events in the drought driven sub-season across different PSAs.

Figure 11 Continued

Dew Point Temperatures During Lightning Strokes in the Drought Season
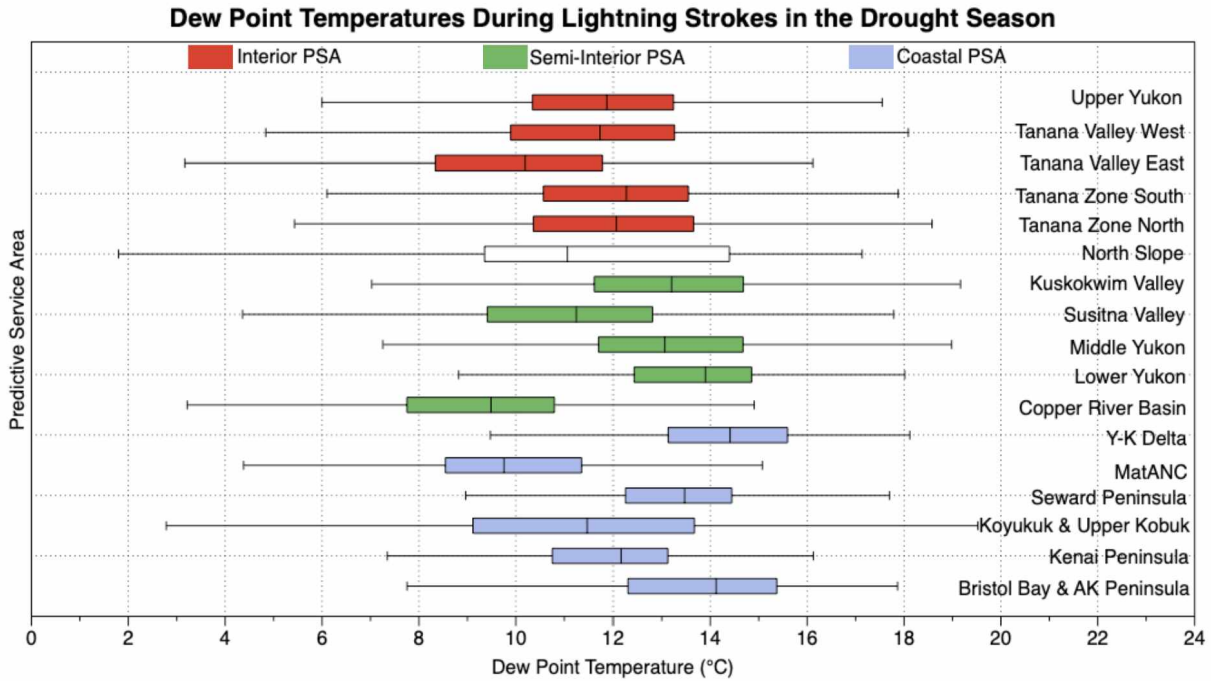
3.3 Case Studies by PSA

3.3.1 Tanana Valley West PSA

The Tanana Valley West PSA is of particular interest and importance to fire managers due to its significantly higher human population and that it has the third highest fire density in acres burned per square kilometer since fire records began in 1940 (Table 1). Containing the city of Fairbanks, the PSA has had numerous significant wildland fire events requiring evacuations, most recently the Shovel Creek Fire in 2019. The results of this case study will begin with a discussion of the upper levels of the atmosphere and progress down to the surface in order to better communicate links between known weather patterns and their impacts on surface conditions.

The Tanana Valley West PSA, like other PSAs to be discussed later, experiences its highest average lightning associated 500 hPa heights during the duff driven sub-season (Figure

12). During the duff driven sub-season, there is a bimodal distribution of lightning associated 500 hPa heights with heights between 565 and 570 decameters being present during most lightning events, though heights of 579 to 581 decameters produce a second maximum. Lightning activity is relatively low in between these two maxima (Figure 12). Lightning activity in the Tanana Valley West PSA is also highly dependent on the direction of 500 hPa and 700 hPa flow. Flow from the northeast at both 500 hPa and 700 hPa is the most favorable for lightning activity (Figure 13), and also produces the wettest thunderstorms (Figure 14). Relative humidity is also highest at the surface during periods of northeast flow (Figure A1.1). A second maximum in lightning can be found with 500 hPa and 700 hPa flow out of the northwest during the duff driven sub-season. Lightning producing thunderstorms under periods of northwest flow are generally drier than thunderstorms during northeast flow (Figure A1.1). For this reason, they may be more likely to ignite a wildfire.

Among other parameters critical to thunderstorm development are measures of instability. Traditionally, convective available potential energy (CAPE) is referenced as an instability measure. This study focuses on the K-Index rather than CAPE, since a high number of strokes were analyzed to have occurred in areas with no CAPE. This raised suspicions of the quality of this dataset and it was replaced by the K-index, another measure of instability constructed using 500, 700, and 850 hPa air temperatures along with 850 and 700 hPa dew point temperatures. For the Tanana Valley West PSA, the K-Index peaks during the duff driven sub-season (Figure 15) with a mean value of 26.6 during lightning strokes. Mean values during lightning strokes in the wind and drought driven sub-seasons were 23.6 and 26.0 respectively.

Warm cloud depth (freezing level minus cloud base height) is higher in the duff and drought driven sub-seasons than during the wind driven sub-season (Figure 16). This is

consistent with the notion that warm rain processes are more dominant in these sub-seasons

compared to the wind driven sub-season.
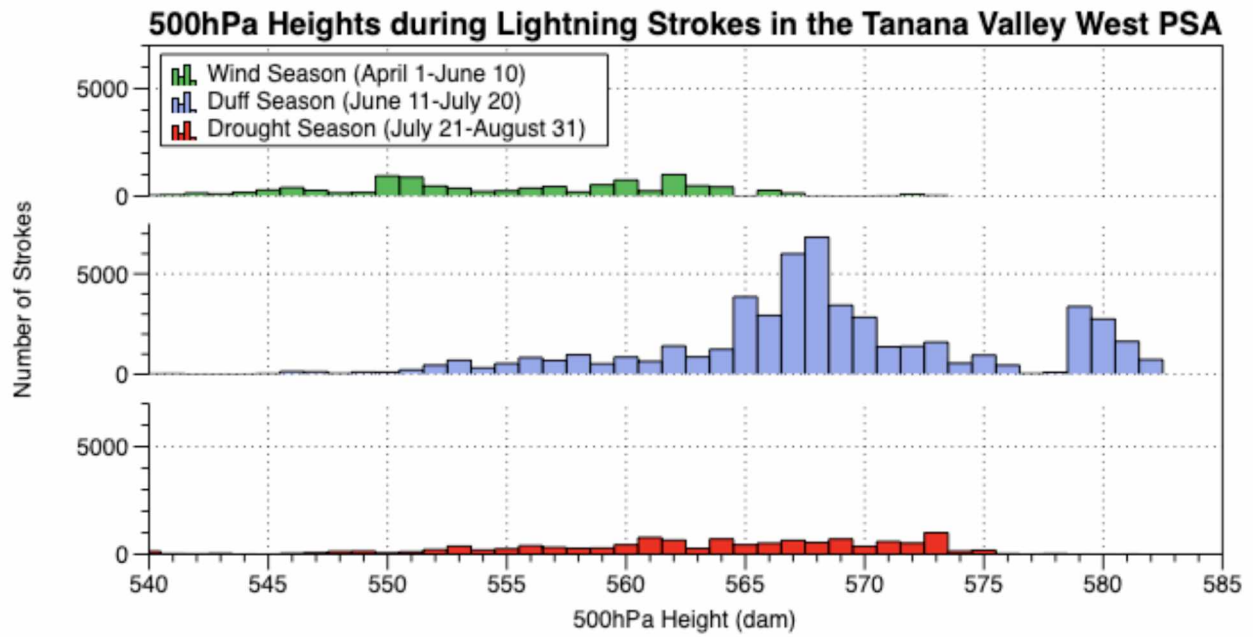
Figure 12: The 500 hPa heights (decameters: dam) associated with lightning strokes in the Tanana Valley West PSA for the 3 sub-seasons.
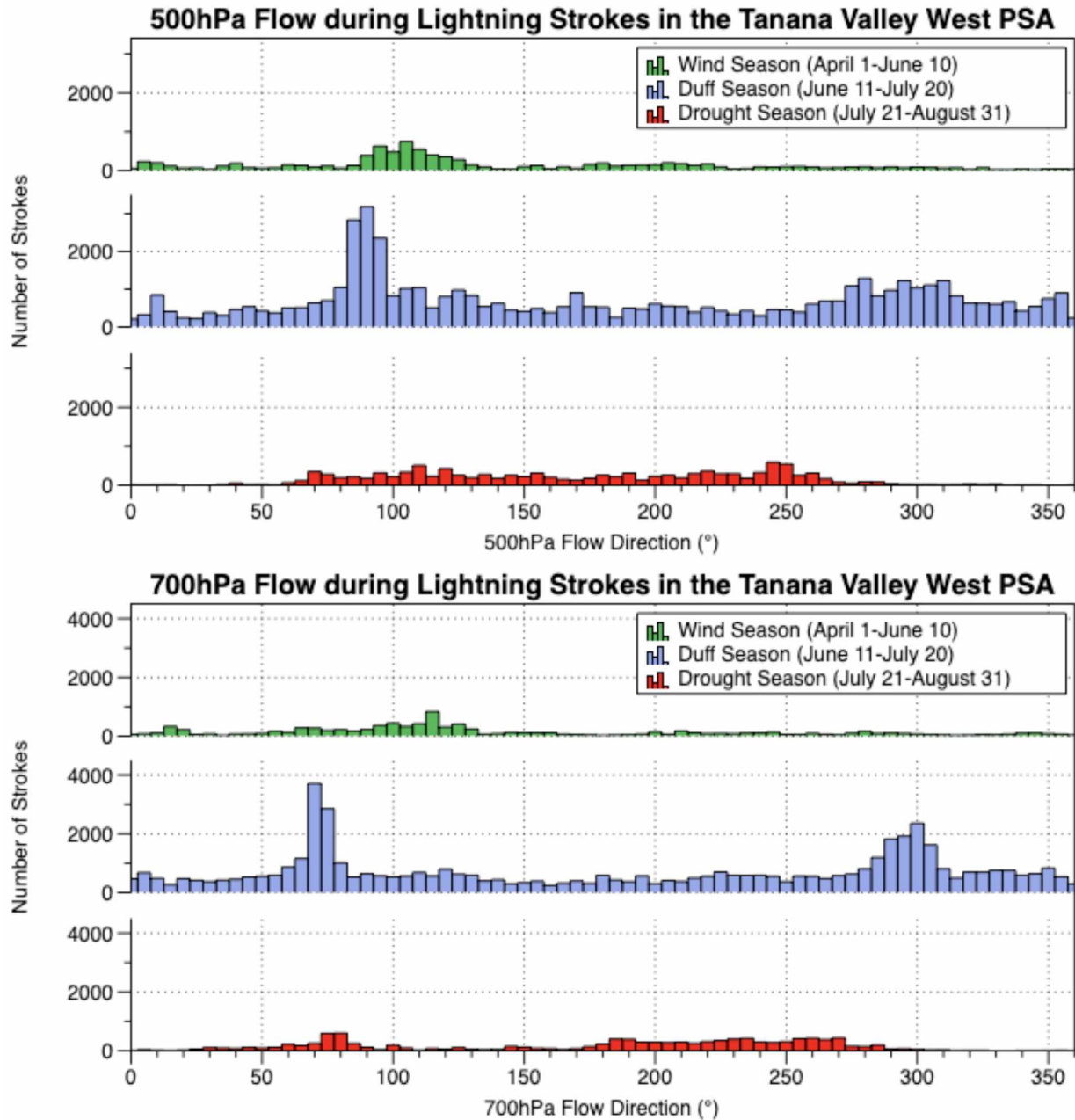
Figure 13: The 500hPa and 700hPa flow associated with lightning strokes in the Tanana Valley West PSA for the 3 sub-seasons. Flow direction is from due north at 0°N and traverses clockwise (i.e., 45° signifies a wind from the northeast direction).
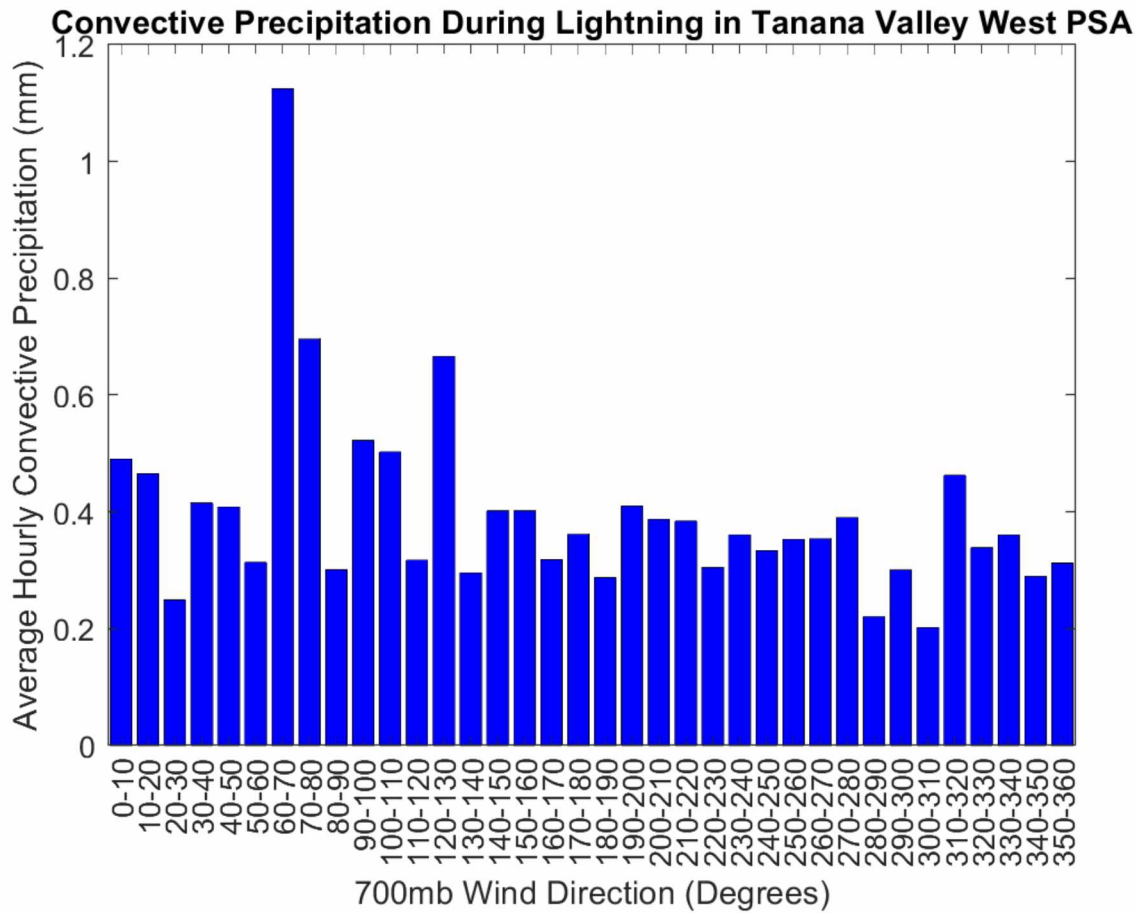
Figure 14: The convective precipitation by 700 hPa flow direction during lightning strokes in the Tanana Valley West PSA.
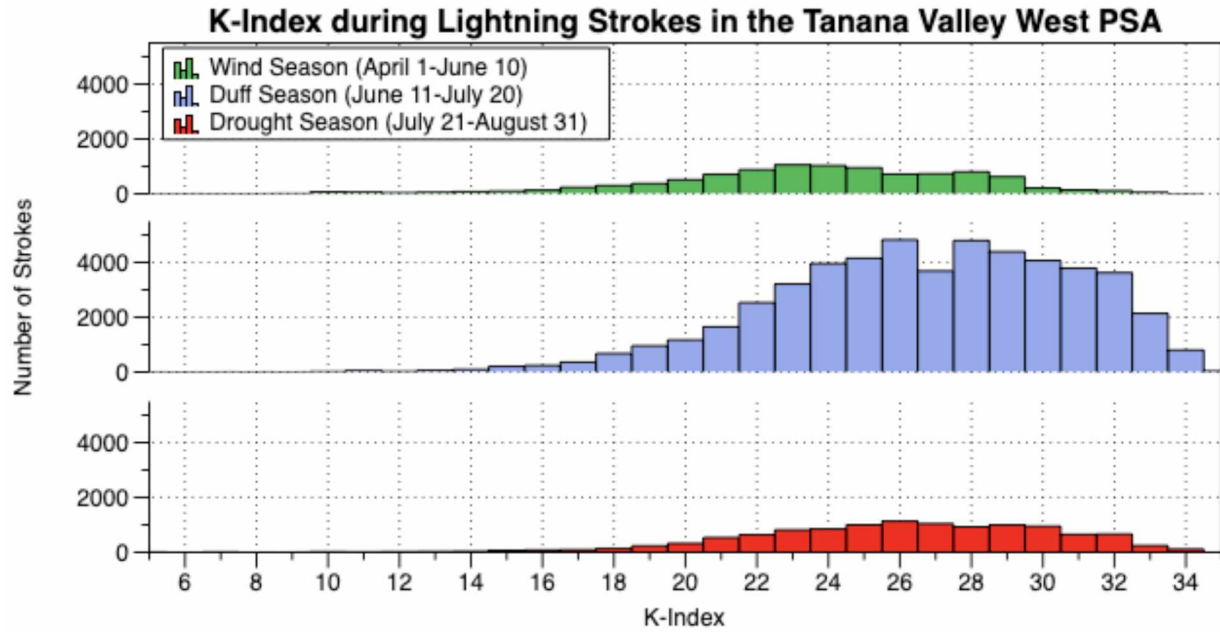
Figure 15: The K-index associated with lightning strokes in the Tanana Valley West PSA for the 3 sub-seasons.
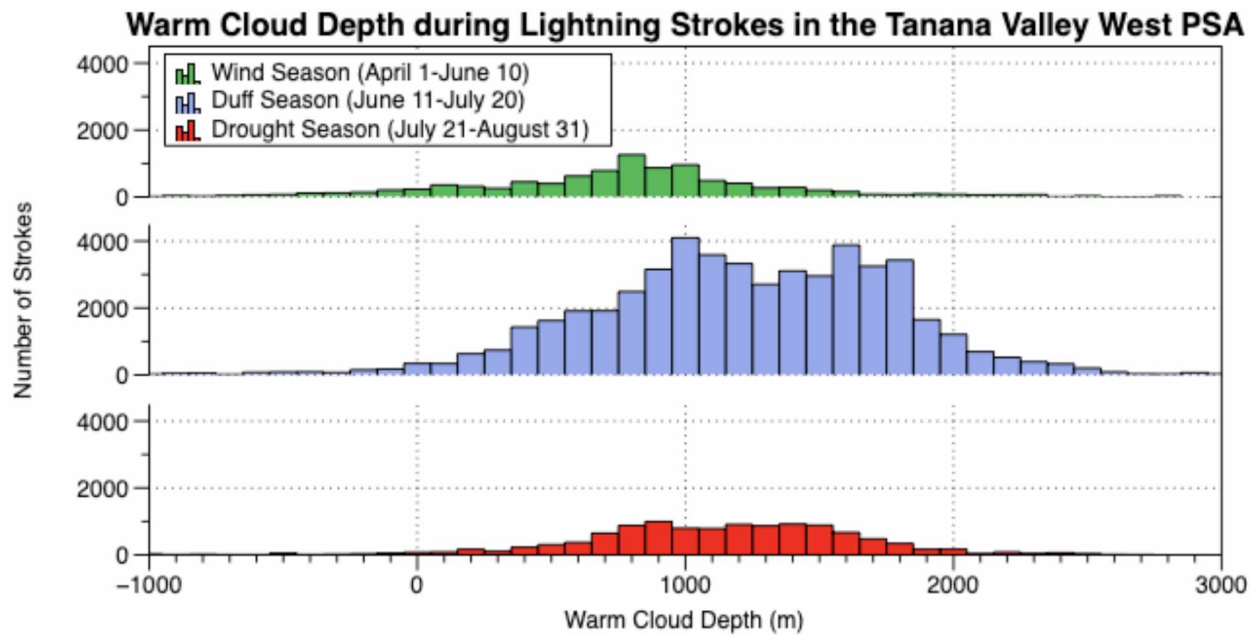
Figure 16: The warm cloud depth associated with lightning strokes in the Tanana Valley West PSA for the 3 sub-seasons.

3.3.2 Upper Yukon PSA

The Upper Yukon is a significant PSA because it has some of the largest fires in Alaska. It is the second largest PSA and also has the second highest fire density in acres burned per total area (Table 2). Lighting associated 500 hPa heights are highest during the duff driven sub-season with a mean of 564 decameters, followed by the drought driven sub-season (563 decameters) and finally the wind driven sub-season (556 decameters), similar to the Tanana Valley West PSA discussed above. A second maximum in lightning strokes with 500 hPa heights of 577 decameters and above is evident in the Upper Yukon PSA during the duff driven sub-season (Figure 17), and a feature similar to that found in the Tanana Valley West. Upon further investigation, July 14-15, 2016 had the second and third highest daily stroke counts in the 2012–2019 record, and 92% of all strokes that occurred with 500 hPa heights of 577 decameters or higher in the Tanana Valley West PSA happened these days. In the Upper Yukon PSA, 73% of all strokes that occurred with 500 hPa heights of 577 decameters or higher occurred during these same two days.

The 500 and 700 hPa flow directions favoring lightning are less defined in the Upper Yukon PSA than in the Tanana Valley West PSA, especially during the duff driven sub-season (Figure 18). Northwest flow at 700 hPa during the duff driven sub-season in the Upper Yukon PSA was favorable for lightning, in contrast to a well-defined maximum in the Tanana Valley West PSA where lightning associated flow was from northeast and northwest at 500hPa and 700 hPa. Additionally, southeast flow at 500 and 700 hPa is somewhat favorable for lightning activity. All directions at 500 hPa except for northeast were conducive for lightning to occur during the duff driven sub-season (Figure 18). During the drought driven sub-season, a southerly

component to both the 500 hPa and 700 hPa flow is associated with lightning, with due south being less favorable than southeast or southwest flow at both levels.

Relative humidities associated with lightning strokes increase as the sub-seasons progress (Figure 19) and are similar to those in the Tanana Valley West PSA (Figure A1.4). The lightning associated humidities are lowest during the wind sub-season and highest during the drought sub-season, though mean relative humidity values are lower overall in the Upper Yukon than in the Tanana Valley West PSA. Temperatures coincident with lightning in the Upper Yukon PSA are coolest during the wind driven sub-season and similar during the duff and drought driven sub-seasons (Figure 20). The highest temperature values during lightning strokes occur in the duff driven season.
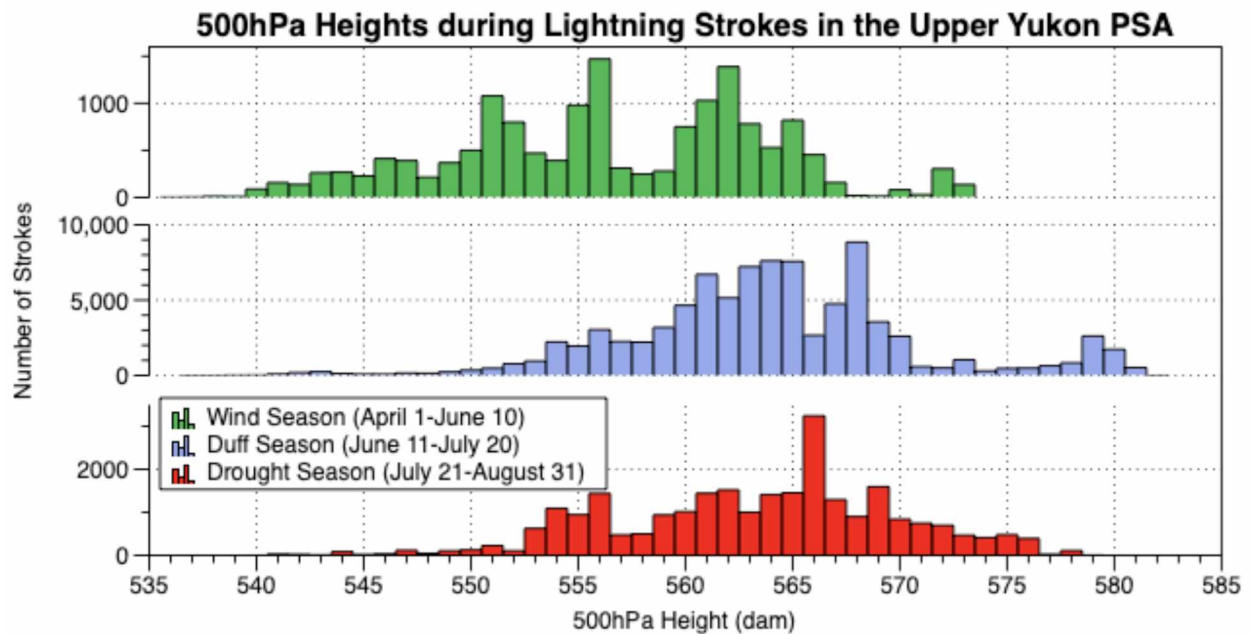
Figure 17: The 500hPa (decameters: dam) heights associated with lightning strokes in the Upper Yukon PSA for the 3 sub-seasons.
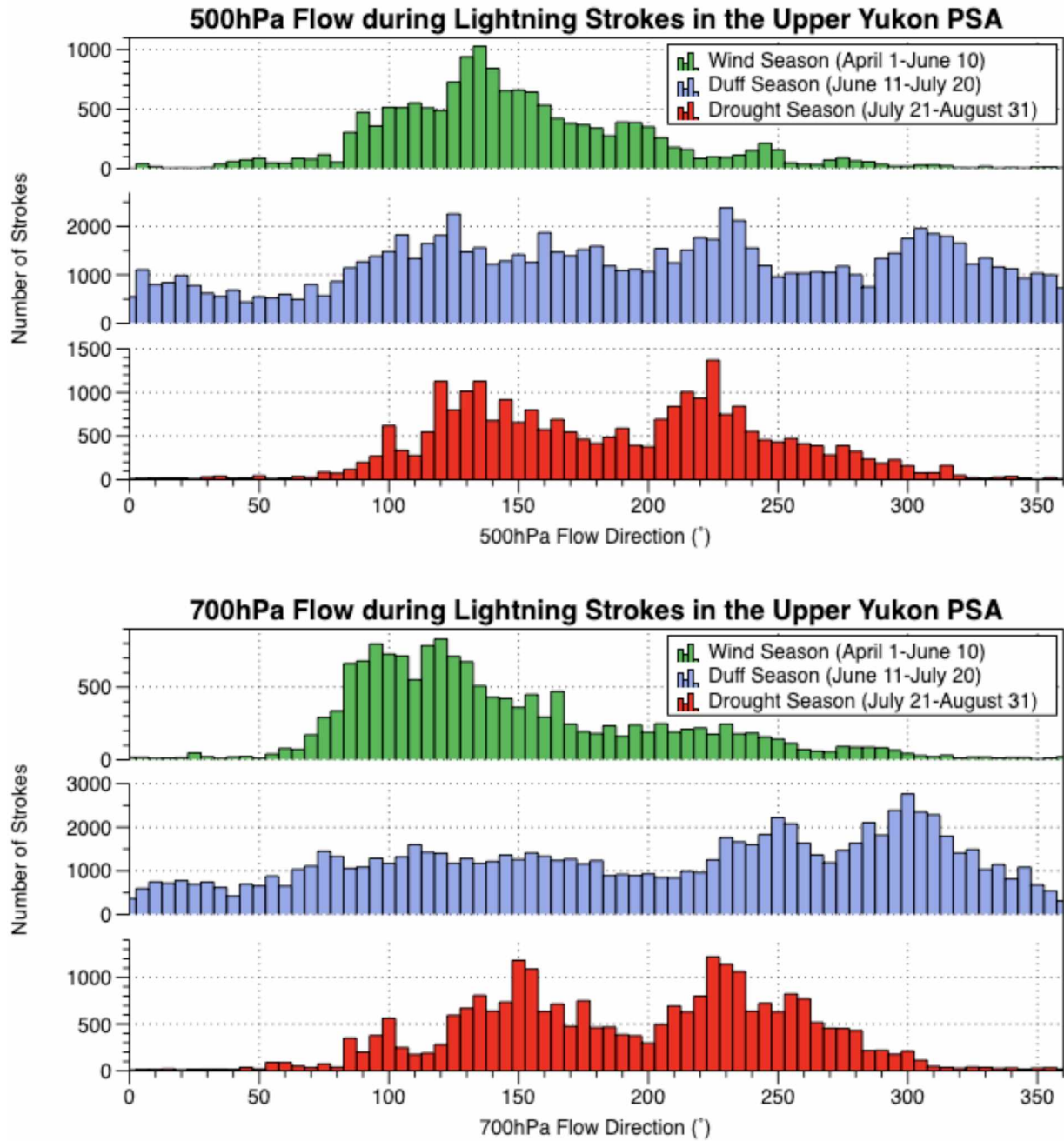
Figure 18: The 500 hPa and 700 hPa flow associated with lightning strokes in the Upper Yukon PSA for the 3 subseasons.. Note that the y-axis scale is different in the sub-panels for visibility of patterns.
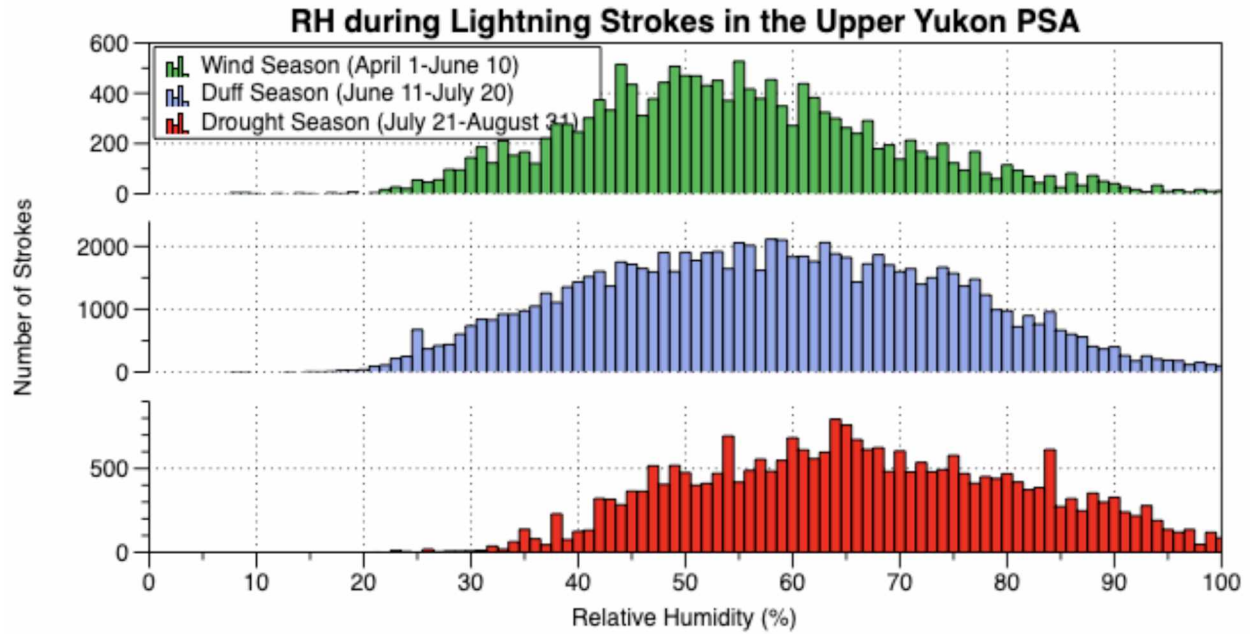
Figure 19: The relative humidity (%) associated with lightning strokes in the Upper Yukon PSA for the 3 sub-seasons. Note that the y-axis scale is different in the sub-panels for visibility of patterns.
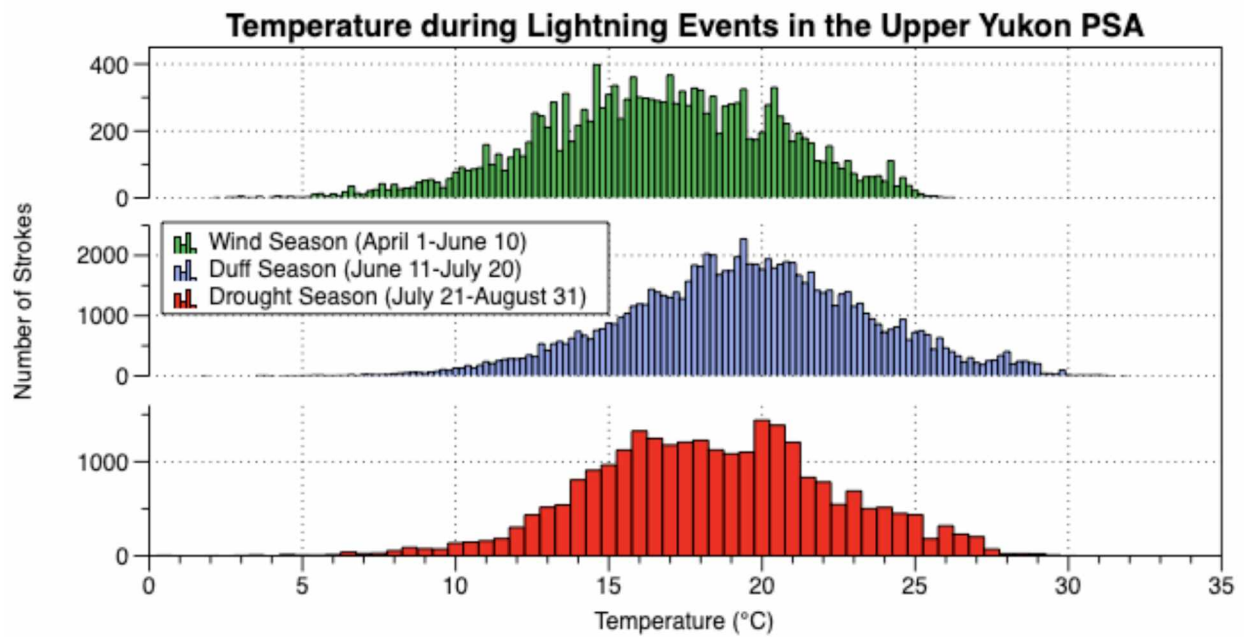
Figure 20: The 2-m air temperature associated with lightning strokes in the Upper Yukon PSA for the 3 sub-seasons. Note that the y-axis scale is different in the sub-panels for visibility of patterns.

3.3.3 Kuskokwim Valley PSA

The Kuskokwim Valley PSA is included in this group of case studies due to the planned installation of additional lightning detectors in this region. It is thought that more lightning occurs here than is reported due to a gap in detection efficiency (Beach, personal communication 2019). Similar to the Tanana Valley West and Upper Yukon PSAs, the Kuskokwim Valley has multiple maximum lightning occurrences in 500 hPa heights, with a defined break during the duff driven season, between 552 and 567 hPa. Even higher heights were less favorable for lightning activity (Figure 21). While most of the duff driven season spike with 500 hPa heights above 575 decameters in the Tanana Valley West and Upper Yukon PSAs occurred over a 2 day timespan in 2016, the less defined spike here was not due to a small number of big lightning days and took place over many different days and summers.

The Kuskokwim Valley PSA has distinct lightning associated peaks in flow direction at 500 hPa and 700 hPa, similar to the Tanana Valley West PSA (Figure 22). During the wind driven sub-season, flow from the east, northeast, north, and northwest at 500 and 700 hPa was most favorable for lightning (Figure 22). During the duff driven sub-season, easterly flow at 500 hPa was associated with lightning while other directions were not as favorable, however this feature did not translate down to 700 hPa, where less of a defined favorable direction was present. During the drought driven sub-season, easterly flow at 500 hPa again was the most favorable for lightning, though southeast flow at 700 hPa was also markedly more favorable than other directions at that pressure level (Figure 22).

In the Kuskokwim Valley PSA, instability peaks during the duff driven sub-season with an average lightning coincident K-Index of 27.3 (Figure 23). Among other PSAs studied in this set of case studies, 27.3 was the highest lightning associated K-Index of any PSA during any

sub-season. During the wind and drought driven sub-seasons, mean lightning coincident K-indices were 23.0 and 26.3, respectively.
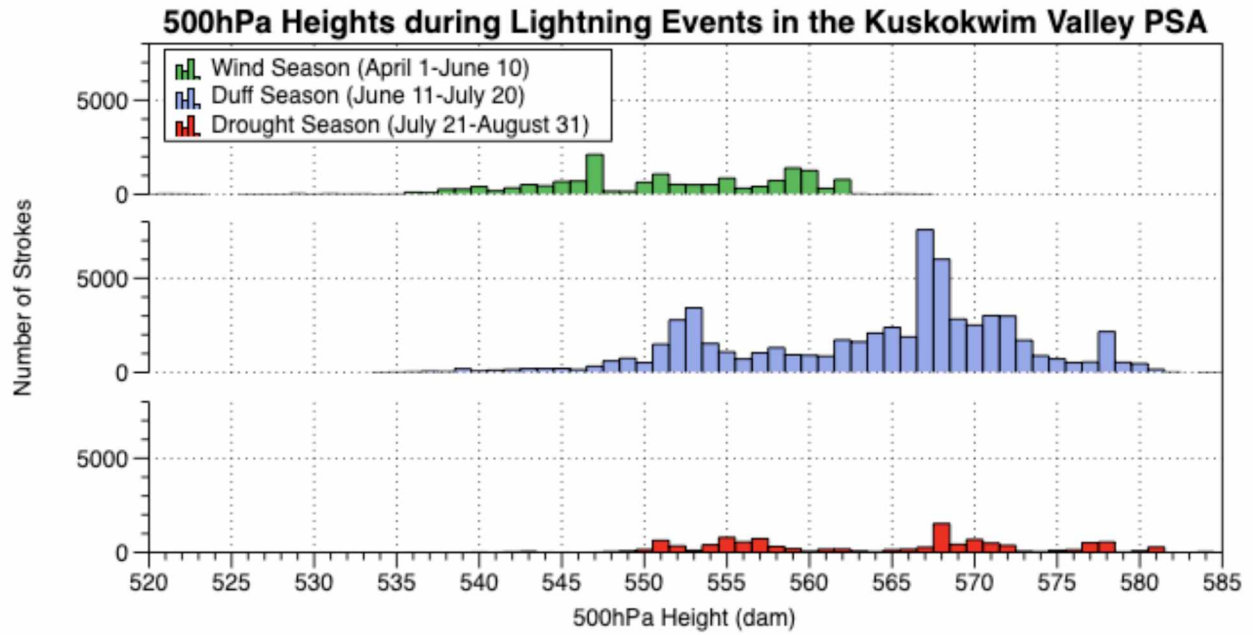
Figure 21: The 500 hPa (decameters: dam) heights associated with lightning strokes in the Kuskokwim Valley PSA for the 3 sub-seasons.
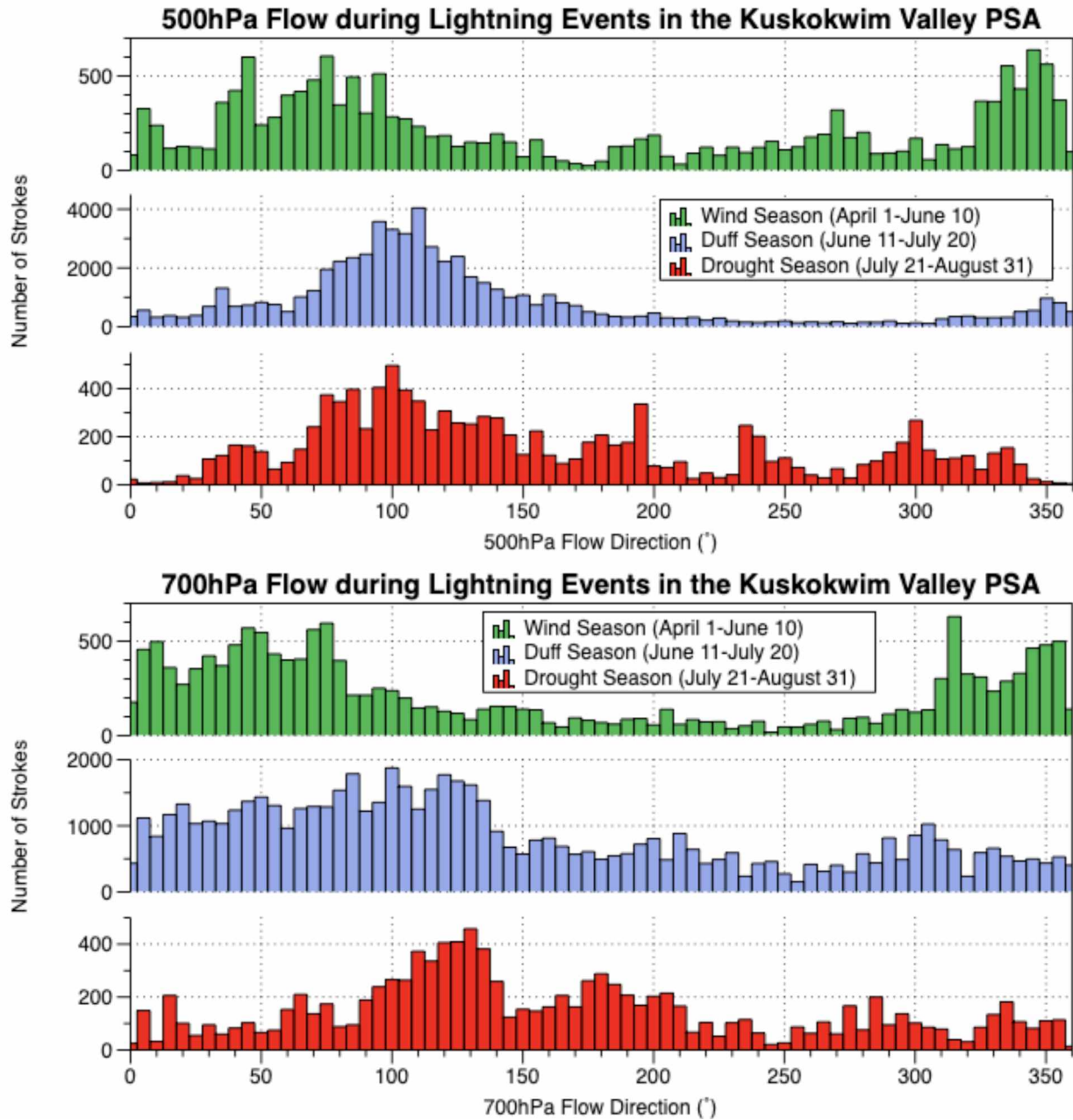
Figure 22: The 500 hPa and 700 hPa flow associated with lightning strokes in the Kuskokwim Valley PSA for the 3 sub-seasons. Note that the y-axis scale is different in the sub-panels for visibility of patterns.
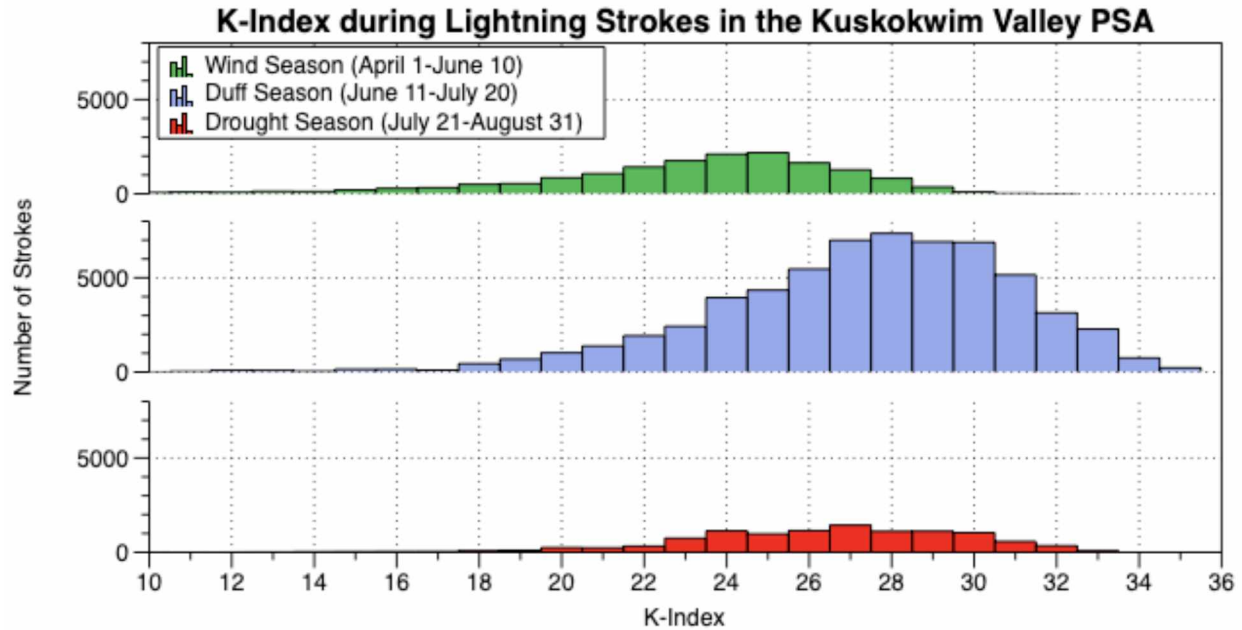
Figure 23: The K-Index associated with lightning strokes in the Kuskokwim Valley PSA for the 3 sub-seasons. Note that the y-axis scale is different in the sub-panels for visibility of patterns.

3.3.4 Seward Peninsula PSA

The Seward Peninsula PSA is included in this study because it has the least variability in lightning activity among the three fire sub-seasons. The majority of lightning occurs in the Seward Peninsula PSA during easterly flow at 500 and 700 hPa (Figure 24), similar to the Kuskokwim Valley though this feature is even more defined in the Seward Peninsula PSA. Since the Seward Peninsula is a coastal PSA on the west coast of Alaska, easterly flow provides the warm continental air required for instability and lightning activity. Flow from other directions is influenced by the relatively cold waters of the Bering Sea and Strait and Kotzebue Sound, where sea ice can linger into the summer months. Despite the markedly different distribution of lightning throughout the fire sub-seasons, 500 hPa heights follow a similar pattern as other PSAs except the North Slope, with the highest lightning associated 500 hPa heights taking place in the duff driven sub-season and the lowest during the wind driven sub-season (Figure 25). The same

pattern is also observed in lightning coincident 850 hPa temperatures (Figure 26). Dew point temperatures also peak during the drought driven sub-season like all other PSAs included in these case studies except the Tanana Valley West (Figure 27). Lightning coincident relative humidities are very similar during the wind driven and duff driven sub-seasons with mean values of 66.1% and 65.9% respectively. However, during the drought driven sub-season, the mean lightning coincident relative humidity was 73.6% and most notably, very little lightning occurred with relative humidities less than 60%, while lightning was prevalent with relative humidities as low as 50% during the wind and duff driven sub-seasons (Figure 28). Lightning coincident warm cloud depth (Figure 29) increases steadily from the wind to the duff to the drought driven sub-seasons, similar to other northern PSAs studied here (Upper Yukon and North Slope).
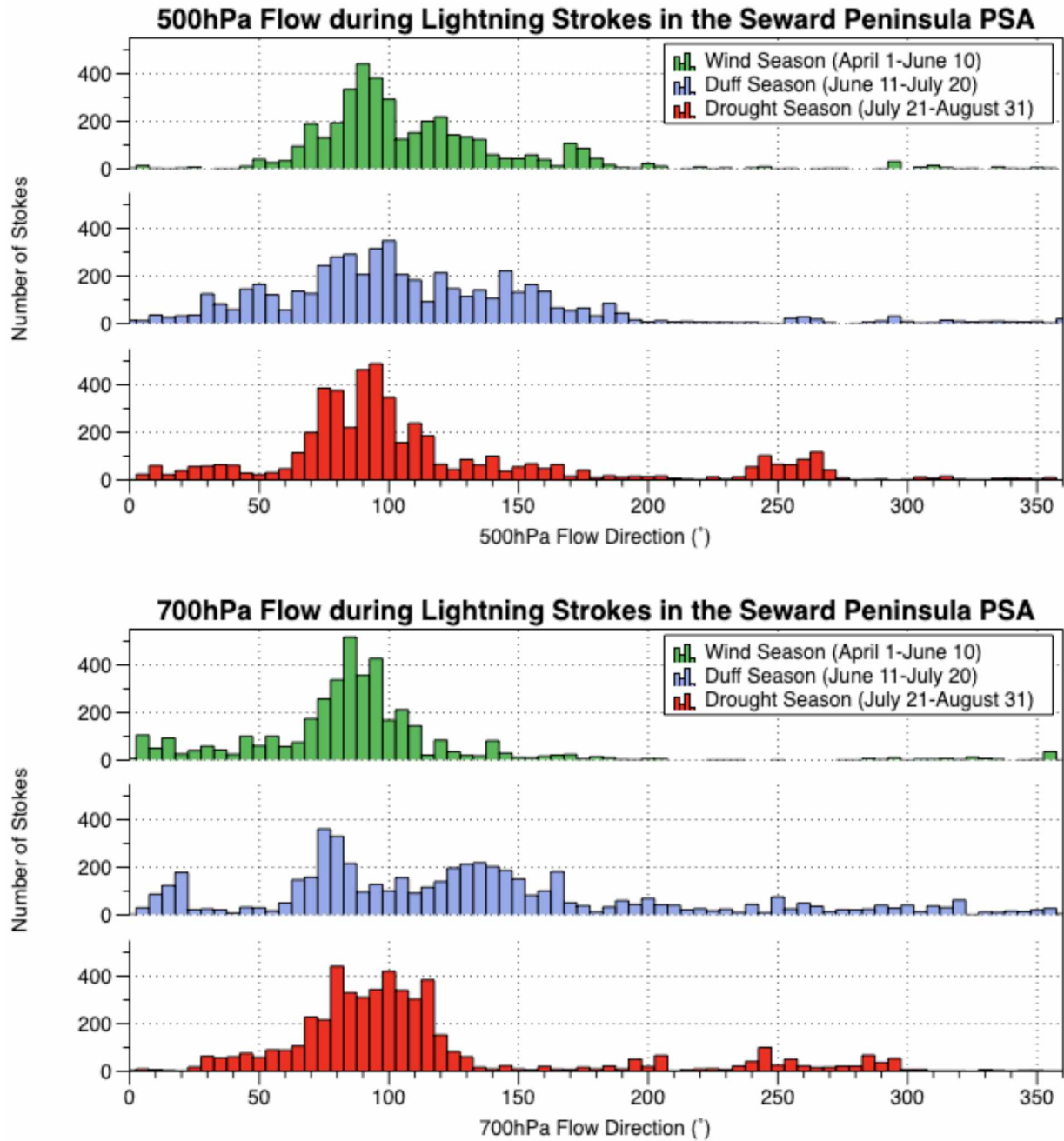
Figure 24: The 500 hPa (top) and 700 hPa (bottom) flow associated with lightning strokes in the Seward Peninsula PSA for the 3 sub-seasons.
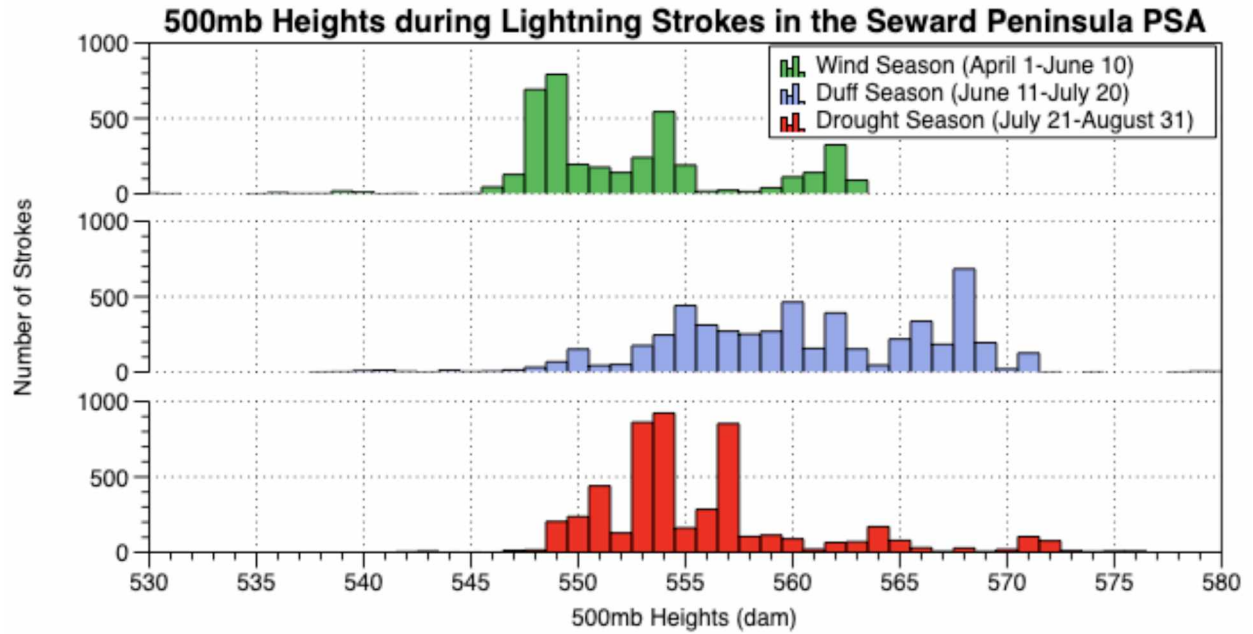
Figure 25: The 500 hPa (decameters: dam) heights associated with lightning strokes in the Seward Peninsula PSA for the 3 sub-seasons.
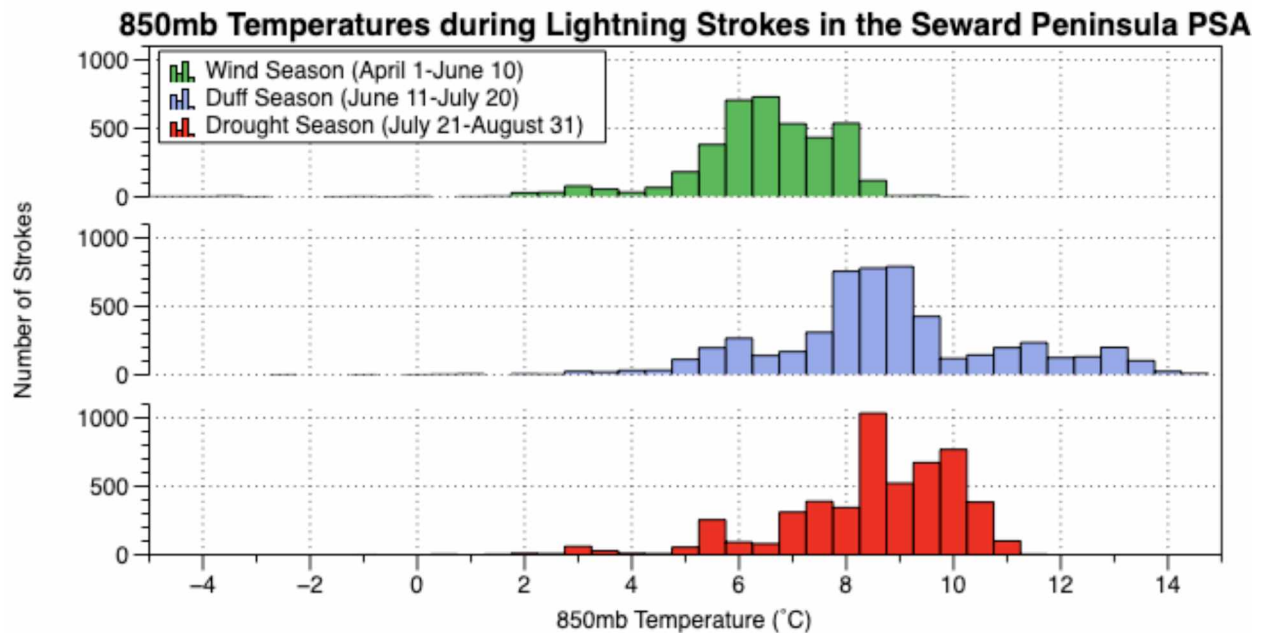
Figure 26: The 850 hPa air temperature associated with lightning strokes in the Seward Peninsula PSA for the 3 sub-seasons.
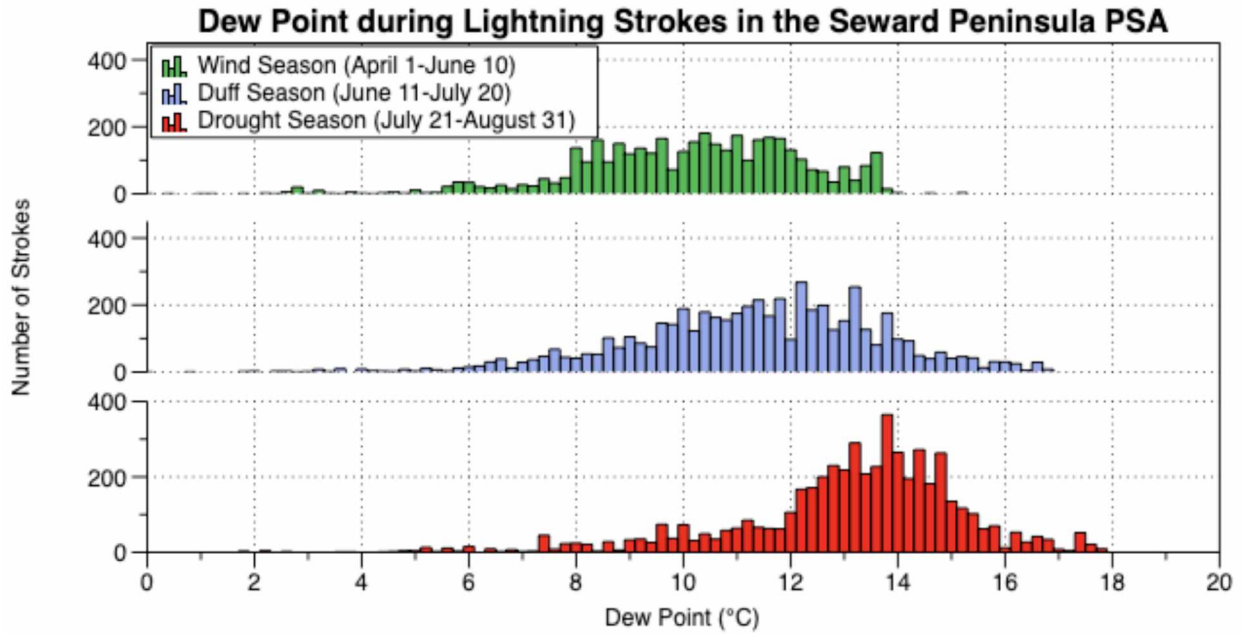
Figure 27: The 2-m dew point temperature associated with lightning strokes in the Seward Peninsula PSA for the 3 sub-seasons.
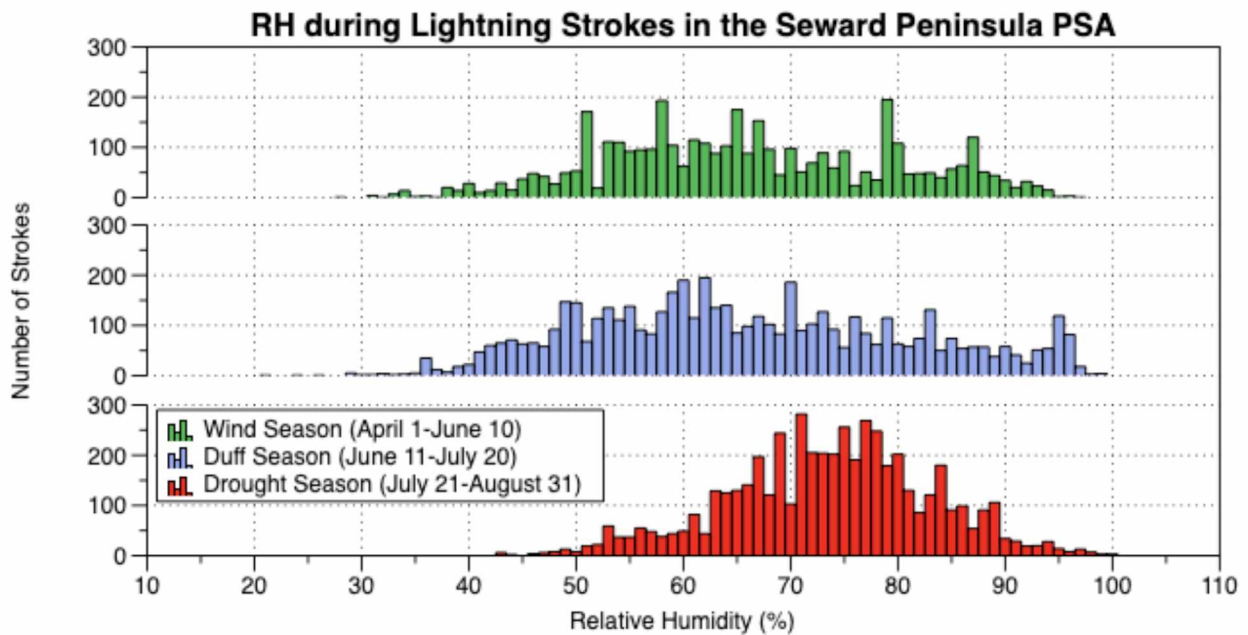
Figure 28: The relative humidity associated with lightning strokes in the Seward Peninsula PSA for the 3 sub-seasons.
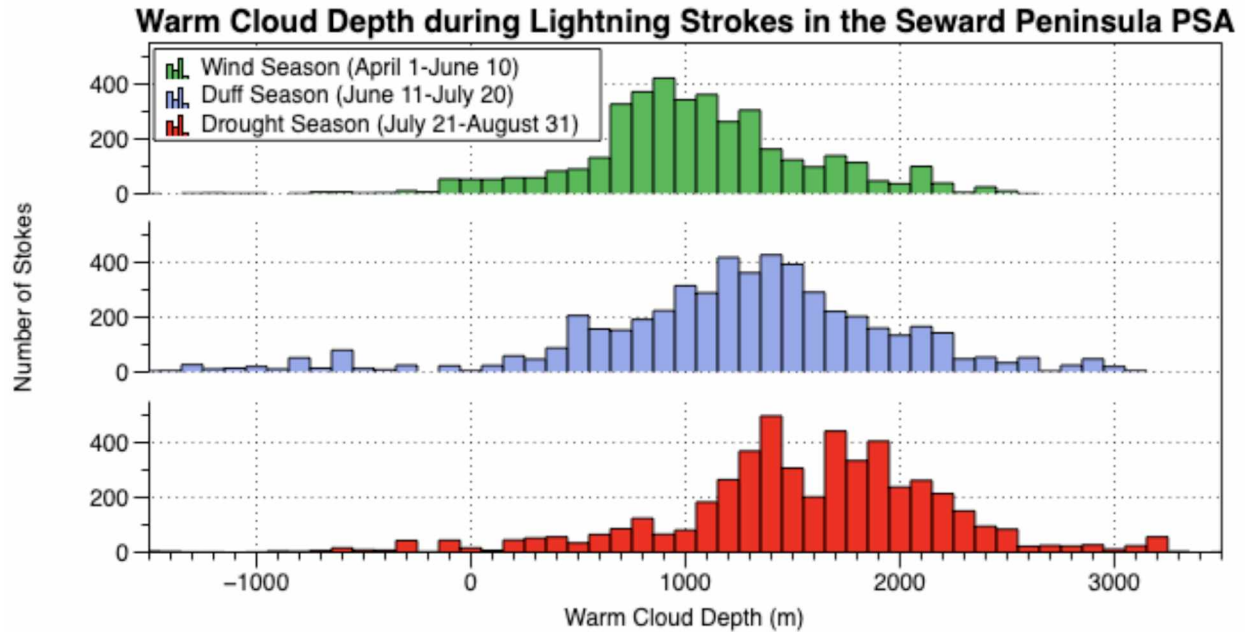
Figure 29: The warm cloud depth associated with lightning strokes in the Seward Peninsula PSA for the 3 sub-seasons.

3.3.5 North Slope PSA

The North Slope is included in this set of case studies because it is a rapidly changing region of the Arctic. Poujol et al. (2020) projects the North Slope to be ground zero for convective storm increases, citing sea ice loss allowing more moisture to travel inland with air masses originating from the Arctic Ocean and the Bering Sea. As mentioned in section 3.2, the North Slope experiences a higher percentage of its total fire season lightning during the duff driven sub-season (83%) than any other PSA.

Unlike other PSAs included in this set of case studies, southerly, offshore flow at 500 and 700 hPa (Figure 30) is required for lightning to occur in the North Slope PSA. This offshore flow is significantly warmer than sea ice and cold-water-impacted onshore flow due not only to continental air being advected from Interior Alaska, but also due to adiabatic compression as this air is forced downslope over the Brooks Range.

57

Unlike other PSAs, lightning coincident 500 hPa heights (Figure 31), surface temperatures (Figure 32), dew point temperatures, 850 hPa temperatures, K-Indices, and freezing levels peak in the drought driven season rather than the duff driven season. Despite this, some of the lowest lightning coincident relative humidities (Figure 33) occurred during the duff driven sub-season when 83% of total fire season lightning occurs.
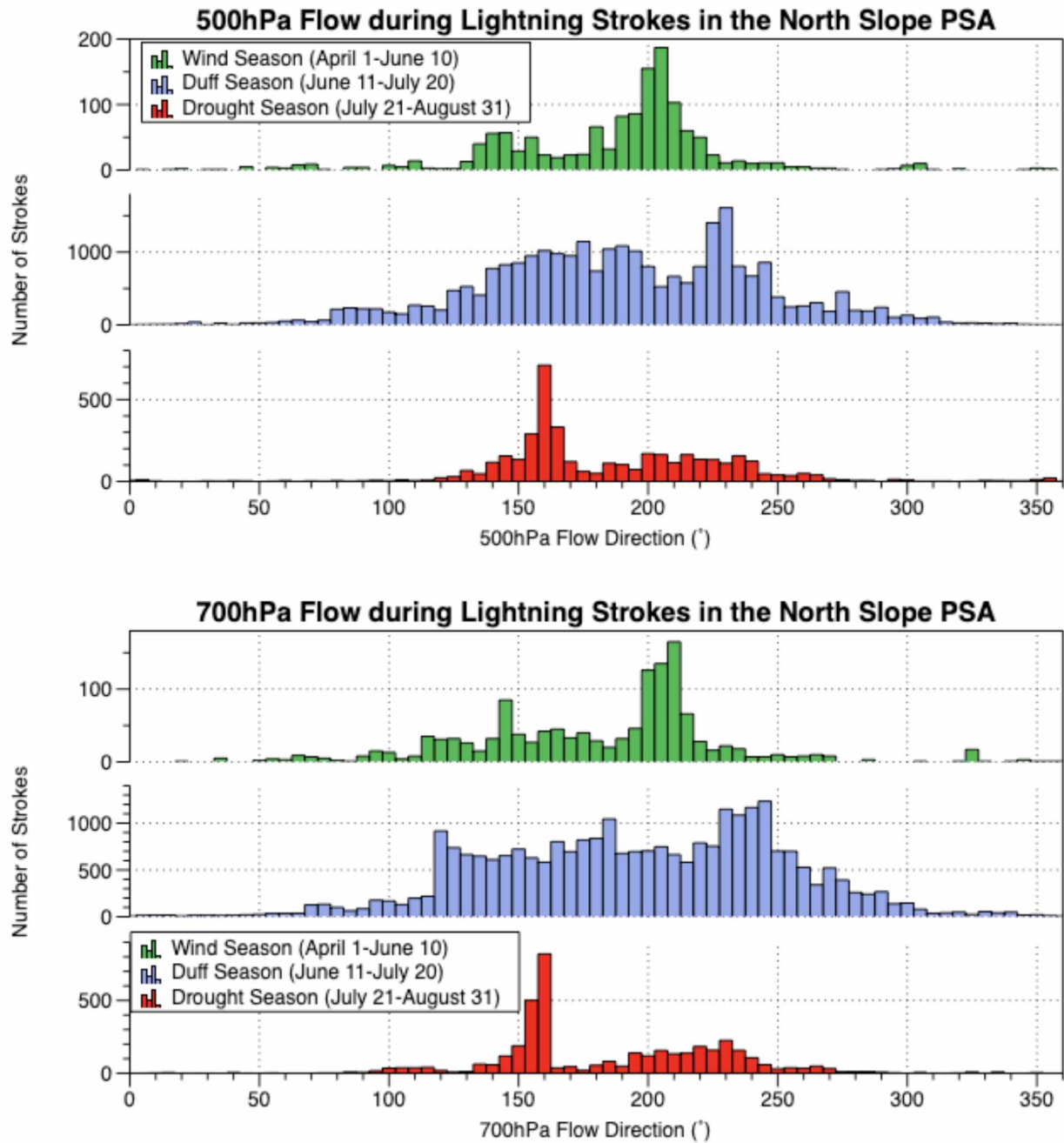
Figure 30: The 500 hPa (top) and 700 hPa (bottom) flow that is associated with lightning strokes in the North Slope PSA for the 3 sub-seasons.. Note that the y-axis scale is different in the sub-panels for visibility of patterns.
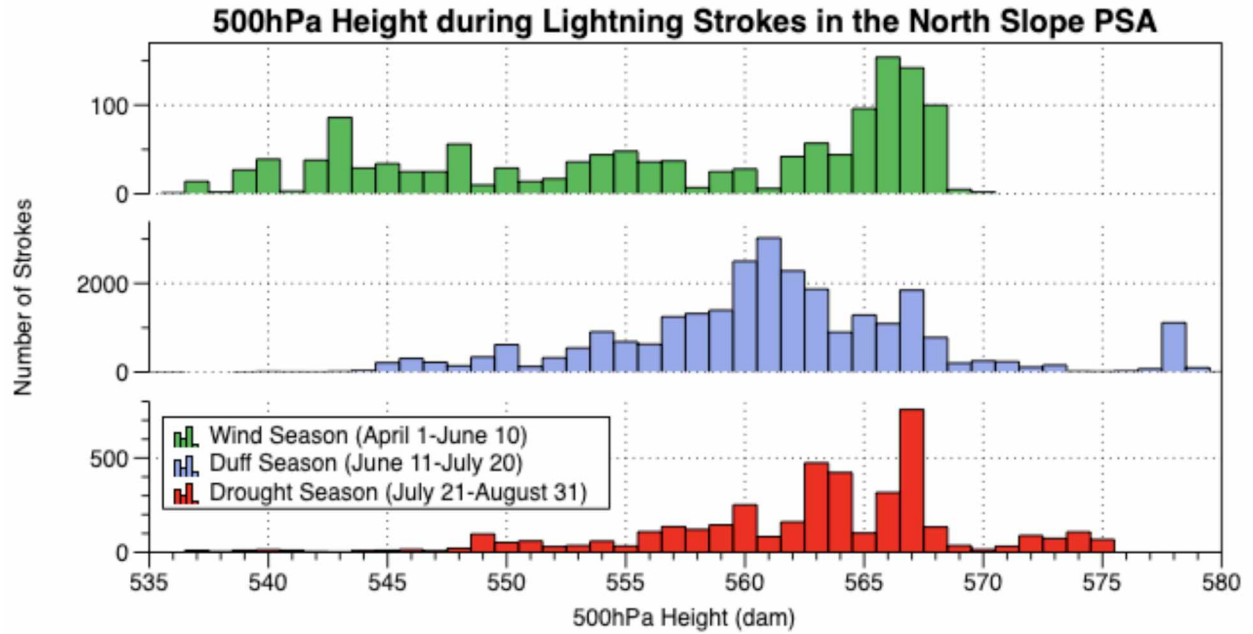
Figure 31: The 500 hPa (decameters: dam) heights associated with lightning strokes in the North Slope PSA for the 3 sub-seasons. Note that the y-axis scale is different in the sub-panels for visibility of patterns.
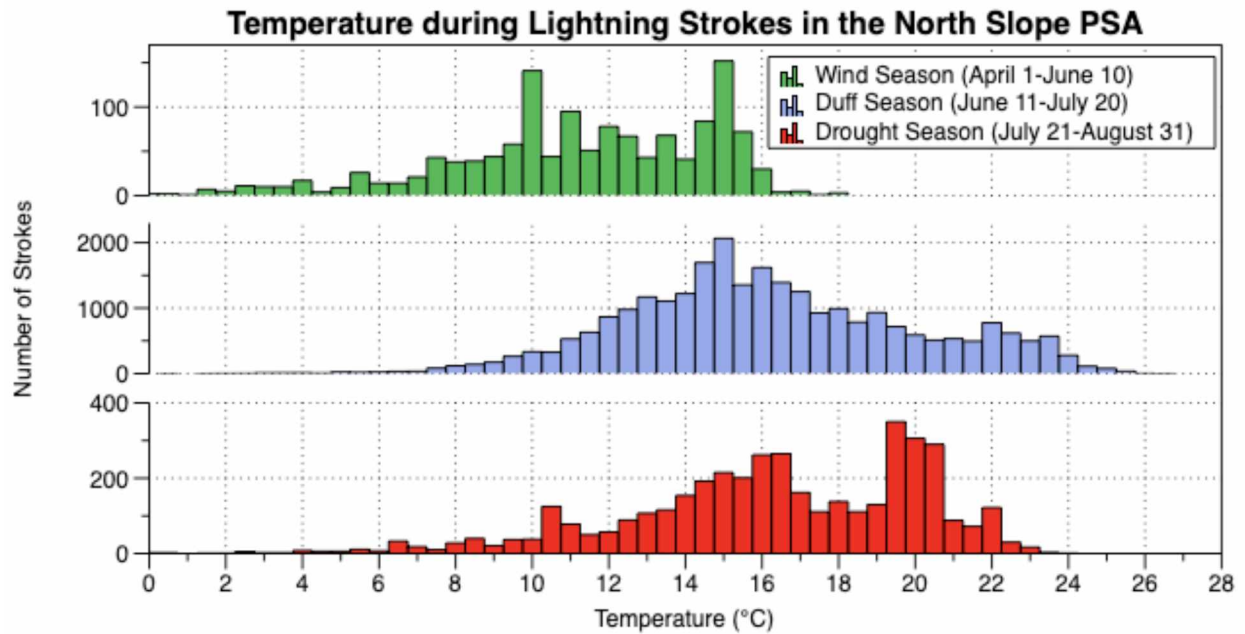
Figure 32: The 2-m air temperature associated with lightning strokes in the North Slope PSA for the 3 sub-seasons.. Note that the y-axis scale is different in the sub-panels for visibility of patterns.
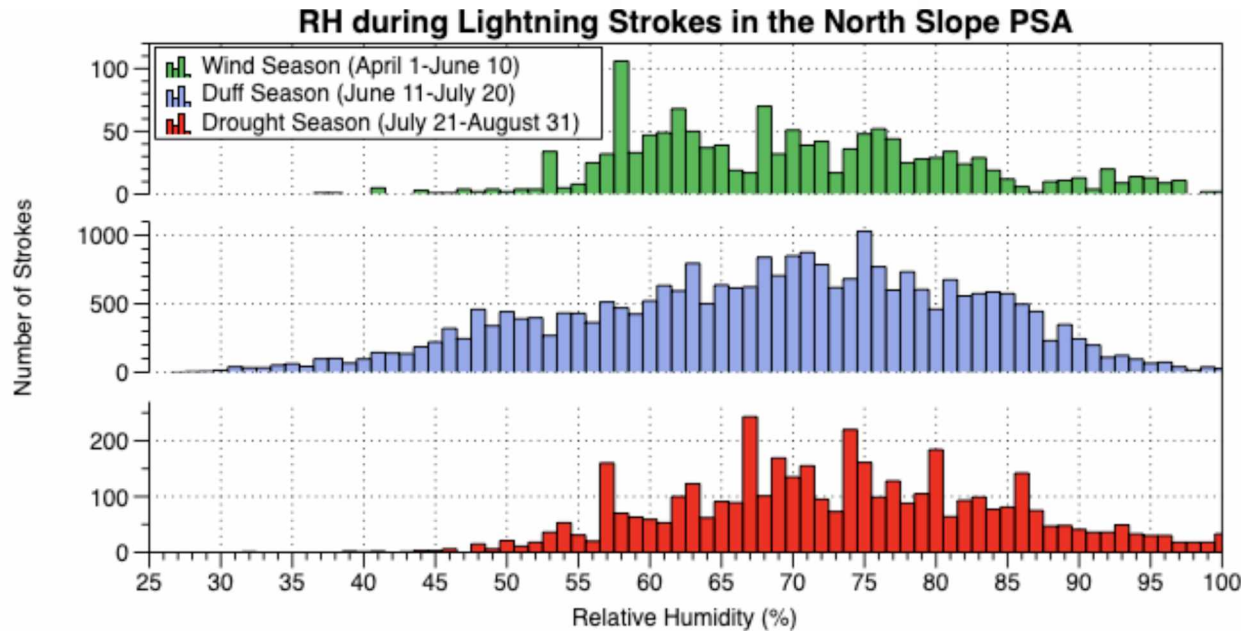
Figure 33: The relative humidity associated with lightning strokes in the North Slope PSA for the 3 sub-seasons.. Note that the y-axis scale is different in the sub-panels for visibility of patterns.

4. Discussion

4.1 Variables Identified as Key for Developing Lightning Outlooks

A main goal of this study was to identify weather parameters that are linked to lightning occurrence so they could be used for developing seasonal and sub-seasonal lightning outlooks. The most significant new parameters associated between the ERA5 reanalysis (serving as observed atmospheric conditions) and lightning count are 500 and 700 hPa flow direction. These variables are generally well represented in the global forecast models and identify the direction of the large-scale circulation that is most favorable for lightning. This flow direction feature varies among each PSA analyzed in the case studies, however, each PSA had a well-defined direction in at least one of the three fire sub-seasons that could be used to identify the periods of higher lightning activity using forecasts from global models, at the medium, long, and seasonal time scales.

CAPE from ERA5 reanalysis was not identified in this study to be well linked to lightning occurrence. While CAPE and instability parameters are widely used to forecast lightning on short term (<3 days) timescales, ERA5 reanalysis CAPE paired with lightning strokes was found to be possibly unreliable due to a large number of lightning strokes occurring when and where zero CAPE was present in the atmosphere despite the 30km ERA5 grid resolution from which values were pulled. For this reason, CAPE was not included in the written thesis. Higher resolution reanalysis data may be required to perform a full investigation of CAPE on a stroke-by-stroke spatial scale.

4.2 Overview of Regional and PSA Level Differences and Sub-Seasonal Differences

Similar patterns in most parameters investigated were seen in all case study PSAs except the North Slope PSA. While the season with the most moisture and warmest temperatures both at the surface and aloft featured the most lightning for these PSAs (the duff driven sub-season), the North Slope PSA's warmest and most moist season during lightning strokes is the drought driven sub-season. Despite this, 83% of fire season lightning still occurs in the duff driven sub-season in the North Slope PSA. A finding during the wind driven sub-season that carries through analysis conducted on the duff and drought driven sub-seasons as well is that the Y-K Delta and Seward Peninsula PSAs behave much more like Interior PSAs than they do Coastal PSAs in terms of lighting coincident weather parameters. Of the Coastal PSAs, Matanuska Valley & Anchorage and the Kenai Peninsula were the only Coastal PSAs that consistently behaved very similarly in this same regard.

Lightning associated convective precipitation also varies significantly between PSAs. In addition to the finding discussed above that the Middle Yukon PSA may experience more dry lightning than other PSAs due to its large difference between median and mean values of lightning associated convective precipitation, a further investigation into dry lightning using ERA5 and an additional high resolution reanalysis package and radar imagery where available may be very worthwhile. The accuracy of both ERA5 convective precipitation in the Middle Yukon PSA as well as the accuracy of the identified locations of lightning strokes there should be verified before any conclusions about dry lightning in the Middle Yukon PSA are determined. With the planned addition of 2 more lightning detectors in western Alaska, the location accuracy of lightning in the Middle Yukon PSA will likely improve. A detailed investigation into dry

lightning and tied to fire ignition could give insight into the importance of different weather parameters and fuel conditions across different PSAs.

4.3 Consistent Lightning Observations

While a large sample size of lighting strokes was analyzed using data gathered in a consistent way from 2012–2019, adding previously collected lightning data from 1986–2011 to this dataset would have certainly improved confidence in results. In order for this to occur, flash data from 1986–2011 must be converted to stroke data to align with stroke data collected from 2012–Present. While difficult, this process may be worth outlining and completing in order to acquire and analyze a larger sample size not only for the similar analysis to that conducted here, but also to analyze changes in lightning patterns over time. This would allow for a more consistent record of lightning data from 1986–Present and extending into the future, though it would still not be able to account for changes in sensor coverage.

An important step to tracking the influence of anthropogenic climate change on the Alaska fire season will be verifying predicted increases in lightning. Due to changes in the Alaska Lightning Detection Network, this has proven to be difficult. With the planned installation of additional lightning detectors, verification of increases in lightning may be best done through analysis of convective build-ups seen on satellite imagery. High resolution reanalysis of convective precipitation could also aid in this investigation, though significant improvements will likely need to be made to current high resolution products in order for this approach to yield reliable findings.

4.4 Next Steps

On the sub-seasonal timescale, relative humidity yielded some intriguing findings that are worthy of further investigation. Specifically, PSAs such as the North Slope PSA where lightning does not occur at low relative humidities during the drought driven sub-season while it does during the duff and wind driven sub-seasons. This is something that may have an impact on fire ignition due to drying of fuels during periods of low relative humidity.

Due to the most lightning and fire ignitions occurring during the duff driven sub-season, a special focus should be placed on this time period. Many fire seasons such as 2020 burn relatively few acres in Alaska. The predictability in these seasons likely lies in predicting weather, fuel, and lightning conditions during the duff driven sub-season since ignitions and weather and fuel conditions must align in this season to suppress the fire season.

Another possible direction of future investigation into lightning in Alaska could be to investigate teleconnections such as the Madden-Julian Oscillation (MJO). Abatzoglou and Brown (2009) found that lightning activity in the CONUS can be related to the MJO. Should lightning in Alaska also be related to the MJO, it could provide a baseline for predictability based on a well forecasted phenomenon. Eastern Pacific teleconnections as outlined in Duffy et al. (2005), as well as the El Niño Southern Oscillation are worthy of investigation for predictability of lightning in Alaska on a long term timescale.

While understanding lightning on the short and long term timescale is a necessary step for forecasting it, forecasting the variables that are associated with lightning on a seasonal timescale is a challenge in and of itself. Long term climate models such as the CFSv2 have shown promising skill in predicting a number of variables in recent years. Another possible approach to future work on lightning forecasting in Alaska is to utilize high resolution models to

attempt to gain skill on the 3 and 4 day planning timeframe. These forecasts could provide, as suggested in Tippett et al. (2018), a predictability baseline against which other approaches can be compared.

4.5 Towards Taking Research to Operations

Routine fire weather planning forecasts are produced twice daily by National Weather Service (NWS) forecast offices in Alaska. These forecasts are used by fire managers in the field as well as by Alaska Fire Service Meteorologists to aid in preparing briefings for fire managers, firefighters, and other interested parties involved in wildland firefighting operations. Fire managers and other operational personnel also request hyperlocal short-term weather forecasts called SPOT forecasts from the NWS for specific locations of importance. Additional coordination calls are often held during active fire weather periods, and to coordinate Red Flag Warnings between the NWS and the Alaska Fire Service Meteorologists. The end goal of this research is for it to be applicable to this process so that it can be used to improve firefighting resource distribution and management. For this to be accomplished, additional details on smaller geographic areas should be investigated in order for thresholds in weather parameters to be established. Additional short-term convective parameters such as the lifted index should be included in this investigation. A decision tree machine learning model or model output statistic (MOS) equation could then be applied to daily conditions to determine if they are favorable for lightning in a smaller and well defined geographic area. Based on the key results, flow direction would likely be one of the first decision tree steps and highest weighted MOS variables.

5. Conclusions

Using Alaska Lightning Detection Network data for the 2012–2019 time period and meteorological reanalysis data from ECMWF ERA5, lightning in Alaska was analyzed on a stroke-by-stroke timescale and a PSA spatial scale. Through this process, meteorological parameters were determined at the time and place of lightning strokes. The resulting database was analyzed to identify key lightning associated meteorological parameters and their distinct features and patterns that could be used to improve the predictability of lightning on seasonal and sub-seasonal timescales. The majority of lightning occurs in the duff driven sub-season across all PSAs. The majority of lightning occurs in Interior Alaska, with the lowest values occurring in the Coastal PSAs. Lightning, particularly in the Interior PSAs, follows a diurnal pattern with lightning on average beginning earlier in the day in the eastern portion of Alaska and later in the western portion of Alaska. This distinction is not as well defined in the Coastal PSAs. Lightning activity peaks in the afternoon between 16:00 and 18:00 Alaska Daylight Time. A higher percentage of lightning in the coastal regions occurs at night (between midnight and 5AM) than in the Interior PSAs, with the exception of a few small regions in the Interior.

During the wind driven sub-season, 2-meter air temperatures are approximately 10°C warmer than climatology and dew point temperatures around 8 °C warmer than climatology during lightning strokes. During the duff driven sub-season, 2-meter air temperatures and dew point temperatures are approximately 5 °C and 4 °C above normal during lightning strokes, respectively. During the drought driven sub-season, 2-meter air temperatures and dew point temperatures were approximately 6 °C and 4 °C above climatology respectively, however lightning associated dew point temperatures were approximately 7 °C above climatology for the North Slope PSA. The Middle Yukon PSA was of particular interest because lightning associated

median convective precipitation values were much lower than mean values, leading us to speculate that this may be due to elevated amounts of dry lightning. This feature was not evident in other PSAs. While this finding may be an artifact of the reanalysis data, or a result of inaccurate locating of lightning strokes, it certainly bears the need for more investigation and could be useful information to fire managers. Grouping PSAs into Interior, Semi-Interior, and Coastal geographical divisions was useful for comparison of analysis conducted on each PSA, however each PSA has its own unique influences beyond proximity to the coast. Similar patterns were often not observed between PSAs within the same geographical divisions. For example, the Copper River Basin and Susitna Valley PSAs have much colder lightning associated temperatures than other Semi-Interior PSAs. This is likely due to higher elevation terrain being extensive in both of these PSAs while it is limited in other Semi-Interior PSAs.

Among case studies conducted on the Tanana Valley West, Upper Yukon, Kuskokwim Valley, Seward Peninsula, and North Slope PSAs, important differences were found at the process level of parameters favorable for lightning activity. The most distinct patterns in each PSA were seen in lightning associated 500 and 700 hPa flow direction. Easterly flow was more common during lightning strokes in the Seward Peninsula and Kuskokwim Valley PSAs while south was the dominant flow direction during lightning strokes in the North Slope PSA. The Upper Yukon and Tanana Valley West PSAs showed less distinction in this, the northeast and northwest flow at both 500 and 700 hPA was favorable for lightning in the Tanana Valley West PSA. In the Upper Yukon PSA, flow from the southeast at 500 and 700 hPA during the wind driven sub-season was somewhat favorable for lightning activity. Northerly flow during all sub-seasons was unfavorable for lightning in the Upper Yukon and North Slope PSAs. Lightning associated relative humidities are highest during the drought driven sub-season across all five

70

PSA case studies. The Seward Peninsula PSA, while similar to other case study PSAs in terms of patterns in lightning associated meteorological parameters, exhibited nearly the same amount of lightning activity during the drought driven sub-season as the duff driven sub-season. The feature was unique to the Seward Peninsula PSA. The North Slope PSA experiences a higher percentage of its lightning activity in the duff driven sub-season than other sub-seasons compared to other PSAs. However, lightning associated temperature and moisture parameters do not peak until the drought driven sub-season. These parameters generally peak during the duff driven sub-season in other PSAs. The case studies highlight the unique conditions influenced by localized geographic conditions in each PSA.

Further research into this topic can be directed in a number of ways. To continue analysis at the hourly scale, employing higher resolution (< 3 km) reanalysis than the ERA5 and high resolution forecast models to gain lightning forecast skill on the three to four day timeframe can also be useful to allocation and positioning of fire resources. On the seasonal and sub-seasonal timescales, linking teleconnections to weather patterns and flow directions identified as favorable for lightning in this study would enhance the ability to construct skillful seasonal outlooks. Using this research, the key parameters identified can be evaluated in seasonal forecast models in order to improve them and increase the skill of seasonal lightning prediction. With higher skill in seasonal lightning outlooks, the quality of decision support provided to fire managers and stakeholders can be improved, and additional costs in fire suppression and resources can be saved.

References

Abatzoglou, J. T., and Brown, T. J., 2009: Influence of the Madden–Julian oscillation on summertime cloud-to-ground lightning activity over the continental United States. *Mon. Weather Rev*, **137**, 3596– 3601. doi:10.1175/2009MWR3019.1

AICC, 2020: Alaska Fire History Perimeter Polygons. Available online: https://fire.ak.blm.gov/content/maps/aicc/Metadata/Metadata/Zipped%20file%20geodatabases/AlaskaFireHistory_Polygons_metadata.xml (accessed on 11 March 2021).

Alvarado, E., Sandberg, D., Pickford, S.G., 1998: Modeling large forest fires as extreme events. *Northwest Science*, **72**, 66-75.

Bhatt, U.S., Lader, R.T., Walsh, J.E., Bieniek, P.A., Thoman, R., Berman, M., Borries-Strigle, C., Bulock, K., Chriest, J., Hahn, M., Hendricks, A.S., Jandt, R., Little, J., McEvoy, D., Moore, C., Rupp, T.S., Stevens, E., Strader, H., Waigl, C.F., White, J., York, A., and Ziel, R., 2021: Emerging Anthropogenic Influences on the Southcentral Alaska Temperature and Precipitation Extremes and Related Fires in 2019. *Land*, **10**, 82. doi:10.3390/land10010082.

Biagi, C.J., Cummins, K.L., Kehoe, K.E., and Krider, E.P., 2007: National Lightning Detection Network (NLDN) performance in southern Arizona, Texas, and Oklahoma in 2003–2004, *J. Geophys. Res.*, **112**, D05208, doi:10.1029/2006JD007341.

Bieniek, P.A., Bhatt, U.S., York, A., Walsh, J. E., Lader, R., Strader, H., Ziel, R., Jandt, R., and Thoman, R., 2020: Lightning Variability in Dynamically Downscaled Simulations of Alaska's Present and Future Summer Climate. *J. Appl. Meteorol. Climatol.*, **59**, 1139-1152. doi:10.1175/JAMC-D-19-0209.1.

Biswas, A.K., and Jayaweera, K.O.L.F., 1976: NOAA-3 Satellite Observations of Thunderstorms in Alaska, *Mon. Weather Rev*, **104**(3), 292-297. doi:10.1175/1520-0493(1976)104<0292:NSOOTI>2.0.CO;2.

Brandt, J.P., 2009: The extent of the North American boreal zone. *Environmental Reviews*, **17**(NA), 101-161. doi:10.1139/A09-004.

Burrows, D.R., 1987: Preattack Planning Report (United States Bureau of Land Management's Alaska Fire Service).

Charba, J., Shafer, P., Samplatsky, F., Kochenash, A., and Ghirardelli, J., 2020: LAMP Alaska Convection and Lightning Verification Report, *NOAA/NWS Meteorological Development Lab*, Office Note 20-1, May 2020.

Cummins, K.L., Murphy, M.J., Bardo, E.A., Hiscox, W.L., Pyle, R.B., and Pifer, A.E., 1998: A Combined TOA/MDF Technology Upgrade of the U.S. National Lightning Detection Network, *J. Geophys. Res.*, **103**(D8), 9035– 9044, doi:10.1029/98JD00153.

Dissing, D., and Verbyla, D.L., 2003: Spatial patterns of lightning strikes in interior Alaska and their relations to elevation and vegetation. *Can. J. For. Res.*, **33**(5), 770–782. doi: 10.1139/X02-214.

Duffy, P.A., Walsh, J.E., Graham, J.M., Mann, D.H., and Rupp, T.S., 2005: Impacts of large-scale atmospheric–ocean variability on Alaskan fire season severity. *Ecological Applications*, **15**(4), 1317–1330.

Farukh, M., Hayasaka, H., and Kimura, K., 2011: Characterization of Lightning Occurrence in Alaska Using Various Weather Indices for Lightning Forecasting. *Journal of Disaster Research*, **6**, 343-355.

Farukh, M., Hayasaka, H., 2012: Active Forest Fire Occurrences in Severe Lightning Years in Alaska. *J Nat Disast Sci.*, **33**, 71-84. doi: 10.2328/jnds.33.71.

Flannigan, M.D., Krawchuk, M.A., de Groot, W.J., Wotton, B.M., and Gowman, L.M., 2009: Implications of changing climate for global wildland fire. *International Journal of Wildland Fire*, **18**(5), 483. doi:10.1071/WF08187.

Flannigan, M.D., and Harrington, J.B., 1988: A Study of the Relation of Meteorological Variables to Monthly Provincial Area Burned by Wildfire in Canada (1953–80), *J. Appl. Meteorol. Climatol.*, **27**(4), 441-452. doi: 10.1175/1520-0450.

Fuchs, B.R., Rutledge, S.A., Bruning, E.C., Pierce, J.R., Kodros, J.K., Lang, T.J., MacGorman, D.R., Krehbiel, P.R., and Rison, W., 2015: Environmental controls on storm intensity and charge structure in multiple regions of the continental United States. *J. Geophys. Res. Atmos.*, **120**, 6575–6596, doi:10.1002/2015JD023271.

Graham, R.M., Hudson, S.R., and Maturilli, M., 2019: Improved Performance of ERA5 in Arctic Gateway Relative to Four Global Atmospheric Reanalyses. *Geophys. Res. Lett.*, **46**, 6138–6147, doi:10.1029/2019gl082781.

Grice, G.K., and Comisky, A.L., 1976: Thunderstorm climatology of Alaska. *NOAA Tech. Memo*, NWS AR-14, 36 pp.

Henry, D.M., 1978: Fire occurrence using 500 mb map correlation. *NOAA technical memorandum*, NWS AR-21. NWS, Anchorage, Alaska.

Kasischke, E.S., and Turetsky, M.R., 2006: Recent changes in the fire regime across the North American boreal region—Spatial and temporal patterns of burning across Canada and Alaska. *Geophys. Res. Lett.*, **33**(9). doi:10.1029/2006GL025677.

Krider, E.P., Noggle, R.C., Pifer, A.E., and Vance, D.L., 1980: Lightning direction finding systems for forest fire detection. *Bull. Am. Meteor. Soc.*, **61**, 980 – 986. doi:10.1175/1520-0477(1980)061<0980:LDFSFF>2.0.CO;2.

Lynch, J.A., Hollis, J.L., and Hu, F.S., 2004: Climatic and landscape controls of the boreal forest fire regime: Holocene records from Alaska. *Journal of Ecology*, **92**, 477-489. doi:10.1111/j.0022-0477.2004.00879.x.

Mülmenstädt, J., Sourdeval, O., Delanoe, J., and Quaas, J., 2015: Frequency of occurrence of rain from liquid-, mixed-, and ice-phase clouds derived from A-Train satellite retrievals. *Geophys. Res. Lett.*, **42**, 6502–6509, doi:10.1002/2015GL064604.

Partain, J.L., Alden, S., Strader, H., Bhatt, U.S., Bieniek, P.A., Brettschneider, B.R., Walsh, J.E., Lader, R., Olsson, P.Q., Rupp, T.S., Thoman, R., York, A.D., and Ziel, R.H., 2016: An assessment of the role of anthropogenic climate change in the Alaska fire season of 2015. *Bull. Am. Meteorol. Soc*, **97**(12), S14–S18.

Poujol, B., Prein, A.F., Molina, M.J., and Muller, C., 2021: Dynamic and thermodynamic impacts of climate change on organized convection in Alaska. *Clim. Dyn.* doi: 10.1007/s00382-020-05606-7.

Poujol, B., Prein, A.F., and Newman, A.J., 2020: Kilometer-scale modeling projects a tripling of Alaskan convective storms in future climate. *Clim. Dyn.* **55**, 3543–3564, doi:10.1007/s00382-020-05466-1.

Rakov, V. (2016). *Fundamentals of Lightning*. 1-248. Cambridge: Cambridge University Press. doi:10.1017/CBO9781139680370.

Reap, R.M., 1991: Climatological characteristics and objective prediction of thunderstorms over Alaska. *Weather and Forecasting*, **6**(3), 309–319.

Romps, D.M., Seeley, J.T., Vollaro, D., and Molinari, J., 2014: Projected increase in lightning strikes in the United States due to global warming. *Science*, **346**(6211), 851–854. doi:10.1126/science.1259100.

Semmens, K.A., and Ramage, J., 2012: Investigating correlations between snowmelt and forest fires in a high latitude snowmelt dominated drainage basin. *Hydrological Processes*, **26**(17), 2608–2617.

Sullivan, W.G., 1963: Low Level Convergence and Thunderstorms in Alaska. *Mon. Weather Rev*, **91**, 82-92.

Tippett, M.K., and Koshak, W.J., 2018: A baseline for the predictability of U.S. cloud-to-ground lightning. *Geophys. Res. Lett.*, **45**, 10,719– 10,728. doi:10.1029/2018GL079750.

Tippett, M.K., Lepore, C., Koshak, W.J., Chronis, T., Vant-Hull, B.. 2019: Performance of a simple reanalysis proxy for U.S. cloud-to-ground lightning. *Int. J Climatol.* **39**, 3932–3946. doi:10.1002/joc.6049.

Veraverbeke, S., Rogers, B.M., Goulden, M.L., Jandt, R.R., Miller, C.E., Wiggins, E.B., and Randerson, J.T., 2017: Lightning as a major driver of recent large fire years in North American boreal forests. *Nature Climate Change*, **7**(7), 529–534. doi: 10.1038/nclimate3329.

Wendler, G., Conner, J., Moore, Berrien., Shulski, M., Stuefer, M., 2011: Climatology of Alaskan wildfires with special emphasis on the extreme year of 2004. *Theoretical and Applied Climatology.* **104**. 459-472. doi:10.1007/s00704-010-0357-9.

White, J.H.R., Walsh, J.E., Thoman, R.L., 2020: Using Bayesian statistics to detect trends in Alaskan precipitation. *Int. J. Climatol.* doi:10.1002/joc.6946.

Appendices

Appendix A Tanana Valley West PSA
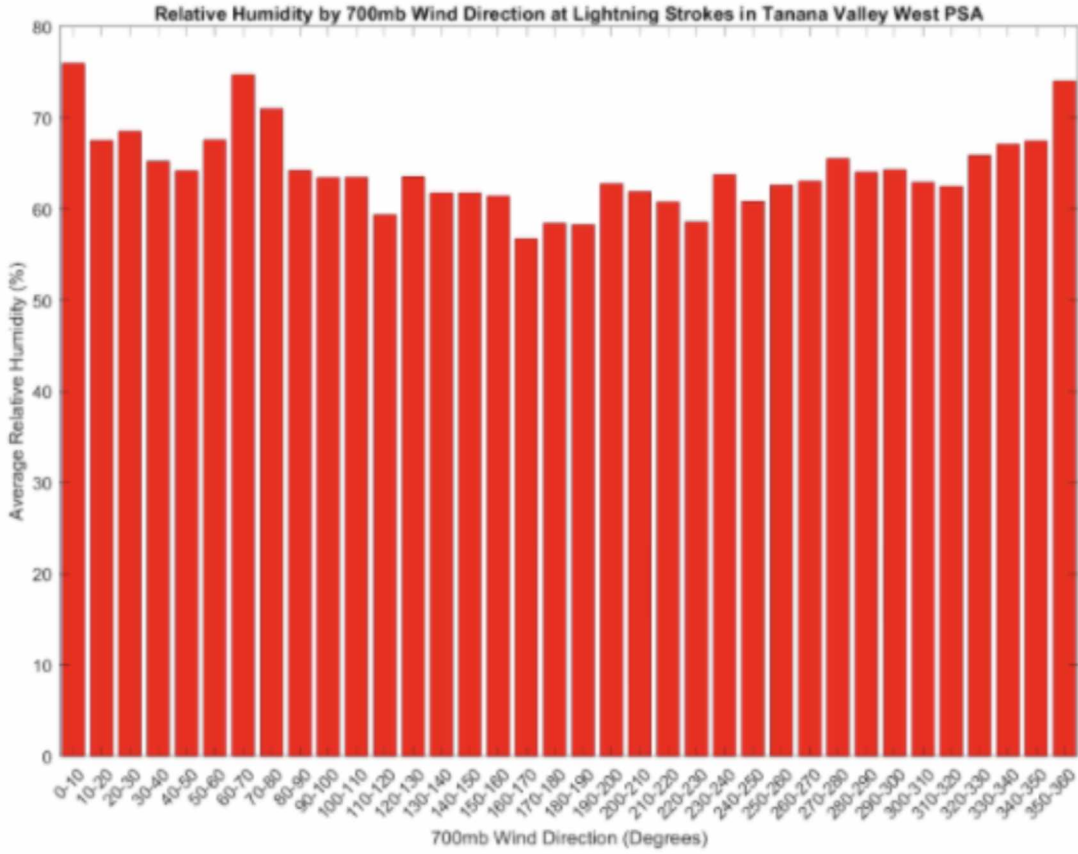
Figure A.1: Relative humidity amounts shown by 700 hPa flow direction during lightning events in the Tanana Valley West PSA.
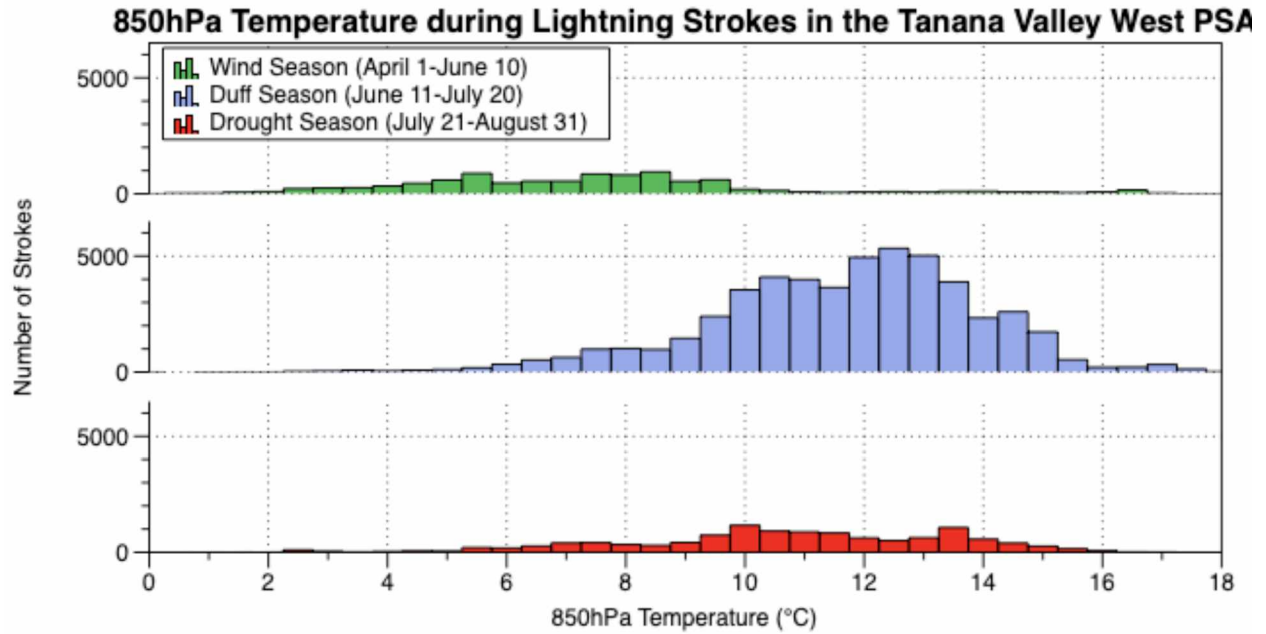
Figure A.2: The 850 hPa air temperatures (°C) associated with lightning strokes in the Tanana Valley West PSA for the 3 sub-seasons.
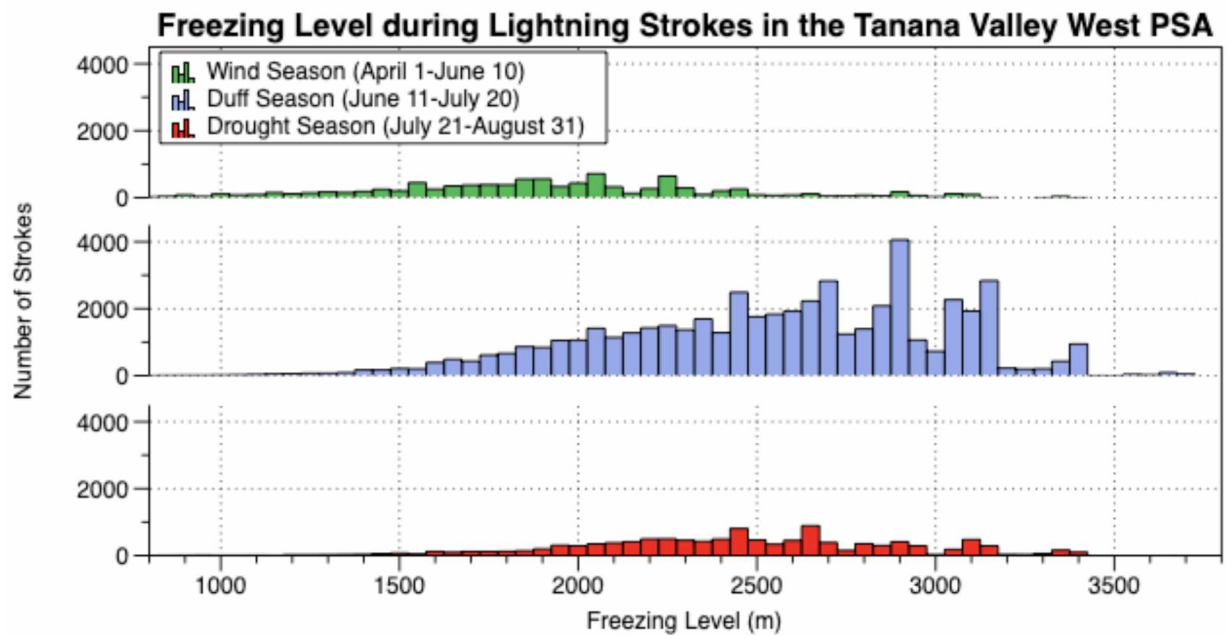
Figure A.3: The freezing level (m) associated with lightning strokes in the Tanana Valley West PSA for the 3 sub-seasons.
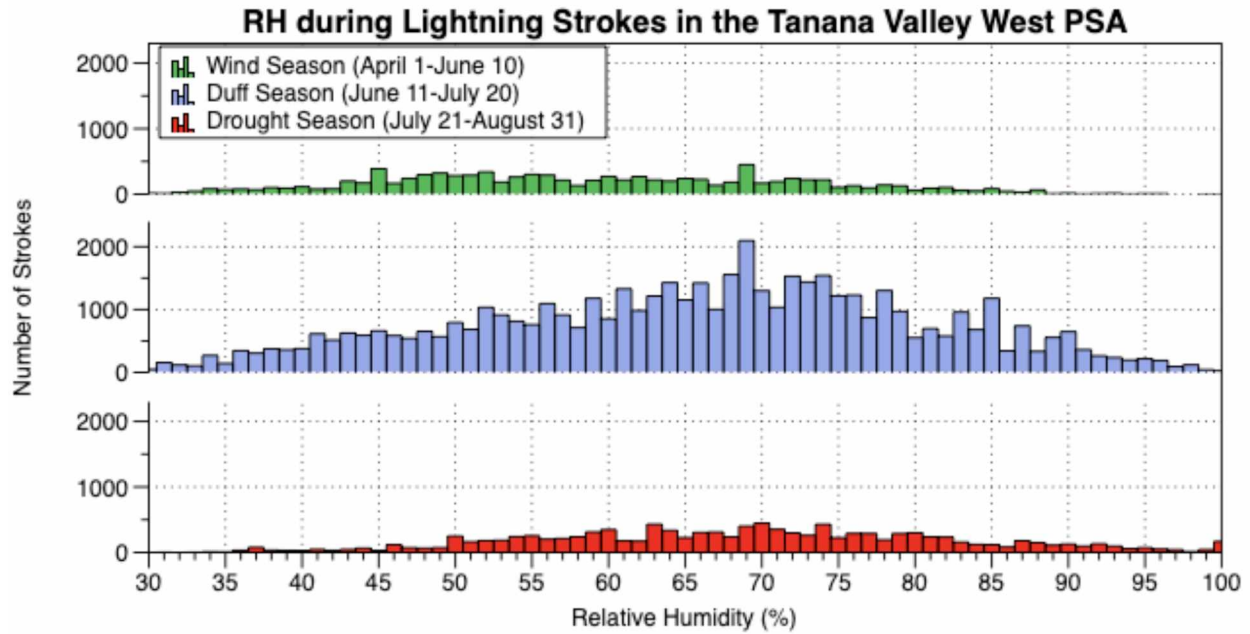
Figure A.4: The relative humidity (%) associated with lightning strokes in the Tanana Valley West PSA for the 3 sub-seasons.
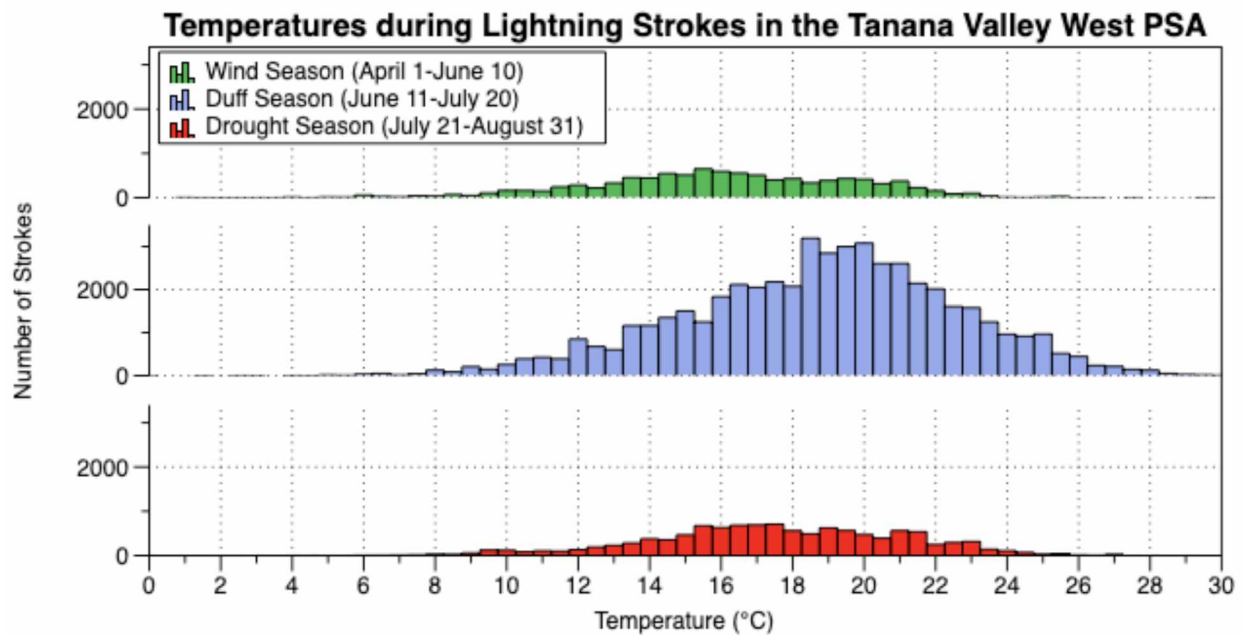
Figure A.5: The 2-m air temperature (°C) associated with lightning strokes in the Tanana Valley West PSA for the 3 sub-seasons.
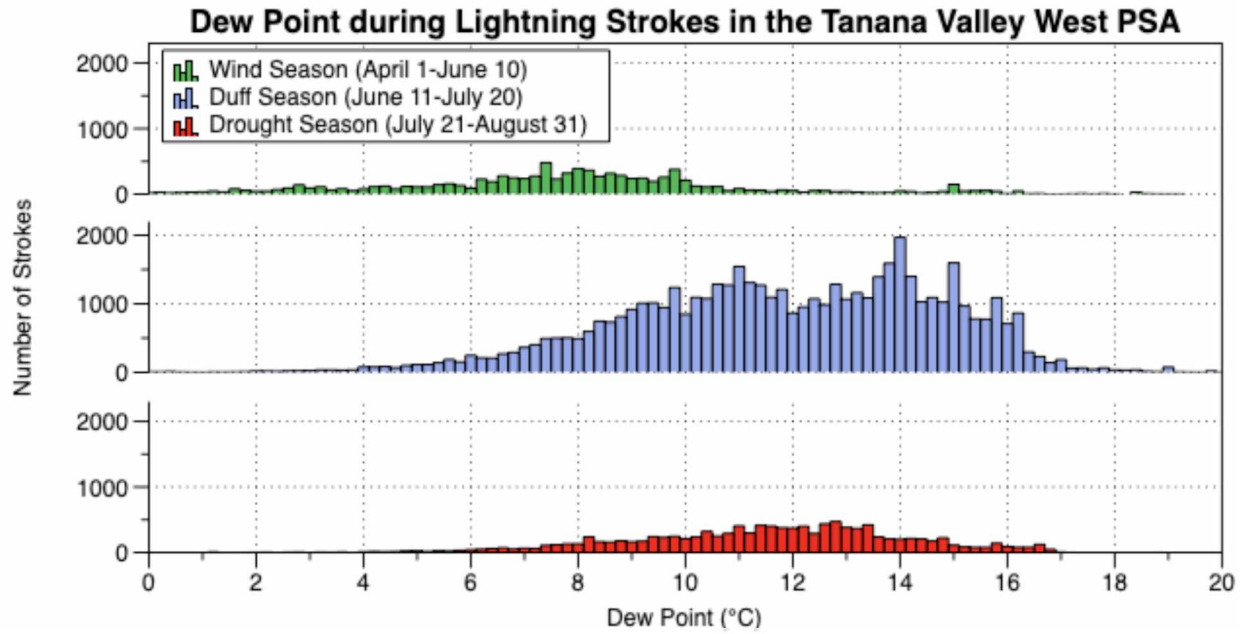
Figure A.6: The 2-m dew point temperature (°C) associated with lightning strokes in the Tanana Valley West PSA for the 3 sub-seasons.
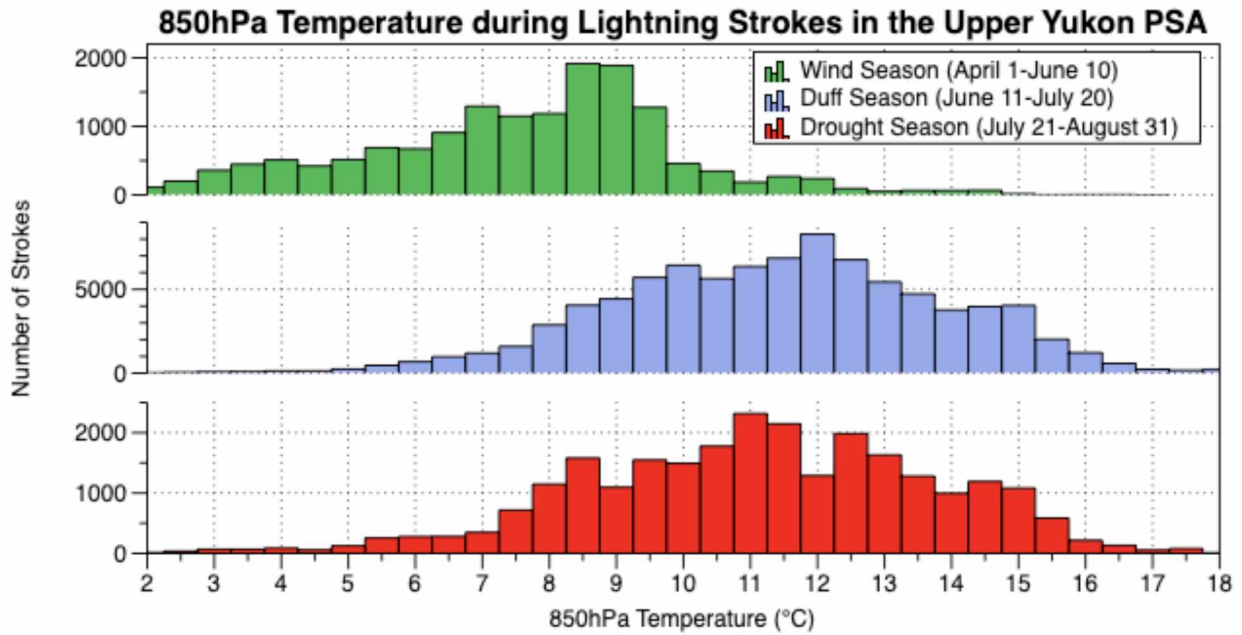
Figure B.1: The 850 hPa temperature (°C) associated with lightning strokes in the Upper Yukon PSA for the 3 sub-seasons.
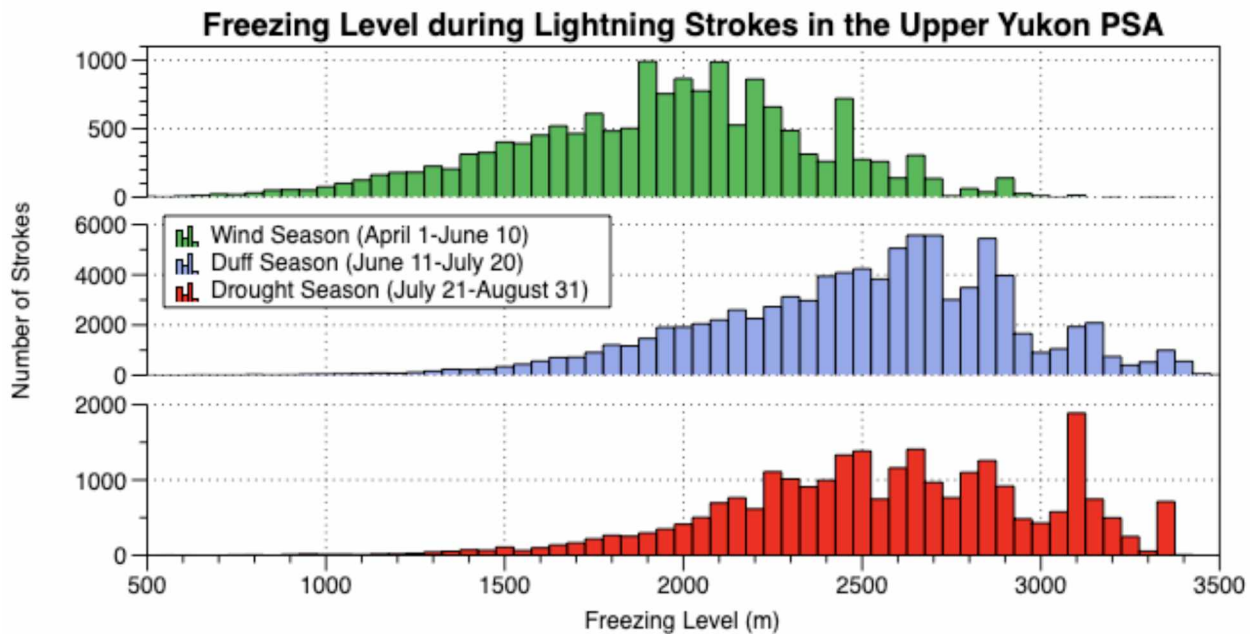
Figure B.2: The freezing level (m) associated with lightning strokes in the Upper Yukon PSA for the 3 sub-seasons.
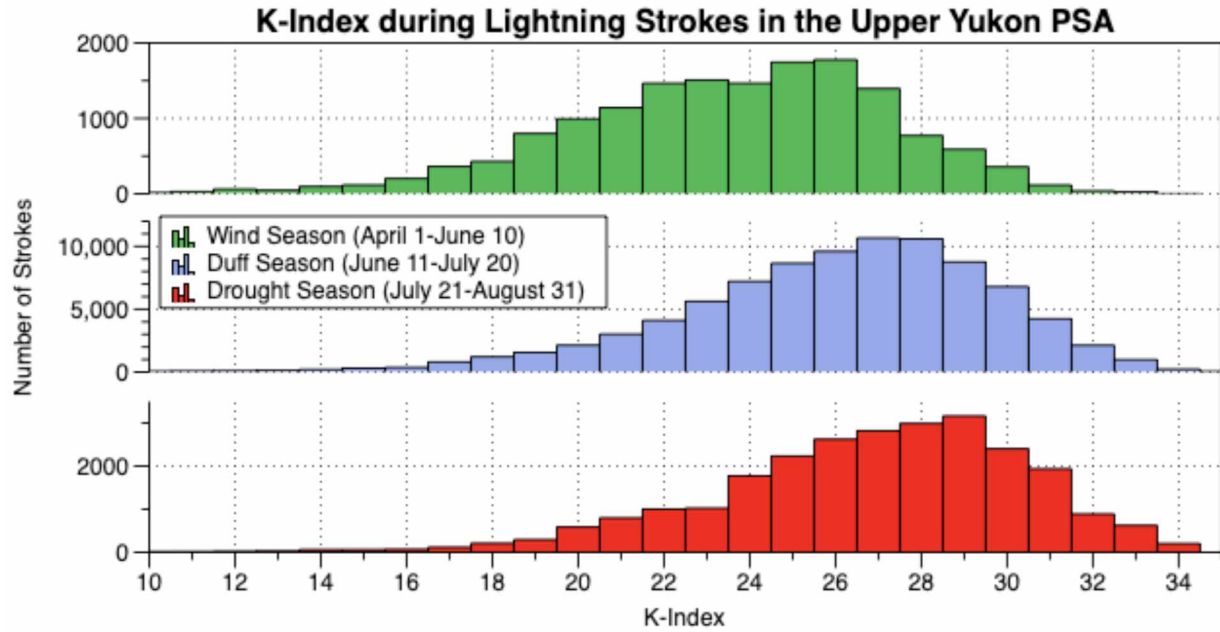
Figure B.3: The K-Index associated with lightning strokes in the Upper Yukon PSA for the 3 sub-seasons.
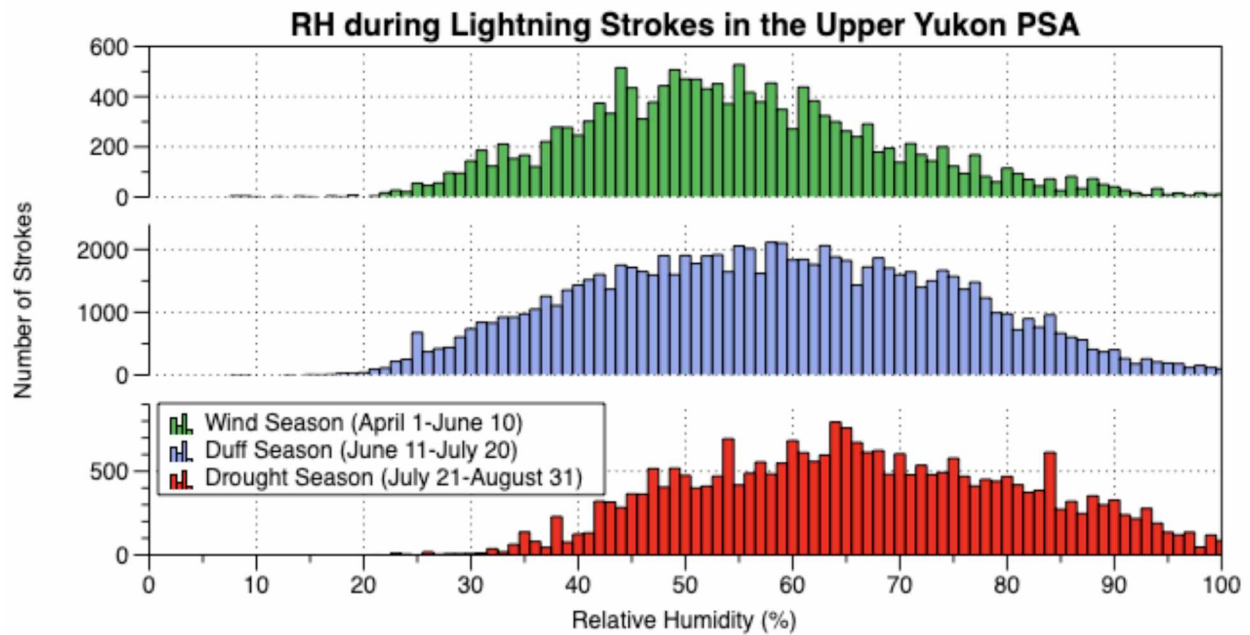
Figure B.4: The relative humidity (%) associated with lightning strokes in the Upper Yukon PSA for the 3 sub-seasons.
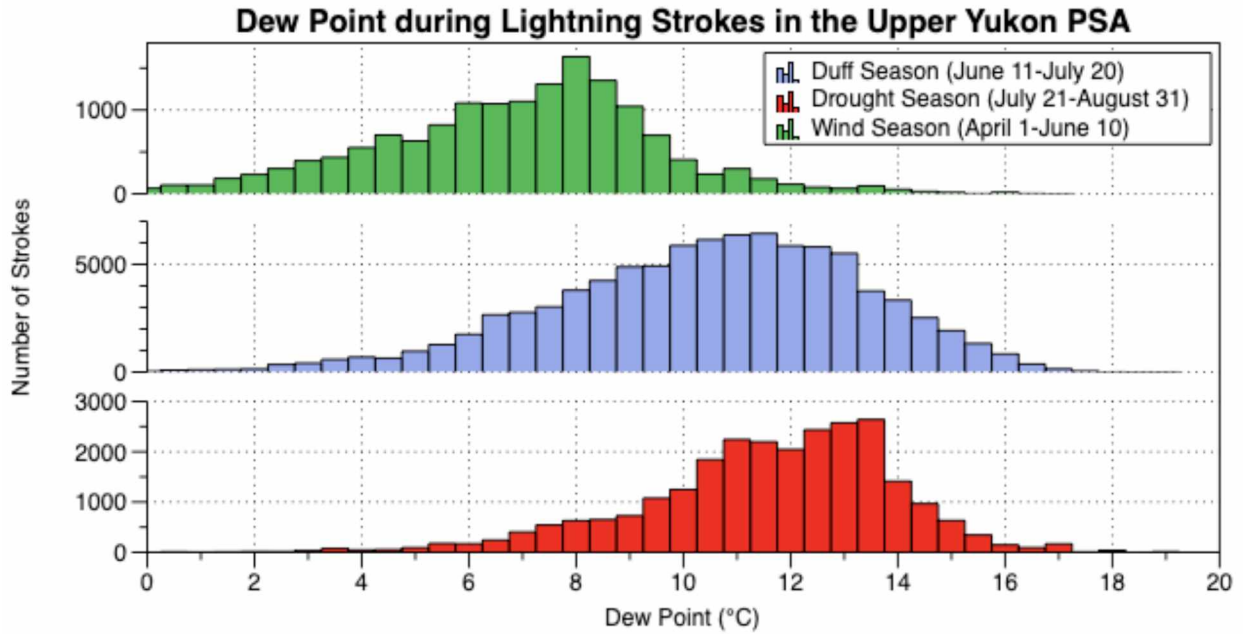
Figure B.5: The 2-m dew point temperature (°C) associated with lightning strokes in the Upper Yukon PSA for the 3 sub-seasons.
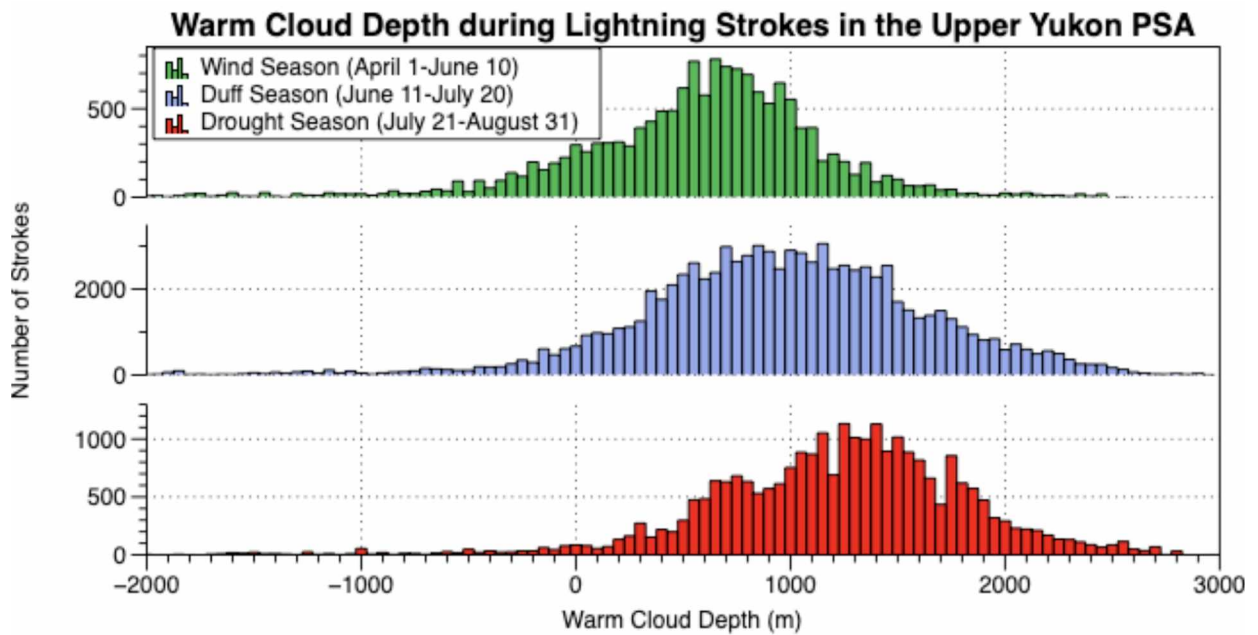
Figure B.6: The warm cloud depth (m) associated with lightning strokes in the Upper Yukon PSA for the 3 sub-seasons.
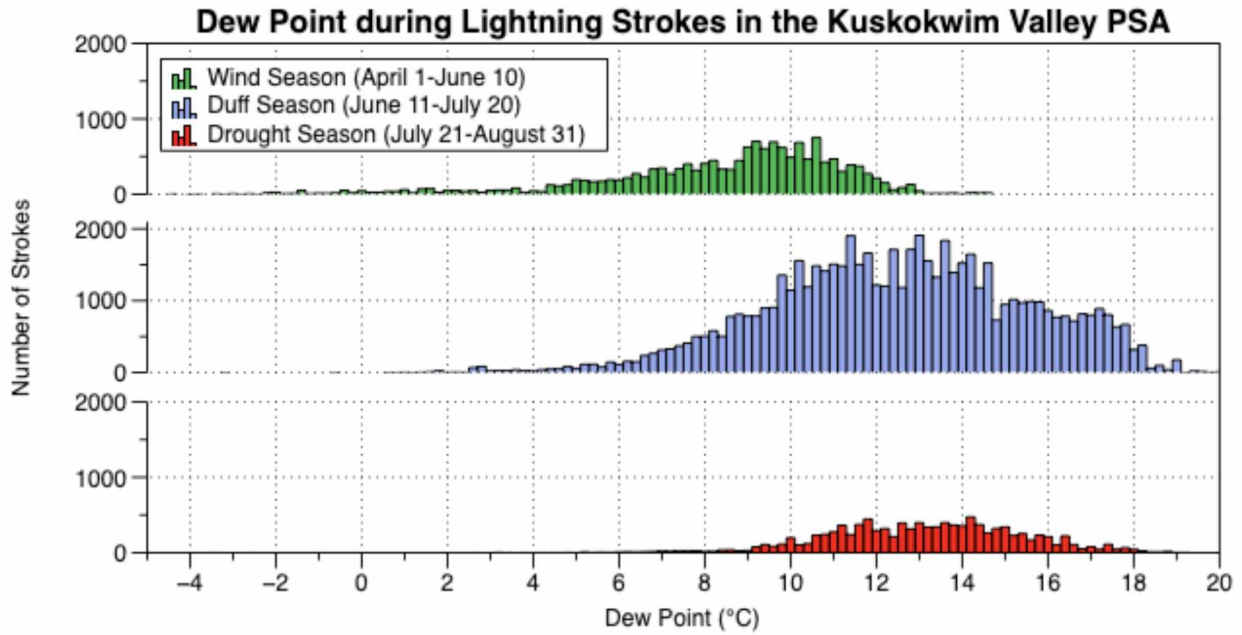
Figure C.1: The 2-m dew point temperature (°C) associated with lightning strokes in the Kuskokwim Valley PSA for the 3 sub-seasons.
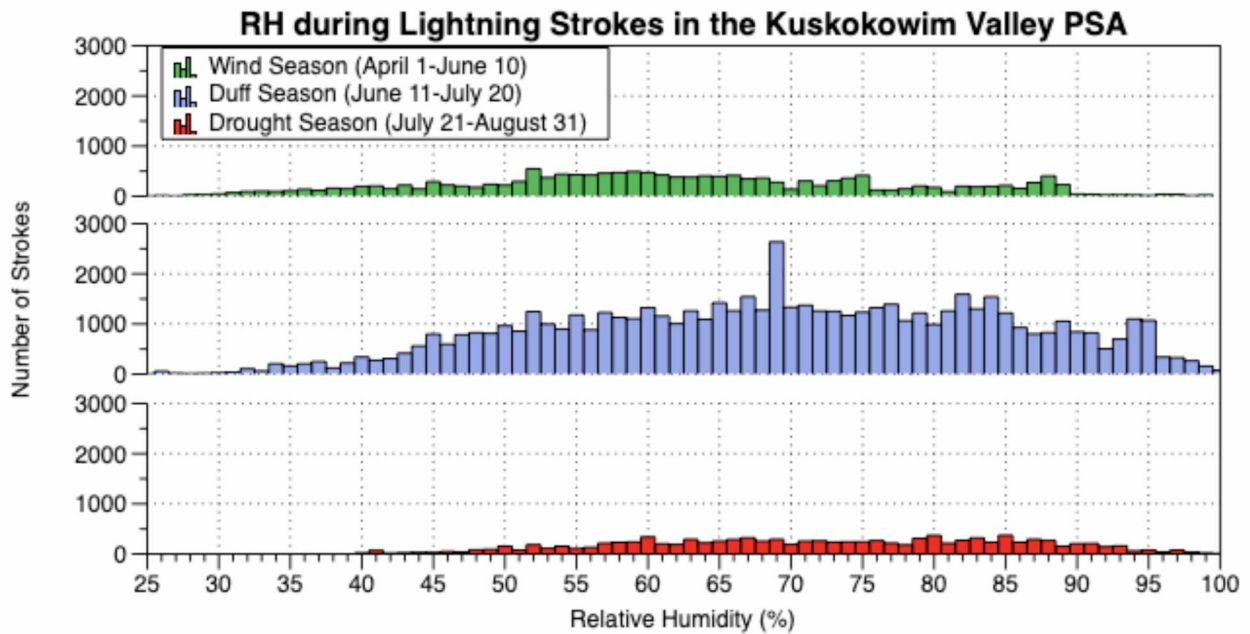
Figure C.2: The relative humidity (%) associated with lightning strokes in the Kuskokwim Valley PSA for the 3 sub-seasons.
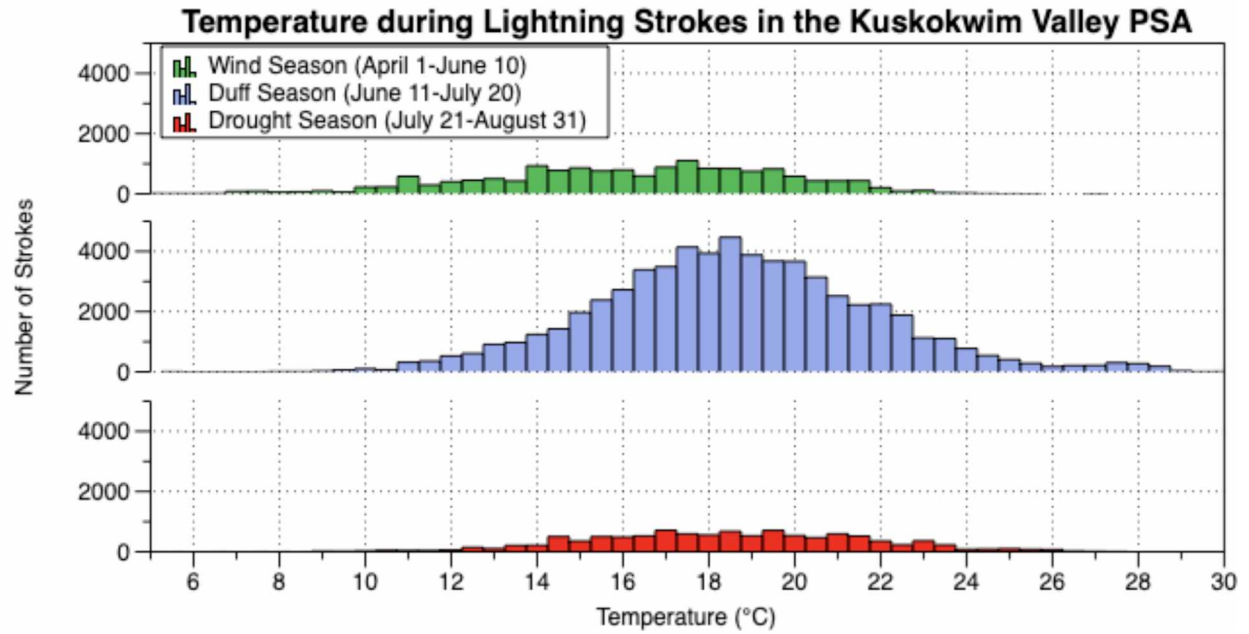
Figure C.3: The 2-m air temperature (°C) associated with lightning strokes in the Kuskokwim Valley PSA for the 3 sub-seasons.
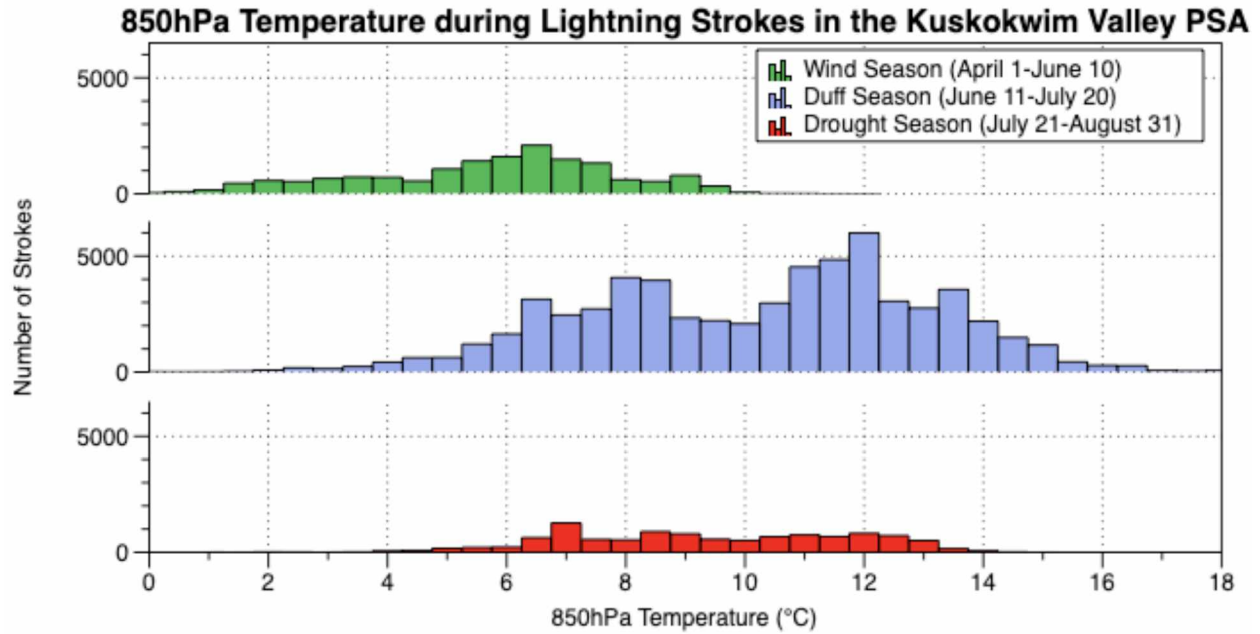
Figure C.4: The 850hPa temperature (˚C) associated with lightning strokes in the Kuskokwim Valley PSA for the 3 sub-seasons.
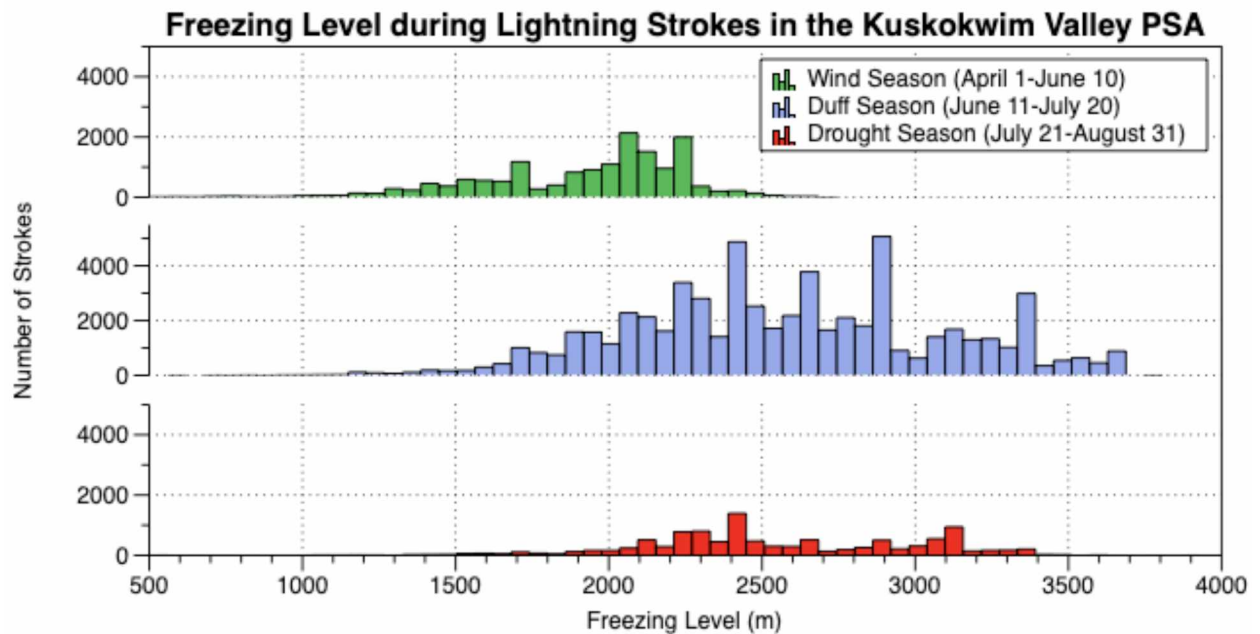
Figure C.5: The freezing level (m) associated with lightning strokes in the Kuskokwim Valley PSA for the 3 sub-seasons.
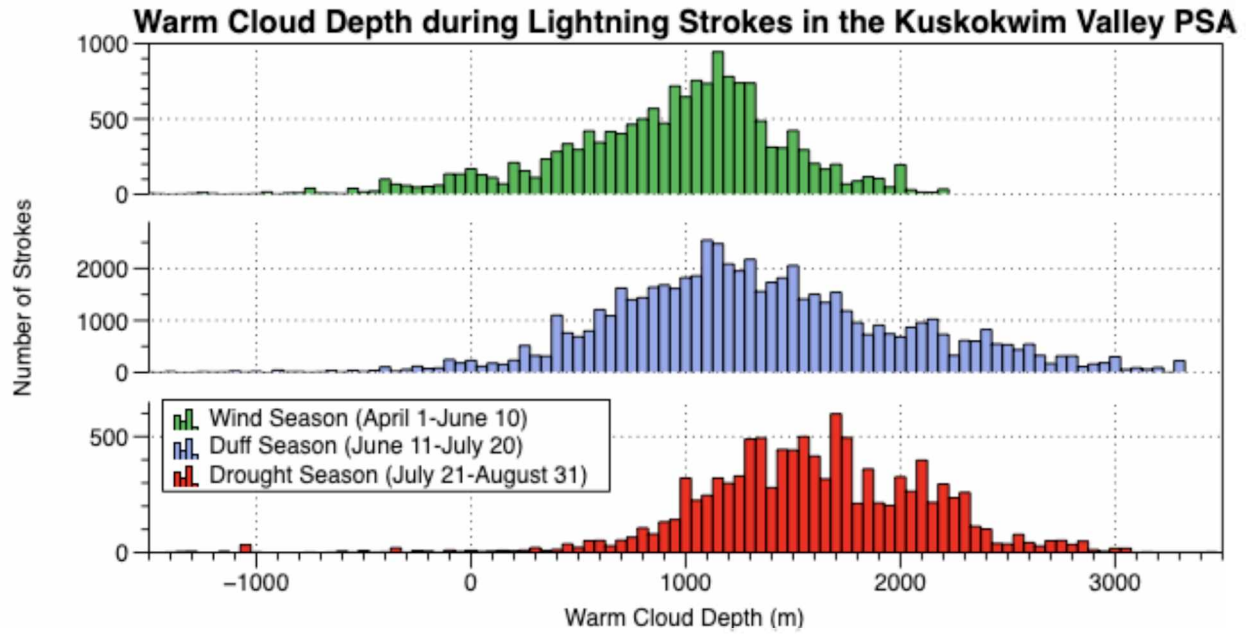
Figure C.6: The warm cloud depth (m) associated with lightning strokes in the Kuskokwim Valley PSA for the 3 sub-seasons.
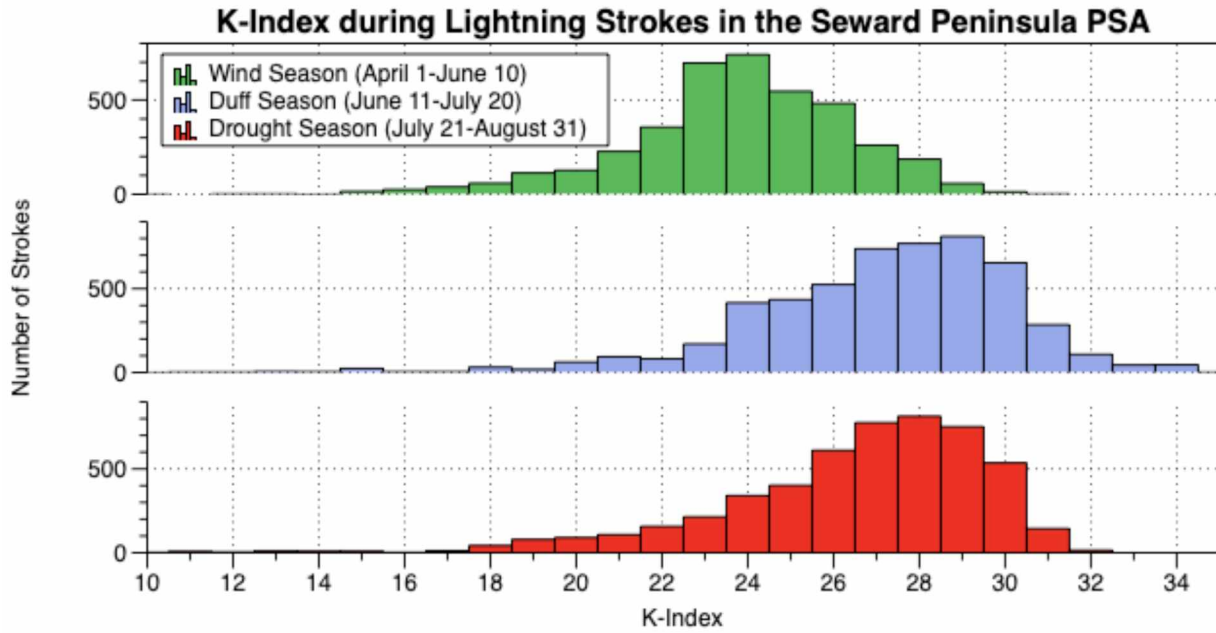
Figure D.1: The K-Index associated with lightning strokes in the Seward Peninsula PSA for the 3 sub-seasons.
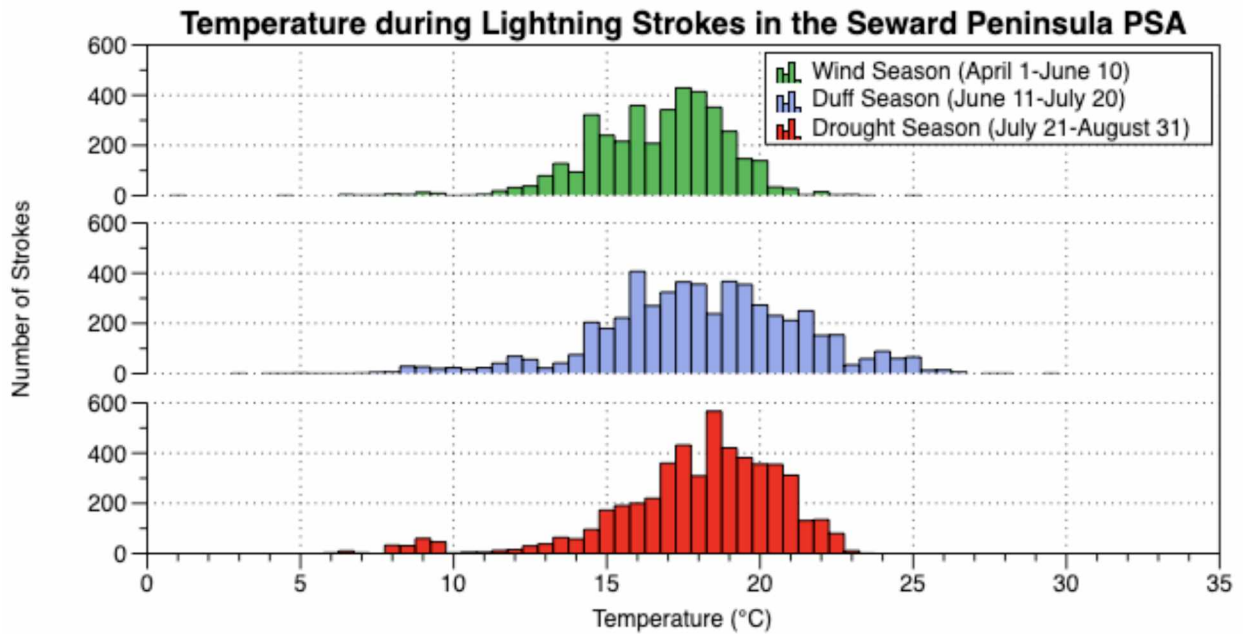
Figure D.2: The 2-m air temperature (°C) associated with lightning strokes in the Seward Peninsula PSA for the 3 sub-seasons.
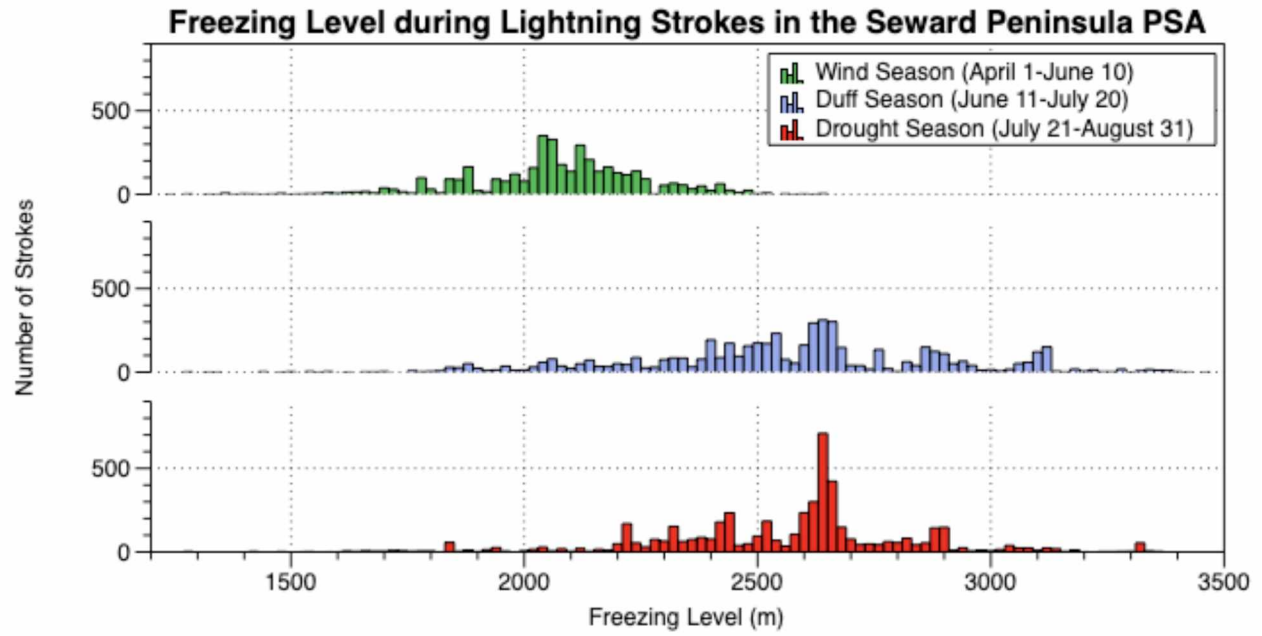
Figure D.3: The freezing level (m) associated with lightning strokes in the Seward Peninsula PSA for the 3 sub-seasons.
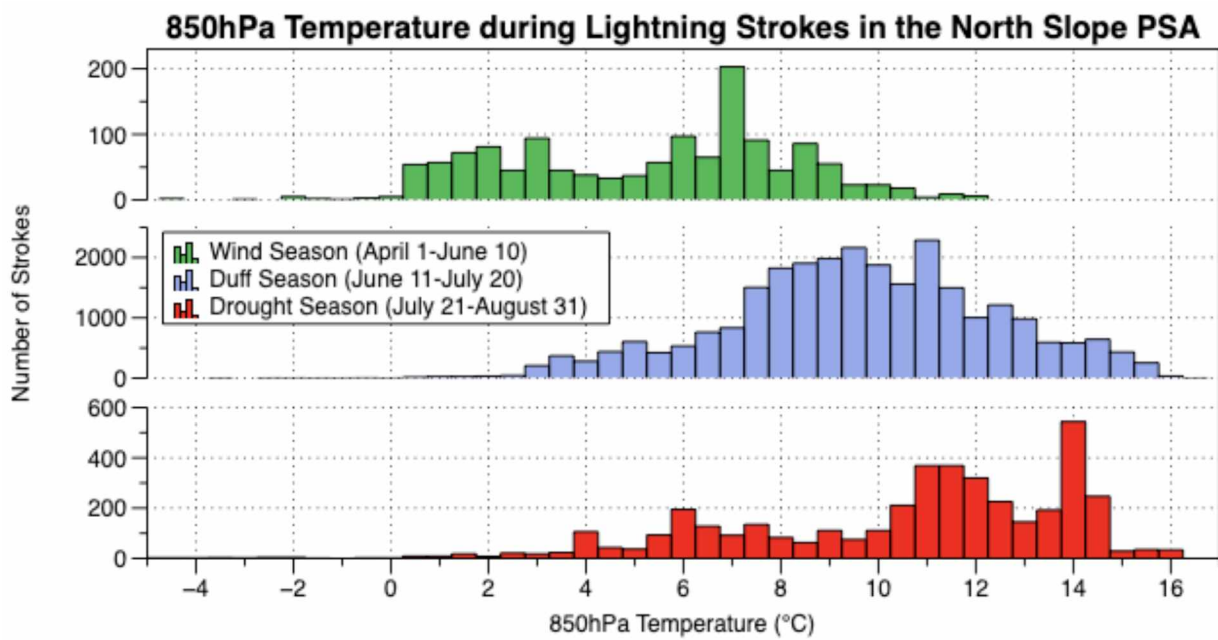
Figure E.1: The 850 hPa Temperature (˚C) associated with lightning strokes in the North Slope PSA for the 3 sub-seasons.
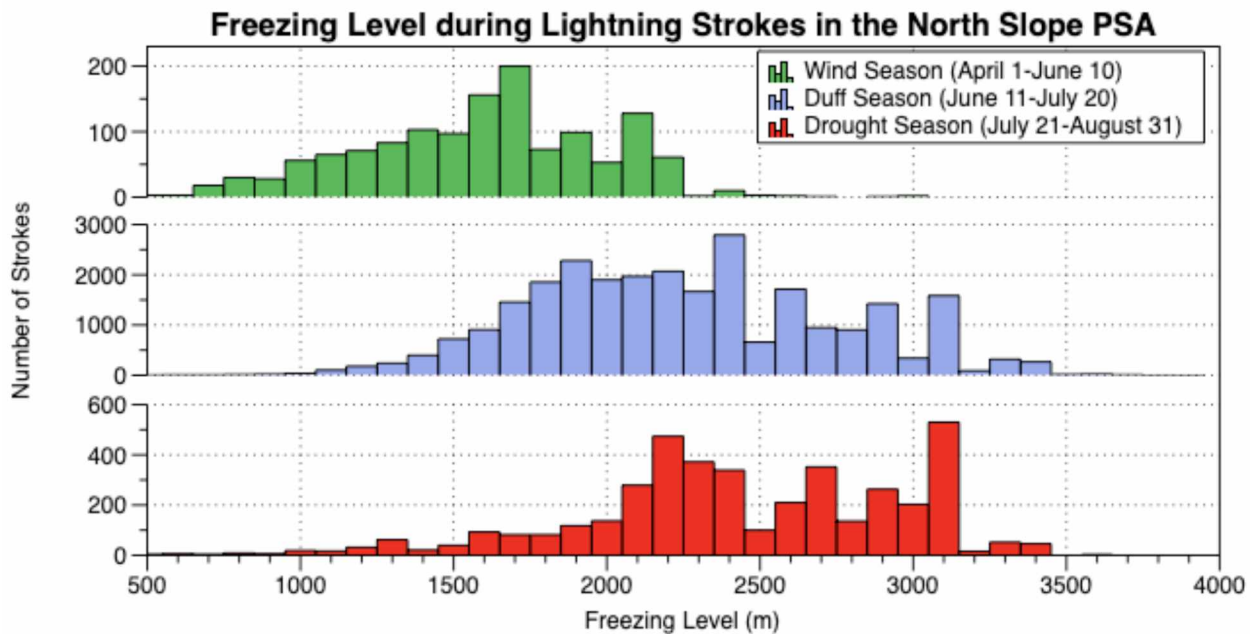
Figure E.2: The freezing level (m) associated with lightning strokes in the North Slope PSA for the 3 sub-seasons.
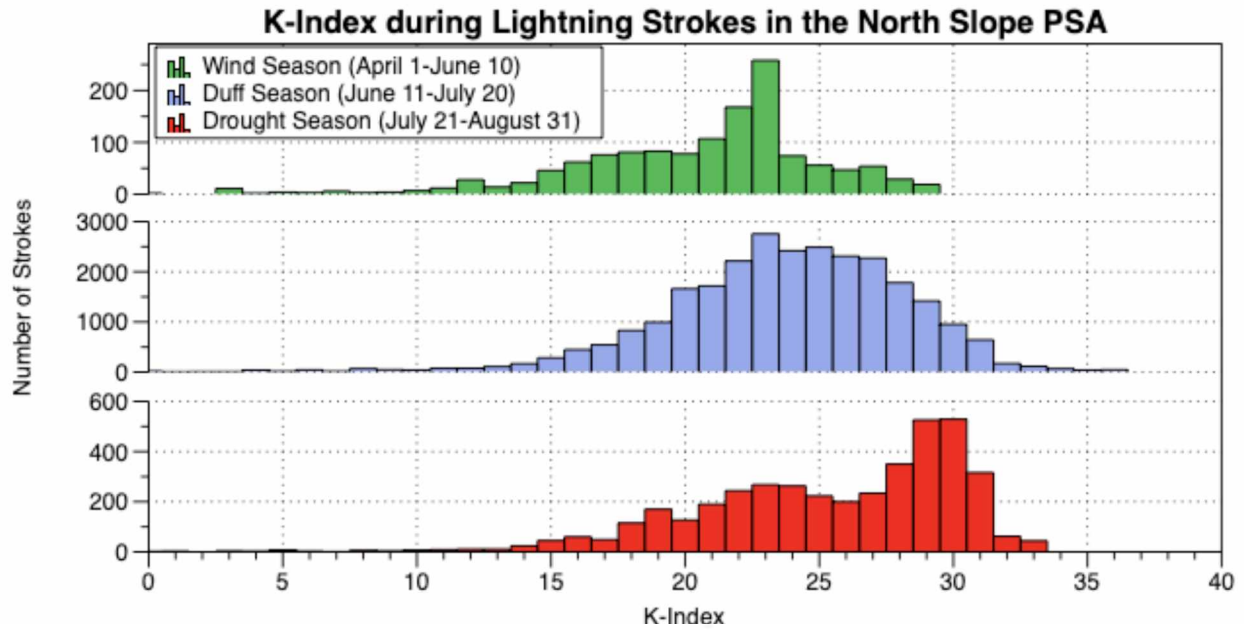
Figure E.3: The K-Index associated with lightning strokes in the North Slope PSA for the 3 sub-seasons.
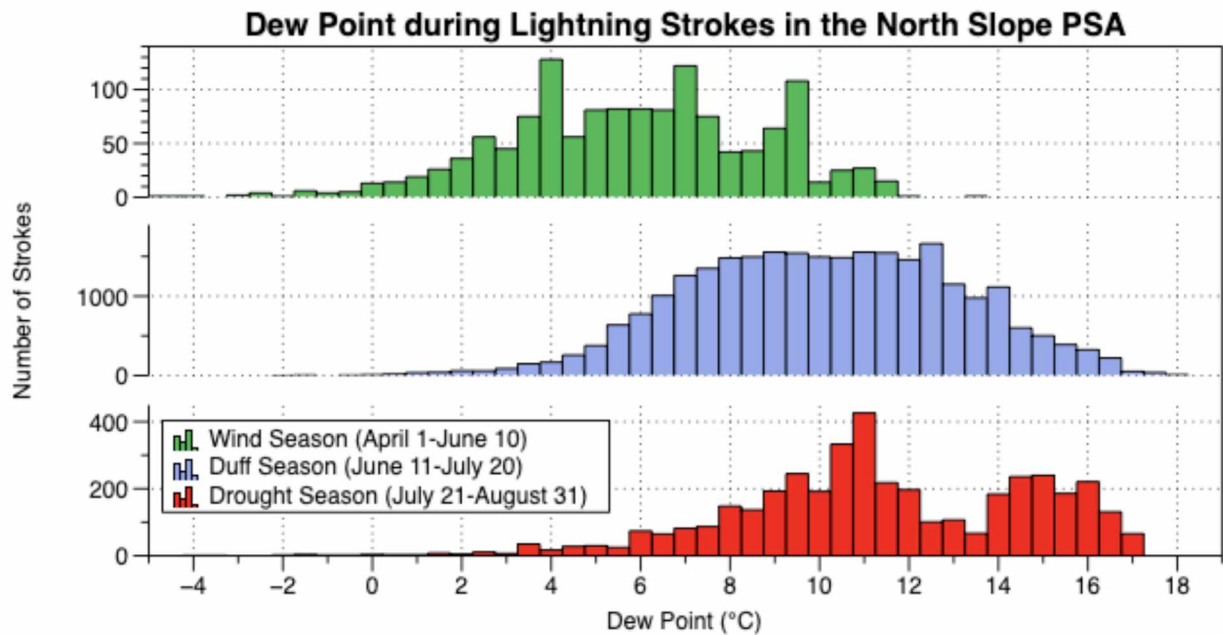
Figure E.4: The 2-m dew point temperature (°C) associated with lightning strokes in the North Slope PSA for the 3 sub-seasons.
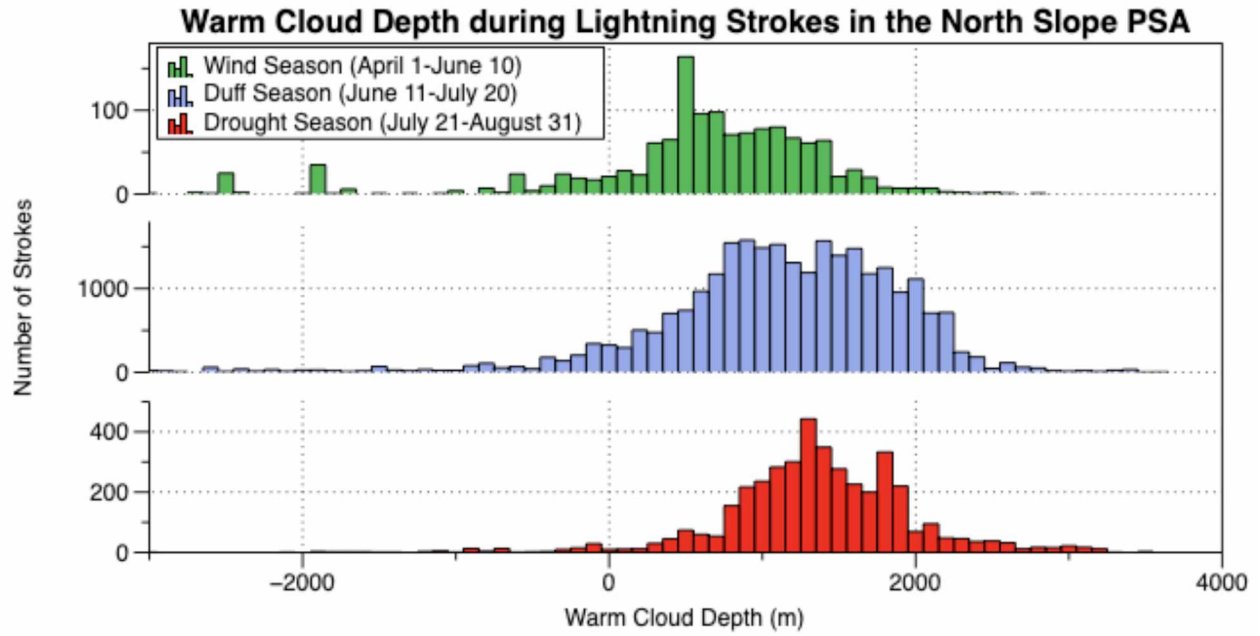
Figure E.5: The warm cloud depth (m) associated with lightning strokes in the North Slope PSA for the 3 sub-seasons.